2-1-2015

Lipid-based nanoparticles for altering immune response: A step towards targeted cancer immunotherapy

Noha Samir Ismail

The American University in Cairo

School of Sciences and Engineering

Nanotechnology Program

Lipid-based nanoparticles for altering immune response: A step towards targeted cancer immunotherapy

A thesis submitted to

The Nanotechnology Graduate Program in partial fulfillment of the requirements for the degree of

Master of Science

By Noha Samir Mohamed Ismail

Under the supervision of:

Associate Professor Nageh K. Allam

Physics Department, The American University in Cairo

Professor Suher Kamal Zada

Biology Department, The American University in Cairo

Associate Bioengineer Ashish Kulkarni

Brigham and Women's Hospital – Harvard Medical School/Harvard-MIT Health Sciences and Technology

September, 2015

Dedication

For my dear mother and father; for their devotion, prayers and endless support

Acknowledgements

In the name of Allah, the Most Gracious and the Most Merciful. All praises are due to Allah for the strengths and his blessing in completing this thesis.

I would like to express my deep gratitude to my advisor and role model Dr. Nageh Allam for giving me the opportunity to be a member in his awesome group. Every time I contact Dr. Nageh Allam he inspires me in a way that gives me the confidence to move forward and proceed. He used to advise, encourage and critically stimulate my thinking in every possible way. Your door was always open for us every time we need to reach you. Thank you for giving me hope, for respecting my passion and helping me highlight my dreams. I wish I will be able to conduct the same invaluable manners throughout my career in shaa Allah.

In addition, I would like to extend my deep gratitude to Dr. Suher Zada for giving me the opportunity to work with her. Dr. Suher Zada always helped me by every possible mean she can do. Thank you for putting your confidence and trust in me from the first time I contacted you. Your sincere advice, support and encouragement helped me a lot to proceed in my work. You were always available and very nice to me. Thank you for pushing me forward and helping me follow my passion.

I want to extend my sincere gratitude to Dr. Ashish Kulkarni and Dr. Shiladitya Sengupta for giving me the opportunity to join their laboratory for Nano-medicine at Brigham and women's Hospital, Harvard Medical school, Harvard–MIT Division of Health Sciences and Technology.

I would like to thank Dr. Ashish Kulkarni for his guidance and supervision throughout the practical work. His technical expertise, training and fruitful discussions throughout the project helped me a lot to proceed in my work. His assistance in experimental designs, critical troubleshooting and protocol optimizations are appreciated. Also I would like to thank all members of Sengupta's group specially Aaron Goldman and Siva Kumar. I would like to thank Seba Rezakhani, Ivana Kostic and Tong for the valuable comments and discussions.

I want to thank Dr. Hanadi Salem for her continuous support for the Nanotechnology program and her assistance whenever needed.

At AUC I would like to thank all my friends from EML group for giving me support and valuable advice from the very beginning, thanks to Icell Sharaf El Din, Basamat Shahin, Ahmed Mohyee, Ahmed Amer, Ahmed Hafez, Walaa Adly, Aya Maher, Mohamed Salama, Mohamed El Ganzoury, Menna Samir. And also special thanks to my friends in Biology, chemistry and physics department: Eman Rabie, Eman Mahmoud, Israa Hussein, Noha Nagdy, Leila Zeko, Asmaa Gamal, Hoda, Wesam Awad, Nahla Hussein, Rehab Kotb, Sara Hussein and Rami Wasfi for sharing positive inspirations, discussions and sincere help. My sincere gratitude to Reem Al Olaby for inspiring me from the very beginning to join AUC.

I would like to express my deep appreciation to the Egyptian group in Boston who supported me a lot during my stay there, I would like to mention Doaa Hegazy, her husband Mahmoud Sakr and their little girl Fairuz for their awesome company, their warm feelings they showered and ultimate assistance and care that made me forget any homesickness feeling, you were more than a family for me thank you. Also I would like to thank Doaa Hamed for her unconditional help since day one in Boston, her advice, help and care are greatly appreciated, thank you for being beside me. Thanks to Tarek Madany, Hany Bardissi and his wife Deina Abdelkader, Yasmin Saleh and Rama Saad for giving hand whenever needed.

I would like to thank the person who were supporting, encouraging and giving me ultimate help, attention and honest care through my journey my friend Aya Samy. Thank you for believing in me and being there for me.

Finally special gratitude to my parents for their unconditional and continuous support during my entire life. I couldn’t have done all of that without their prayers and honest wishes for me. Thanks to my mother for encouraging me to proceed in my academic dream since day one and thanks for my father for being supportive and putting trust and confidence in me.

Financial support from the American University in Cairo is gratefully appreciated.

Abstract

Since cancer is an extremely heterogeneous disease of origin, scientists are always trying to define novel approaches that can eliminate this disease. Over decades now, surgery, radiotherapy and chemotherapy have been the conventional methods to eradicate cancer. Unfortunately, cancer resistance has developed, in which tumor cells became resistant to the majority of chemotherapeutics. Consequently, people started to use combination therapy as a more intensified protocol to counteract the aggressiveness of cancer. However, the results are not satisfactory till now and lots of optimizations are needed in order to make sure that synergistic not antagonistic effects are happening.

That is why scientists started to revisit cancer immunotherapy field after long years of its discovery. They are trying to understand more about the manifestations that occur in case of tumor induced immunosuppression. They are rapidly defining new approaches for harnessing the immune system against cancer. Different methodologies are developed in the last ten years, yet optimizations are still in process. The significant hurdle in the field of cancer immunotherapy is the selectivity towards certain immune cell population. In other words, how selective targeting could be achieved with high affinity to the cell of interest. That led to the evolution of cancer nano-immunotherapy where nanoparticles are engineered in a certain manner that can elicit a selective interaction with the target receptor. Many studies have revealed how nanotechnology is a promising tool in harnessing immune system against cancer.

However, targeting as a technique is still paving the way for the optimum particle-cell interaction. In the current study, we are paving the way to target immune cells infiltrating the tumor. The challenge here is that the population of cancer cells themselves are much more than the immune cells. In this study, the response of different immune cell lines towards internalization of different surface charged lipid-based nanoparticles (NPs) was investigated at different time frames. The hypothesis is whether specific immune cell line isolated from melanoma tumor model and lymphoid organ like spleen could be targeted with liposomes having different surface charges, could this be considered a novel approach for targeting immune cells passively depending only on surface charge.

In the first part, three sets of fluorescently labelled nano-liposomes were engineered as a model for different surface charges, the cationic DOTAP NP, anionic DOPG NP and near neutral DOPC NP with mean diameter of 220, 190, 210 nm and Zeta Potential of +36, -48 and -17.4 mV respectively. Physical stability of the NPs was evaluated by monitoring the changes in size and zeta potential. B16 melanoma cancer model was induced subcutaneously in C57BL/6 black mice (10 weeks age), divided into four groups each of five mice. CD11c Dendritic Cells (DCs), CD11b macrophages, CD90.2 T-cells and CD49b Natural Killer (NK) cells were isolated from the tumors and spleens of each group. The three sets of NPs were tested against the isolated cell lines. The cellular uptake (internalization) was assessed by normalizing the fluorescence of the cells against their protein concentration, then all samples were acquired to flow cytometry, and shifts in fluorescence histograms on horizontal axis were monitored against PE channel on the vertical axis. Results reveal the presence of preferential internalization of specific surface charge over others in some cell lines in different time frames. For the first time differences in the internalization pattern are reported in the same immune cell line isolated from two different contexts tumor and spleen. These results might serve as a guideline for a rational design of successful nano-carriers that can maximize the targeting, and hence the therapeutic efficacy towards certain population of immune cells.

In the second part and in the sense of screening the different pathways that contribute to immunosuppression, STAT3 (Signal Transducer and Activator of Transcription 3) pathway is considered one of the promising targets that when inhibited will reverse the immunosuppressed status of DCs. The molecular STAT3 inhibitor is investigated for the first time for its ability to offer superior properties in terms of specificity of STAT3 without affecting the other STATs and eliciting immunomodulatory effect. Pegylated nano-liposomes were synthesized with size of 190 nm loaded with conjugated form of the drug which is drug-cholesterol in order to maximize the loading efficiency reaching 82±4% and physical stability with minimal changes in size and zeta potential. Cryo-TEM revealed the formation of predominant unilamillar structures. The efficacy of conjugated drug-NP was evaluated *in-vitro* on different cells: Bone Marrow derived DCs (BMDCs), DC cell line, B16F10, 4T1 and MDA-MB-231. The BMDCs primary cultures were generated from bone marrow of C57BL/6 mice femurs. The purity of CD11c lineage of BMDCs was assessed by flow cytometry and showed 70-80% purity. In order to mimic the tumor microenvironment surrounding DCs in the tumor i.e. induce immunosuppression and downregulation of DCs surface receptors, high levels of phospho-STAT3 (pSTAT3) were induced via conditioning DCs with different conditioning media of B16, LLC, and 4T1. It has been revealed that B16 conditioning media induced the highest amount of pSTAT3 based on western blot, flow cytometry and cytokine analysis. DCs by then showed downregulation of CD80, CD86 and major histocompatibility complex class II (MHCII). Finally, the drug-NP and free drug (5µmole) were added to the immunosuppressed DCs for 24hrs and maturation status was assessed using flow cytometry. Expression of CD86, MHCII and CD80 were evaluated after gating CD11c double positive population. No significant change was observed in case of CD80. Slight increase was observed in case of CD86. However, surprisingly there was a dramatic increase in MHCII with 3 folds higher expression in case of free drug and 1.3 fold with drug-NP in only 24 hrs, this reflects sustained release of the drug from the NP. These results demonstrate the potential of the STAT3 inhibitor in reversing the immunosuppressed status of DCs in tumor microenvironment and its immunomodulatory role for the first time.

Table of Contents

List of Figures

List of Tables

List of Abbreviations

APC:	Antigen presenting cells
BCA:	Bicinchoninic acid
BCG:	Bacille Calmette–Guérin
Bcl-2:	B-cell lymphoma 2
BSA:	Bovine serum albumin
CD:	Cluster of differentiation
$CD4^+$T cells:	Cluster of differentiation 4 on T helper cells
CTLA4:	Cytotoxic T-lymphocyte-associated protein 4
DCM:	Dichloromethane
DCs:	Dendritic Cells
DC-SIGN:	Dendritic Cell-Specific Intercellular adhesion molecule-3-Grabbing Non-integrin
DCBM:	Dendritic cells derived from bone marrow
DLS:	Dynamic light scattering
DMAP:	Dimethylamino Pyridine
DMEM:	Dulbecco's Modified Eagle Medium
DMF:	Dimethylformamide
DOPC:	Dioleoyl-sn-Glycero-3-Phosphocholine
DOPG:	1,2-dioleoyl-sn-glycero-3-phospho-(1'-rac-glycerol) (sodium salt)
DOTAP:	Dioleoyl-3-Trimethylammonium-Propane
DOTMA:	1,2-di-O-octadecenyl-3-trimethylammonium propane
DPPC:	1,2-dipalmitoyl-sn-glycero-3-phosphocholine
DSPE-PEG:	1,2-distearoyl-sn-glycero-3-phosphoethanolamine-N-[amino(polyethylene glycol)-2000] (ammonium salt)
EDC:	1-Ethyl-3-(3-Dimethylaminopropyl) Carbodiimide
EDTA:	Ethylenediaminetetraacetic acid
EGF:	Epidermal growth factor
FACS:	Fluorescence activated cell sorting
FBS:	Fetal bovine serum
FDA:	Food and drug administration
FITC:	Fluorescein isothiocyanate

FOXP3:	Fork head box P3
GM-CSF:	Granulocyte-macrophage colony-stimulating factor
HBSS:	Hank's Balanced Salt Solution
HEPES:	(4-(2-hydroxyethyl)-1-piperazineethanesulfonic acid
HIV:	Human immunodeficiency virus
HPV:	Human papilloma virus
IFNα:	Interferon-α
IL-:	Interleukin
INF-γ:	Interferon gamma
JAKs:	Janus kinases
LPS:	Lipopolysaccharides
MDSC:	Myeloid Derived Suppressor Cells
MHC:	Major Histocompatibility Complex
MRI:	Magnetic resonance imaging
MTS:	Tetrazolium compound 3-(4,5-dimethylthiazol-2-yl)-5-(3-carboxymethoxyphenyl)-2-(4-sulfophenyl)-2H-tetrazolium
mRNA:	messenger RNA
NP:	Nanoparticle
NMR:	Nuclear magnetic resonance
NK cells:	Natural killer cells
NKT:	Natural killer T-cells
NHS-Fluorescein:	5-(and 6-)carboxyfluorescein, succinimidyl ester
PBS:	Phosphate-buffered saline
PBST:	Phosphate Buffered Saline (PBS) solution with the detergent Tween® 20
PC:	Phosphatidyl choline
PD1:	Programmed cell death protein 1
PD-L1:	programmed death ligand 1
PE:	Phycoerythrin
PEG:	Poly-Ethylene-Glycol
PLGA:	Poly (lactic-co-glycolic acid)
pSTAT3:	Phospho-STAT3
RIPA:	Radioimmunoprecipitation assay buffer
RPMI:	Roswell Park Memorial Institute medium

SAR:	Structure activity relationship
siRNA:	small interfering RNA
STAT3	Signal transducer and activator of transcription
T_{reg}:	Regulatory T-cells
TAC:	Tetrameric Antibody Complexes
TBST:	Tris-Buffered Saline and Tween 20
TCRs:	T-cell receptor
TDF:	Tumor Derived Factors
TGF-β:	Transforming growth factor-beta
TLC:	Thin layer chromatography
TLR:	Toll-like Receptor
TNF:	Tumour Necrosis Factor
VIN:	Vulval intra-epithelial neoplasia
VEGF:	Vascular endothelial growth factor

Chapter one

1. Introduction and scope of the thesis

1.1 Cancer immunotherapy from the very beginning

Cancer immunotherapy is meant to manipulate the immune system against cancer as a different therapeutic strategy in oncology field. In the 19th century, scientists noticed the co-incidence of erysipelas infection along with cancer regression. In 1868 specifically, a German scientist successfully treated neck carcinoma after inoculation of erysipelas extract (cutaneous bacterial infection) intra-tumoral. The exact mechanism by then was still unrevealed, but it was clinically proved that upon pathogen injection in cancer patients the body develops a kind of reaction that helps counteracting the tumor growth leading to its eradication. After world war II, significant immunological discoveries have evolved while studying mice tumor models such as the definition of major histocompatibility complex (MHC), dendritic cells (DCs), etc.[1] In 2001, there was a major breakthrough in the field of cancer immunotherapy, when three teams published in *Nature Genetics* the discovery of FOXP3 which is expressed on $CD4^+$ T cells known as Tregs. After that, Tregs were not only known with their immune self-tolerance, but also immune cancer tolerance.[2]

Our immune system in its simplest form consists of mesh of cells and lymphoid organs, they all together provide our body with protection against infectious microbes and might also help in counteracting developing cancer in a way or another. Anatomically our immune system on the organ level embrace two types of organs; primary lymphoid organs including bone marrow and thymus, secondary lymphoid organs including spleen, lymph nodes, Peyer's patches and mucosal associated lymphoid tissue. On the cellular level, there are two components, innate immunity and adaptive immunity. Innate immunity such as neutrophils, macrophages and natural killer cells are responsible for mediating reactions against infections at entry portals like skin and mucosal surfaces. Adaptive immunity on the other hand needs time to respond to a certain trigger like (T-cells and B-cells), they have the ability to differentiate into memory cells that can act upon certain trigger in case of re-infection. [3,4,5]

Tuning the immune system today is becoming of a great interest due to the prevalent rule of the immunity in case of encountering any disease. Today, one of the most effective therapeutic intervention is vaccination. However, vaccine technology up till now remains abstract in front of some infectious diseases such as malaria, HIV, hepatitis C and tuberculosis. Our context here is concerned with cancer immunotherapy which mainly deals with manipulation and stimulation of the immune system to constrain and hopefully eliminate a specific tumor. Putting in consideration that not usually activated immune system do the job the right way, sometime times it might attack self-healthy tissues in a process known by autoimmunity.

1.2 Paradigm Shift: targeting immune cells instead of cancer cells

Curing cancer was and still is one of the biggest challenges in the human related diseases facing the whole medical community. To date, cancer therapeutics have been mainly depending on a combination strategy, i.e. surgery, radiotherapy and the cytotoxic chemotherapeutics. Not to mention that all the previous strategies are conventional and approved, but rather old. The first known radical breast cancer mastectomy was performed in 1773, and since then, this kind of surgery practice spread worldwide.[6]

After that, radiotherapy has been performed for the first time in 1896.[7] The revolution of cytotoxic chemotherapeutics in the 1930s was in a continuous development, especially during World War II and with using Nitrogen mustard[8]. Later on, a lot of collaborative efforts were able to find the best possible combinations with the best optimized protocols through running thousands of randomized clinical trials on cancer patients. However, the outcome of these combinations was not optimum and did not provide improvement in terms of survival rates in some cancers such as glioblastoma and lung cancers. In addition, these combination therapeutics showed awful side effects because of their high toxicity profiles. That is why the majority of cancer research directions in the last 20 years have been focusing on finding solutions that can provide better selectivity to cancer cells and less toxicity to healthy cells.[9]

The progress that has been made in biochemistry field allowed the proper engineering of small molecules that can specifically bind to over expressed proteins in cancer cells and inhibit certain oncogenic activity. This targeted protein could be membrane receptors, intracytoplasmic or intranuclear.[10] In the best case scenario, this small molecule will be able to inhibit that specific pathway which is responsible for tumor cell proliferation. Actually, this situation represents ideal type of cancer that originates from a single driver mutation and is able to respond to single monotherapy. But actually, most cancers have multiple mutation origin, and therefore, this necessitates the design of multi-targeted therapy.[11]

Apart from therapeutic inventions via vaccination, there is an increasing demand to monitor and measure the status of the immune system which makes the thing more complicated, because of the complex nature of the immune system that is disseminated all over the body making the clinical analysis a major hurdle.[12–14] **Figure 1.2-1** illustrates the important basic immunological discoveries and key clinical trials for cancer immunotherapy since 1898.

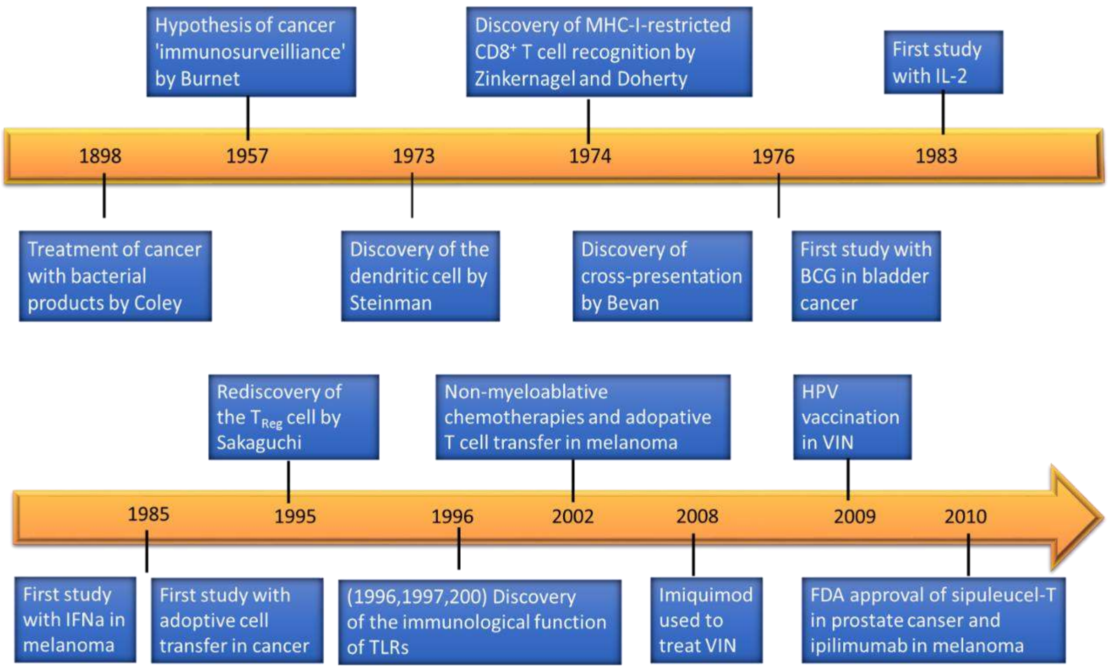

Figure 1.2-1 Cancer immunotherapy timeline (r*eproduced*) [1]

1.3 Tumor microenvironment

The fact that cancer is by nature of extremely heterogeneous origin and coupled with immunosuppression caused by the presence of the tumor itself and its microenvironment represented in the tumor derived factors (TDFs), indicates the extent of hurdles new therapies are facing in the oncology field. The objective of the new therapeutic modalities is to act against cancer taking into account that this will not happen unless the status of the immune system is restored in a away like inhibiting the signals coming from the immunosuppressive microenvironment. This objective actually suggests the concept of having combination of multimodal therapeutics that can target more than one trigger at the same time.

Our immune system play a critical role in any cancer progression in a process called immunoediting which comprises three phases; first is elimination of cancer cells by domination of immunosurveillence, second is the equilibrium where the surviving cancer cells acquire a kind of resistance to elimination and then proceed to the third escape phase where they escape and continue to grow in an uncontrolled manner and eventually get promoted to malignancy.[15,16]

1.4 Immuno-suppression mechanism

Tumors have their own ways to circumvent the immune attack by different immunosuppressive mechanisms, most of them work in parallel to each other. Mediators like prostaglandin E2, adenosine VEGF and TGF-β influence the whole tumor microenvironement scene through direct and indirect immunosuppressive impacts. These derived factors affect the whole immune orchestra through multiple smart ways, they can hinder from DCs maturation and turn them tolerogenic instead of immunogenic thus affecting the efficient priming of T-cells and indirectly inhibiting their penetration capabilities into the tumor bed, or directly inhibiting either by disturbing the effector T-cell activation or promoting the regulatory T-cell expansion. i.e. when tumor cells produce adenosine under hypoxic conditions, they suppress the T-cell activation while enhancing the T_{reg} expansion. VEGF also contributes to the suppression of proper T-cell function and development.[17] Tumor cells can also evade the T-cell priming through the tumor derived factors that can directly contribute to MHC down regulation or through disturbing any other component in the machinery of antigen processing. Not only that, but tumor cells have the ability to develop special surface ligands that can help them induce anergy or exhaustion to the T-cells like PD-L1. The tumor itself comprising the tumor microenvironment is infiltrated by a variety of immunosuppressive subsets of leukocytes in addition to those T_{reg} cells. It has been noticed that their extent of infiltration is always correlated to the poor diagnosis.[18] Myeloid derived suppressor cells (MDSC) also have their impact in tumor immunosuppression. Their mechanism still not well understood, however the suggested explanation is based on their contribution in several mechanisms such as reactive oxidative species, nitric oxide, IL-10, arginase and TGF-β and some reports suggested that MDSC directly induce T_{reg} expansion. Tumor stromal cells as well play an important role as we know in tumor expansion, but in our context here they have immune-modulatory roles, they promote recruitment of immunosuppressive cells that suppress effector T-cells. All the previous indicates that further studies are needed in order to determine which of these mechanisms has the most immunosuppressive effects and which of these mechanisms can barely determine the immune status of the patient.[19]

To date, our understanding to the events that govern the generation and regulation of anti-tumor immunity suggests that the possible routes for therapeutic intervention will be either promoting the efficiency of antigen presentation through antigen presenting cells specially the professional ones like DCs and promoting production of effector T-cells or overcoming to some extent the immunosuppression in the tumor microenvironment. The first stimulus that triggers the whole orchestra begins with capturing a tumor antigen by APC. This captured antigen will be cross presented on MHC and then home to the lymph node. Important thing to mention is the context where the antigen was captured and presented. If the previous incidence happens in the presence of immunogenic maturation stimulus, DCs will have anti-tumor effector response through T-cells, and if such stimulus is not received, DCs will elicit tolerance that leads to effector T-cell anergy and production of regulatory cells. It is important to mention also that the immune response elicited to T-cell depends on the status of DC maturation and mode of interaction of T-cells co-stimulatory moieties with DC surface receptors.[20]

Figure 1.4-1 reveals how immunotherapy catches most of the cancer research groups' attention. In 2014, immunotherapy was surprisingly ranked number one ahead of targeted chemotherapy and gene therapy that have been dominating the cancer research field for decades. This fact reflects how immunotherapy is representing the future trend for cancer therapies. Also, in the same year the percentage of drug approvals in oncology field constituted 22% as shown in **Figure 1.4-2**.

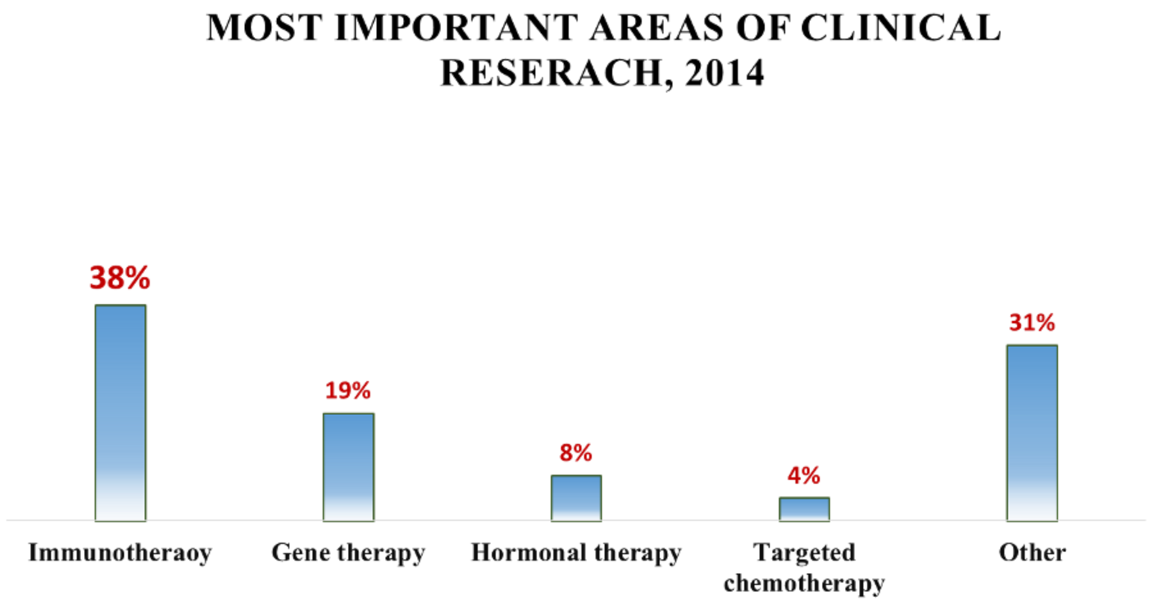

Figure 1.4-1 Rank of different clinical research areas in 2014 (reproduced) [21]

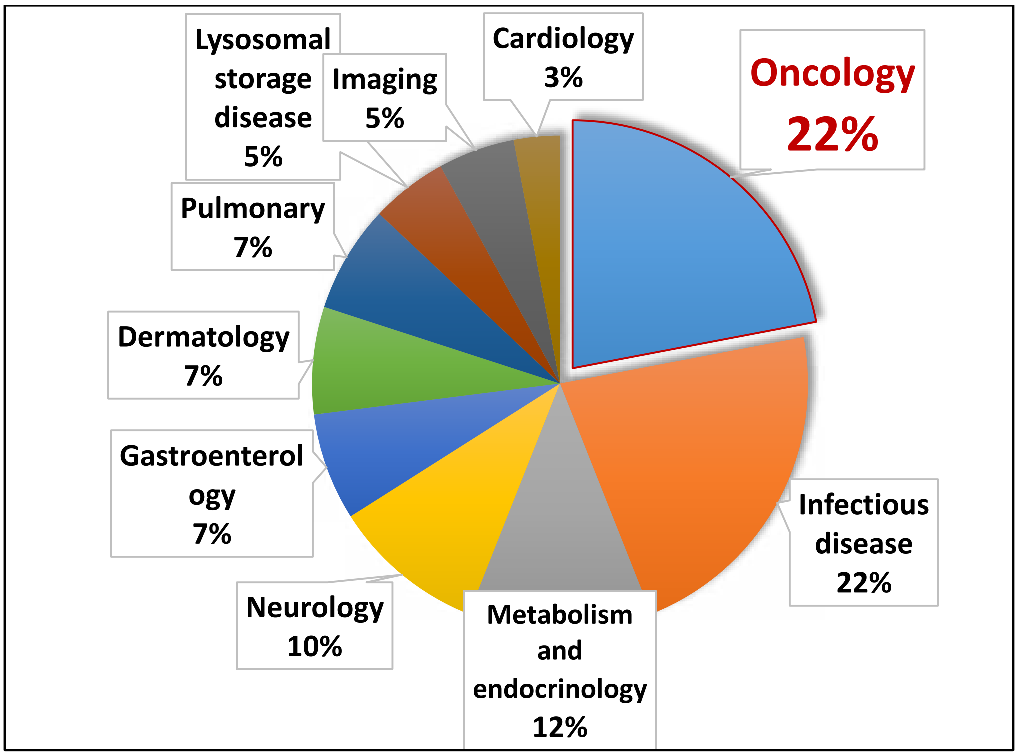

Figure 1.4-2 Drug approval categorized by therapeutic area in 2014 (reproduced) [22]

1.5 Different strategies to harness the immune system against cancer

Over decades great efforts have been made to treat cancer using the immune system, although this dates back over almost a century but the progress is still slow. Recently, many clinical trials showed success in the induction of anti-tumor immune response and this success provided an incremental improvement in the field. Generally, the approaches that can be used for anti-tumor immune response induction are categorized into two main categories; antigen specific and non-antigen specific. Antigen-specific comprises adoptive cell transfer of autologous cancer specific cells and different therapeutic vaccination techniques, whereas non-antigen specific strategies comprise non-specific immune stimulation and immune check point inhibition as well. [23]

1.5.1 A) Non-specific immune stimulation

Immune cell stimulation such as T-cells and APCs like DCs can be achieved in a non-specific way either via their stimulation or via depletion (inhibition) of immunoregulatory cells like T_{reg} cells. Cytokines such as IL-2 and INF_{α} can be used to stimulate effector T-cells. These cytokines are already approved for the treatment of renal carcinoma and melanoma. Complete remission has been observed with IL-2 treatment in selected melanoma patients. However, still there are limitations that hinder from their common use due to the toxicity that is associated with their prolonged use. Other approaches aim at full activation of APC using adjuvants like TLR ligands, for example imiquimod is a TLR7 agonist that has been approved for basal cell carcinoma treatment. For bladder cancer, BCG adjuvant has been considered as a standard therapy and approved for this type of cancer. T_{reg} cells have been inhibited by targeting the IL-2 receptor with daclizumab antibody (anti-CD25) or low dose cyclophosphamide (chemotherapeutic) as shown in **Figure 1.5-1**. It is worth saying that specificity of these approaches still representing major challenges. There are other targeted anti-cancer drugs and chemotherapeutics that have the ability to induce immunogenic apoptosis and cause immune-stimulation or inhibition of suppressive cells or interfering with the inhibitory pathways. Novel treatments that can fully harness the immunogenic properties of the proposed drugs need to be further addressed. [23]

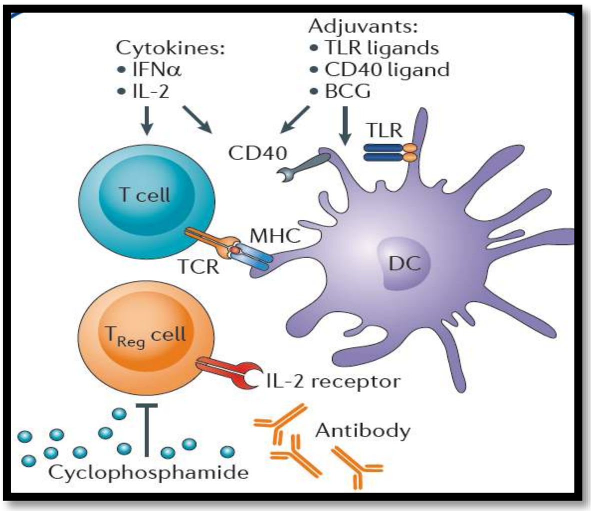

Figure 1.5-1 Examples for the non-specific immune stimulation that might occur with T-cells and APCs. [23]

1.5.2 B) Immune checkpoint blockage

Figure 1.5-2 illustrates the cross talk between the T-cell and APC or tumor cell, specifying the possible receptor interactions that play significant role in down-modulation of T-cell activity through its recognition for the processed antigen on the MHC molecule. By blocking those immune-checkpoints, the overall T-cell status will be either activated or showing better survival. The CTLA4-B7 is one of the major interactions that dictate the pattern of the T-cell response. Also, the PD1-PDL1 interaction represents a prominent role in the effector phase of the T-cell. Ipilimumab which is a CTLA4 antibody has been approved for metastatic melanoma. Immune checkpoint blockage approach is considered one of the less costly and less laborious since it does not depend on the concept of personalized medicine, in other words, it is not tailored according to the patient. This fact gives this approach a privilege than adoptive cell transfer or cellular vaccine, but there will be always a risk from development of autoimmune response. [23]

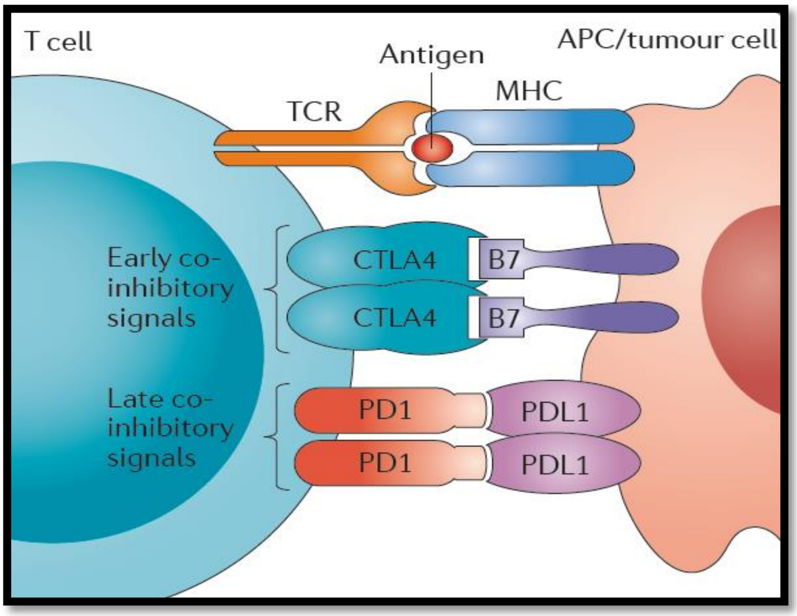

Figure 1.5-2 The interaction between T-cells and APCs specifying the possible receptor interaction[23]

1.5.3 C) Adoptive cell transfer

Effector cells can be isolated from the patient, carefully selected and then expanded while *ex-vivo***.** These expanded cells can be re-injected as such into the patient without being exposed to antigen or get activated in case of APCs. There are two major strategies that are being addressed these days as illustrated in **Figure 1.5-3**. The first is after resection of the tumor and most probably it will be melanoma, T-cells infiltrating the tumor will be isolated and cultured outside, whereas they get expanded *ex-vivo* when they get incubated with IL-2. After getting enough population from the polyclonal T-cells, they are re-injected again to the patient. The second strategy is to isolate T-cells from peripheral blood. Then via genetic engineering, the T-cells will get modulated and become expressing TCRs which are tumor antigen specific followed by re-infusion to the patient. The advantage of this strategy is that good count of T-cells can be isolated and re-infused into the patient, while the potential disadvantage is that the genetically engineered T-cells might express limited antigen specificity repertoire. [23]

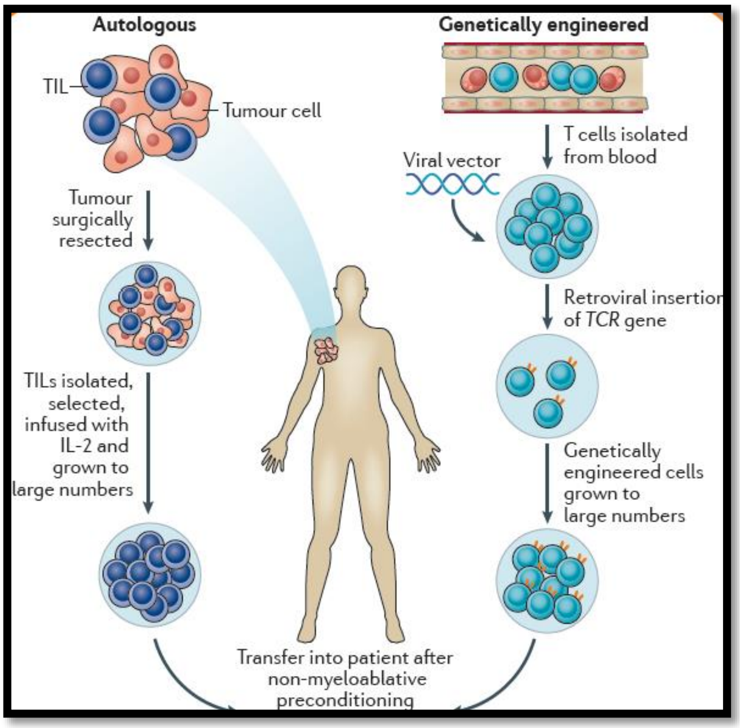

Figure 1.5-3 Major strategies for adoptive cell transfer[23]

1.5.4 D) Different vaccination approaches

The primary aim of designing immunotherapeutic vaccines is to introduce the tumor antigen in an appropriate context that can efficiently prime T-cells. In other words, is to educate the T-cells through proper presentation from the APCs stimuli signals. Tumor antigens can be obtained in form of synthetic peptides or protein or even encoded by virus or plasmid DNA. Also, some idiotype antibodies have been recognized for their tumor specificity and are used as tumor vaccines. Another strategy that can help us circumvent the need to identify the specific antigen for each tumor is direct extraction from the tumor, whereas tumor cells will be isolated and irradiated then re-administrated to the patient. On the other hand, APCs themselves can be isolated from the patient blood stream, expanded, activated by adding adjuvants or cytokines, loaded with antigen then re-administrated to the patient. The previous strategy was used in the development of prostate cancer vaccine sipuleucel-T. It is worth saying that tailor made vaccination approaches are tedious and expensive, in addition they require extremely complex production procedures. These challenges hinder from the progress in this field seeking a complete response[23] as summarized in **Figure 1.5-4.**

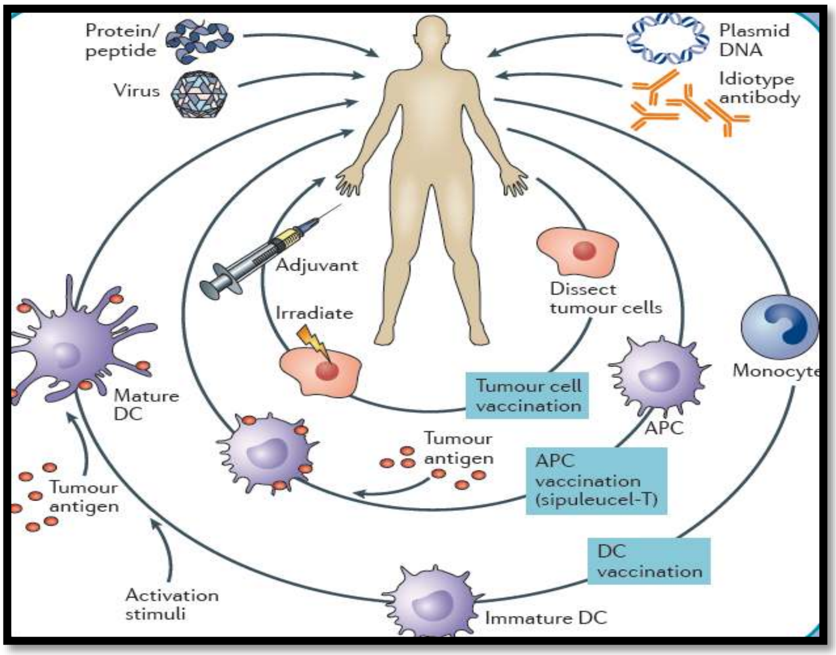

Figure 1.5-4 Possible vaccination strategies[23]

1.6 Nanotechnology and immune system

Today with the privilege of being able to synthesis extremely small particles in the nano-range and make use of nanoscience and nanotechnology, we can reach superior properties than the bulk scale. Nanoparticles have their own physicochemical properties that make them promising in the field of cancer immunotherapy in form of drug delivery, diagnostic and theranostic modalities. Since nanoparticles are of a near range to immune cells diameter, they can interact with the immune cells, bind to the surface and then get internalized. Different nanoparticle characteristics will govern the way of interaction with the immune cells. If a specific immune cell needs to be targeted, the ideal nanoparticle will keep its integrity without being disturbed by the complex biological environment.[24] In the current study we will investigate the possibility of using nano-liposomes to target different immune cells in different contexts.

1.7 Scope of thesis

Lipid based nanoparticles like liposomes have been grabbing attention in the medical field due to their near zero toxicity, biodegradability and their approval by the FDA as drug delivery carrier. A critical field like cancer immunotherapy deals with a very sensitive and delicate type of cells which are immune cells. Consequently, any therapeutic intervention requires high level of integrity and selectivity to avoid any mess that could happen in the immune system. The hypothesis here is whether nanoliposomes with different surface charges can show different internalization pattern with different immune cell lines in different time frames and whether pegylated nanoliposome can play immunomodulatory role in DCs.

Chapter 2 The first part gives a general overview on how and what nanoparticles can alter the immune response. How tailoring nanoparticles affect mode of interaction. Examples on particulate vaccines and background on liposomes. The second part gives an overview on dendritic cells. How cancer can cause suppression of their functional maturation. Current strategies to modulate and reprogram this suppression. A promising drug like LLL12 and its potency to fix the improper signals.

Chapter 3 The first part gives details of experimental methods regarding synthesis, preparation, characterization of fluorescent labeled nano-liposomes and their internalization testing against *ex-vivo* model immune cell lines. The second part gives details of experimental methods regarding synthesis, preparation characterization of LLL12-pegylated liposomes and their testing against bone marrow derived dendritic cells.

Chapter 4 presents the results and discussion concerning the internalization of fluorescent labelled liposomes, their uptake efficiency and flow cytometry analysis.

Chapter 5 presents the results and discussion concerning the ability of LLL12-pegylated liposomes to reprogram the downregulated dendritic cells (proof of concept).

Chapter 6 conclusion and future perspectives.

Chapter two

2. Review of relevant literature

2.1 Micro and nanoparticles for tuning immunity

Our immune system could be the major cause of a disease or the major cause of curing this disease, in the sense of either acting against cancer or acting on a tissue causing destruction in case of autoimmune diseases. That is why there is always a need to suppress or amplify this immune reaction. Recently, great work has been done in creating novel designs in micro and nano-particles that can deliver drugs, imaging agents or have the ability to stimulate immune cells through their chemical and physical properties. This will lead to the development in vaccine delivery, immune response promotion against tumors or suppression in case of autoimmunity.

Synthetic micro and nano-particles play a major role in solving out a lot of hurdles cancer immunotherapy is facing today. Nanoparticle engineering comprehensively addresses delivery systems and adjuvants in vaccines and diagnostic agents to be able to study ongoing immune responses while *ex-vivo* expansions monitoring. By nano-biotechnology a lot of applications could be tailored in the sense of addressing diverse conditions with major implications on the health care sector. [25–27]

2.2 Tailoring particle interactions on a single-cell level

Cells are communicating to each other on a single base level, their membrane characteristics play a major role in their function and dictates how they will react with the surrounding environment. One of the most crucial cell-cell interaction that will eventually trigger an immune response is priming T-cells through one of the major APCs; macrophages or dendritic cells. Nanoparticles can be designed in a way that they can present receptors, functionalized with ligands and co-ligands and be able to mimic the activated APC leading to T-cell efficient priming. What makes nanoparticles of a great interest in this context is that they can entirely replace the APC and be used directly in adoptive therapy and vaccine technology. By modulating nanoparticle properties like size, surface charge, shape and elastic properties, the cellular uptake and degree of internalization will differ and provide optimized drug delivery platform.[28]

The contact between DCs and T-cells is presented in what is known by immunological synapse. The DCs will capture the pathogen fragment and display its peptide (antigen) to the T-cells through establishing the MHC. DCs are professional APCs, they can determine the efficiency of the immune response towards a particular trigger through instructing T-cells, they can instruct T-cells via co-stimulatory ligands, after which soluble cytokines are released at the synaptic cleft.[28,29]

Since that DCs play a major role in the response of the adaptive immunity, scientists thought of designing micro and nano-particles that can entirely mimic the surface of the DCs and have the ability to establish a good contact with T-cells. This method will provide an artificial stimulation for T-cells either *in-vitro* or *in-vivo*. Recently, engineering of multifunctional artificial APC such as biodegradable poly (lactide- *co* -glycolide) (PLGA) conjugated with avidin-palmitate is considered a kind of surface modification that allows the decoration of the particle with stimulatory ligands. It has been noticed that when this type of delivery system is incubated with T-lymphocytes using two different sizes one in micro range and the other in the nano range but having the same co-stimulatory ligands, the larger micro-particle shows better internalization.[30,31]

2.3 Role of particle shape

After the incredible advances in the micro and nanotechnology in the biomedical field especially in immunity modulation, there has been a growing interest to study how and what are the properties that govern the overall efficacy of a delivery, in terms of binding and internalization within immune cells like macrophages. This eventually aims at unrevealing a magic particle that can resist phagocytosis. Engineering particle surface chemistry in a way that can block the protein adsorption and hinder from any subsequent interaction in a process called opsonization requires much effort from the scientists. The most common strategy to counteract this opsonization process is the particle pegylation, anchoring a layer of poly-ethylene-glycol (PEG). PEG creates steric hindrance on the surface of the particle that ends up by resisting protein interaction. Recently, it has become obvious that not only the surface chemistry dictates how the particles will interact with the phagocytes, but also geometrical shape and mechanical properties show a significant role in deciding the fate of the particle.[32,33]

It has been shown that the isotropic particles show enhanced internalization than the anisotropic particles that was reasoned by the incomplete actin formation along the length of the anisotropic geometry. But, there is always an interplay between cellular response and particle geometry, for example HeLa cells showed much more efficient internalization with rod-like high aspect ratio shapes. These contrasting differences arise from different endocytic/phagocytic pathways, meaning that there is a preferential internalization pathway than another according to the cell type. Uncoated silica particles with different shapes (disc, sphere, and cylinder) but almost same volume revealed that disc shape showed higher accumulation in lungs than liver compared to spheres.[34]

In case of poly (maleic anhydride) / lipid particles, higher uptake of irregular shaped nanoparticles 350 nm took place in spleen more than spherical shapes of similar size and composition. To sum up, these studies confirm that shape is an important factor, and a good attention to the design should be taken in consideration, especially if we need to target or avoid APCs in different organs.[35]

2.4 Micro- and nano-particle vaccine

Modern vaccine technology put a lot of effort to design a purified antigenic subunit that can provoke certain immune response and circumvent the dangers associated with the live attenuated vaccines. However, the limitation of purified antigenic subunit lie in the weak immune-response they can provoke, which requires the addition of adjuvants. The primary target of vaccine is APC since they have an efficient ability to initiate and sustain cellular and humoral immune response. DCs in particular are recognized by their strong ability in priming T-cells.[36,37] DCs can process antigen through MHC molecules in the cross-presentation process. Vaccines can be injected intradermaly or subcutaneously, drain through lymph nodes to DCs or get internalized directly at the injection site. Once the antigen get internalized by APCs like macrophages or DCs, it will be processed on the MHC molecule. The features of the nanoparticulate antigen should be designed such that can rapidly release antigen onto the MHC once it get internalized before being digested by the acidic endosomal media, as there is a narrow time frame between both actions.

2.5 Liposomes

Lipid-based nanoparticles like liposomes constitutes a membrane of self-assembled lipid bilayer, their sizes range between 90 to 200 nm. Liposomes are mainly formed of phospholipids and cholesterol that surround the aqueous portion, **Figure 2.5-1**. Phospholipids are characterized by their hydrophilic heads and hydrophobic tails. That is why this type of nanoparticles provide flexible platform for almost all kinds of molecules, since they have a unique nature that allows them to either encapsulate hydrophilic molecule within the inside compartment or entrap hydrophobic molecule in the outer compartment within the hydrophobic bilayer.[38]

These superior characteristics of liposomes rendered them a great potential for a successful drug delivery platform, based on the fact that they elicit slow or sustained release kinetics that is reflected on the therapeutic aspect in the sense of improved accumulation of the entrapped compound. On the other hand, they narrow the toxicity profile of the entrapped compound since they limit and control the biodistribution pattern.[39] Taking into consideration that liposomes have the basic requirement for a nanoparticle to be considered from the first nanoparticles that are FDA approved, as they are biocompatible, biodegradable, and owing to their lipid nature they have the ability to cross the membranes. Liposomes have been recommended and used as a safe delivery platform for vaccines, chemotherapeutic drugs, and gene therapy.[40] While it is important to mention that one of the major challenges of the conventional liposomes is their short circulation time. That is why long circulating liposomes or stealth liposomes have been established to circumvent this problem. Those modified liposomes are designed in such a way they have steric effect that contributes to prolonged half life time.

Since liposomes are FDA approved and they have proven their superior characteristics, they reached advanced clinical trials. Examples for their use as anti-cancer platform are the liposomal doxorubicin, cisplatin and cytarabin. Liposomal doxorubicin reduced to a great extent the side effects that were usually associated with this drug like renal damage and heart failure. Liposomes also act as a good candidate for entrapping oligonucleotides such as siRNA.

Cancer vaccine targeting DCs and DNA complexes has been reported for its formulation based on liposome with great anti-tumor immunity. In addition, liposomes are now studied as a carrier for contrast agents, they offer a safe biodegradable platform for *in-vivo* multi-color MRI for mapping the lymph node.[41]

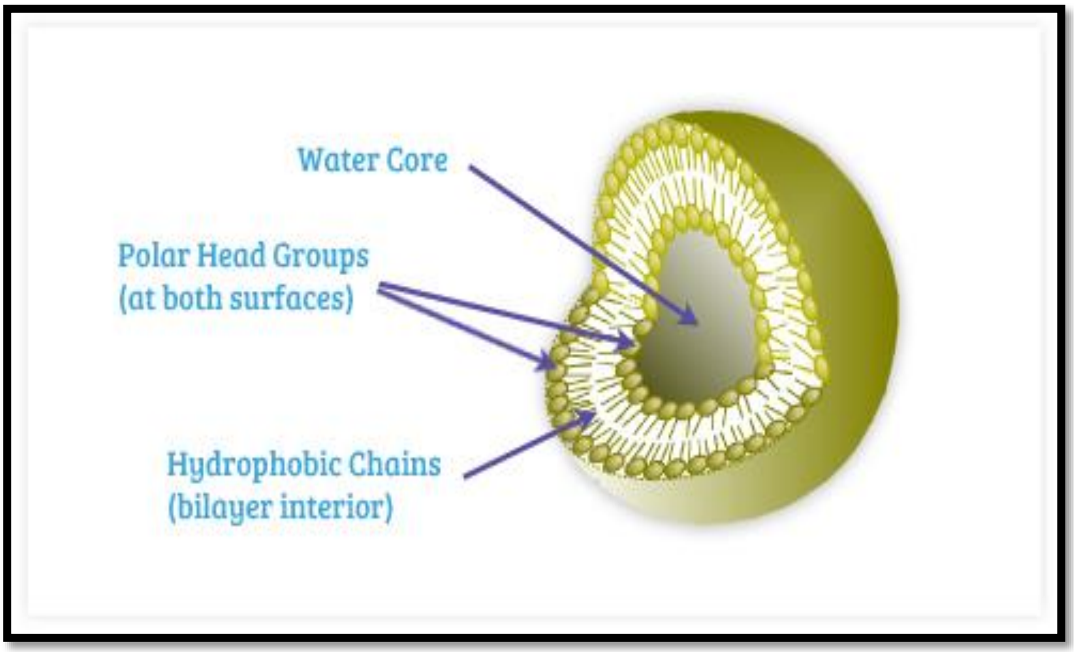

Figure 2.5-1 Liposome structure[42]

2.6 Effect of surface charge on cellular uptake

Engineering a nanoparticle that has targeting ability can be achieved by two ways either active targeting, where the nanoparticle is functionalized by a certain ligand that has binding affinity to the receptor of interest. Or by making use of the natural properties of the nanoparticle and utilize the passive targeting strategy, where we can play with the particle physicochemical properties in order to target certain population than other, **Figure 2.6-1**. Physicochemical properties like size, shape and surface charge directly affect the uptake behavior that differs from one type of cell to another one. Particulate system with different surface charge will elicit different pharmacokinetic patterns. A step before internalization should first takes place which is binding or attachment. The way and degree of attachment vary according to the surface charge. Consequently, playing with particle surface charge could control binding to specific tissue or cell.[43] Liposomes can be categorized according to their charge into three groups: cationic, which possess cationic group like amino group like DOTMA and DOTAP liposomes. They showed superior transfection ability in both *in-vitro* and *in-vivo* experiments.

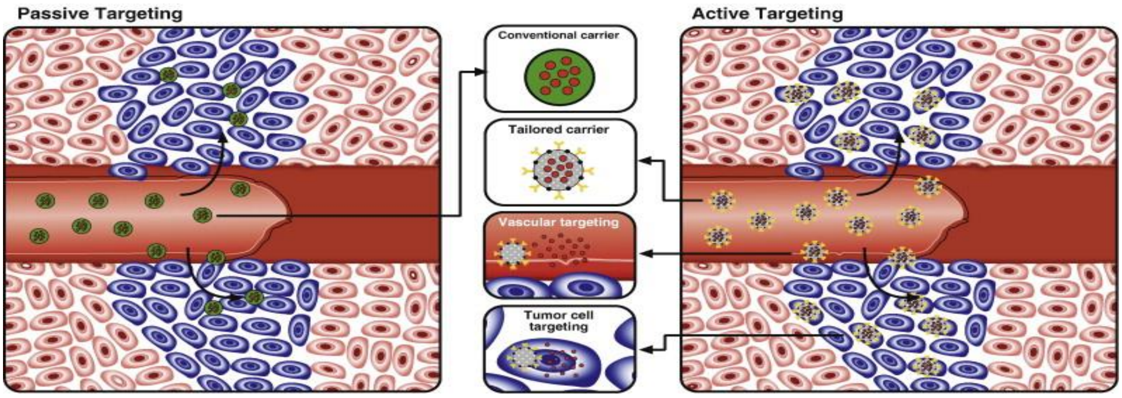

Figure 2.6-1 illustrates the targeting approaches: Passive and Active[44]

Anionic, which possess anion group like DOPG and neutral or zwitterionic that has both charges like DOPC and DPPC, structures are shown in **Figure 2.6-2**. Here we are trying to test whether there will be preferential internalization of certain surface charge within certain immune cell line in *ex-vivo* cell lines.

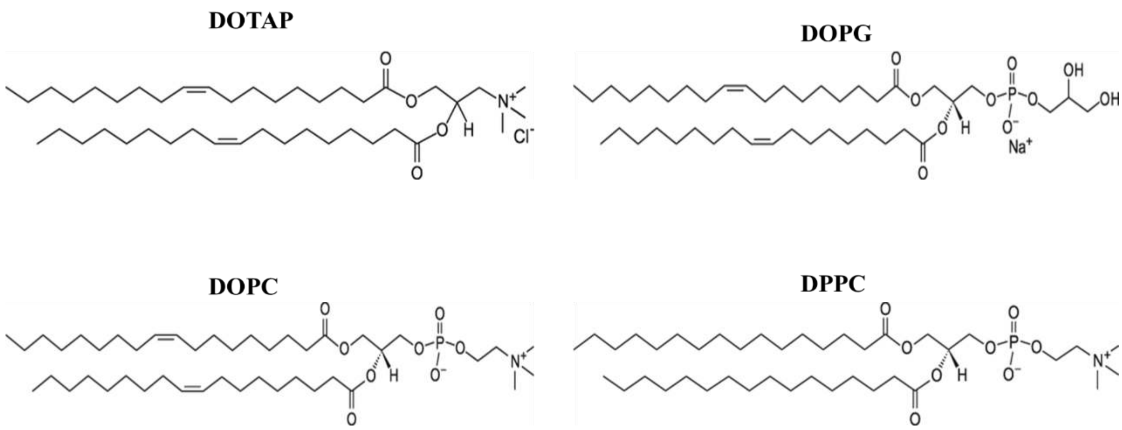

Figure 2.6-2 Structures of different lipids[45]

2.7 Dendritic cells and STAT3

In order to have and maintain proper and adequate immune response, there should be healthy and functioning bone marrow derived APCs. One of the characteristics of cancer is the abnormality that happens in the myeloid lineage. This abnormality is symbolized in two major manifestations; accumulation of the immature myeloid cells and most importantly is the defective differentiation and maturation of the most professional APCs, dendritic cells. Presence of malfunctioned DCs with high numbers impair from the proper antitumor immune response.[46,47] In other words, decreased numbers of mature DCs and accumulation of immunosuppressive myeloid cells contribute to the development of immune tolerance. All these events help in the development of tumor escape from the control of the immune system. It is well known that the factors that mediate the abnormal differentiation of the myeloid lineage is the infiltration of the tumor derived factors such as; IL-6, IL-10, TGF-β, VEGF, etc.[48,49]

A major challenge that cancer immunology is trying to understand is how tumor cells have the ability to elicit a global shutdown for the immune stimulating mediators or signals in the sense of cytokine or stimulatory molecules in the tumor microenvironment.[50,51] The suggested scenario is that these elicited effects take place locally because generally cancer patients do not experience systematic immunosuppression except those of late stage. The question now is what are the mechanisms that make the tumor cells produce immunosuppressive factors that later on render tolerogenic DCs ?[52,53] what makes cancer cells dominate the immune cells and take the control over them in the sense of angiogenesis, survival and invasion? If we managed to understand the signaling pathways for tumor microenvironment regulation, we will be able to identify targets for cancer immunotherapy.[54] Recently, scientists identified an important signaling pathway that acts as a mediator in tumor immunosuppression which is STAT3; signal transducer and activator of transcription 3.[55,56] STAT3 is considered a negative regulator to T helper cells and potent activator for immunosuppressive genes. STAT3 mediates the crosstalk between tumor cells and immune cells, this happens upon its activation via tumor derived factors such as IL-6, IL-10, etc., these events lead eventually to immunosuppression. Owing to all previous reasons, STAT3 is considered a potential target for cancer immunotherapy.[57,58]

2.8 STAT3 biology

In normal state, STAT3 pathway regulate gene expression of proliferation, survival, migration and invasion in addition to angiogenesis. STAT3 plays role in embryo development at his early stages. Normally, STAT3 is under controlled regulation so that signals are only within the physiological response in benign cells.[59,60] Activation of STAT is associated with Janus kinases (JAKs). JAKs are phosphorylated by cytokines or signals such as TNF, IL-6, EGF, TGF-β,etc,[61,62]consequently the phosphorylated JAKs initiate cascade of multiple phosphorylations to the tyrosine residue of the cytokine receptor within the cytoplasmic domain.[63,64] Unphosphorylated monomeric STAT get recruited to the activated sites through interaction between the phosphotyrosine domains at the activated receptors and the SH2 domain of STAT. Consequently, JAKs phosphorylate the tyrosine of STAT domain at C- terminal. Finally, STAT gets separated from the receptor and undergoes dimerization to other STAT monomers then translocate to the nucleus and binds to the DNA in the promoter of the target genes.[65,66] Pathway is shown in **Figure 2.8-1**.

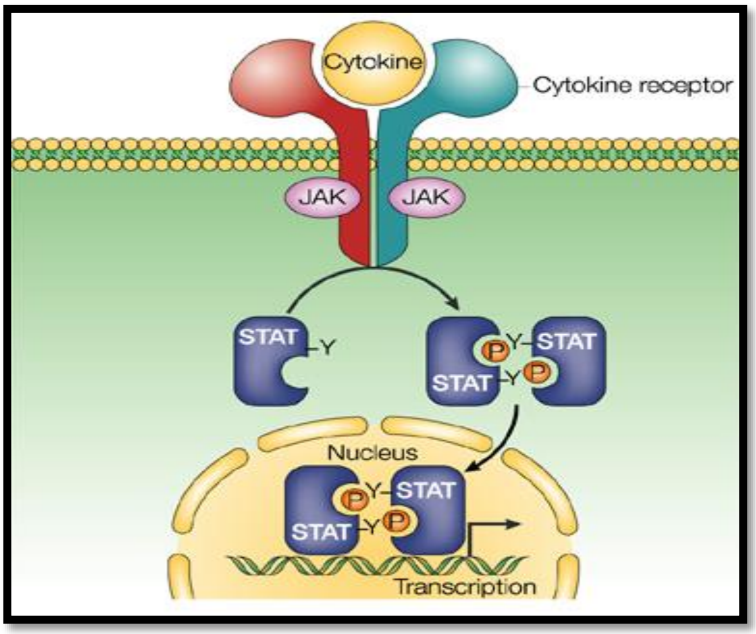

Figure 2.8-1 JAK-STAT pathway[67]

2.9 Suppression of DC functional maturation

It is well established that DCs are professional in inducing anti-tumor immune response, on the other hand when they experience stress from the tumor microenvironment, they fail to reach the maturation status and remain immature, showing insufficient expression levels of MHC class II, CD80 and CD86.[52,53,68] These manifestations lead to failure of DCs to prime T cells, not only that but they can be involved in immune tolerance. Previous studies showed that STAT3 activity in tumor cells suppress DC maturation by affecting the expression of MHC class II. IL-6, IL-10, IL-12 and VEGF mediated the STAT3 inhibitory action on DC maturation. Studies revealed that disrupting signaling of STAT3 leads to activation of T-cells.[69]

2.10 STAT3 signaling and immune cells

Scientists investigated whether STAT3 signaling is critical to induce inhibitory actions on DC maturation. They reported that blocking STAT3 signaling either by interfering with the STAT3 gene itself or by using STAT3 phosphorylation inhibitors, abolished the inhibitory effects on DC functional maturation and showed decreased numbers of immature CD11c-CD86 and CD11c-CD80.[69] In agreement with the previous studies, it has been reported that when tumor derived factors induce STAT3 signaling in immature myeloid cells, they prevent from their differentiation to mature DCs.[70] Accumulation of immunosuppressive population of myeloid cells is partially due to STAT3 activation. It has been shown also that IL-6 mediates inhibitory effect on DC maturation through being STAT3 dependent.[71]

2.11 Inhibition of STAT3 in the preclinical trials in different tumors

As mentioned before STAT3 has physiological functions that regulate biological processes, and high expression of phosphorylated STAT3 (pSTAT3) than normal contributes to malignant manifestations and immunosuppression. STAT3 targeting is becoming of a great interest and is representing a novel approach to prevent or treat cancer. To target STAT3, there are several strategies that tackle the signaling pathway; a) Controlling the upstream negative or positive regulators, either by enhancing the negative STAT3 regulators or by inhibiting the positive ones. b) Utilizing RNA interference, which is an approach that affects translation of STAT3 mRNA using siRNA or anti-sense STAT3 oligonucleotides. C) Direct targeting of STAT3 protein and this approach is considered efficient since it directly inhibits STAT3 protein. STAT3 has three domains: SH2, DNA-binding and NH2-terminal. These domains are considered potential targets for development of STAT3 inhibitor. Numerous novel molecular inhibitors that target SH2 domain were selected and designed via structured based virtual screening. These inhibitors also showed activity against STAT3 dimerization and DNA-binding in cell lines and animal models.[72]

In general, targeting STAT3 with small molecule inhibitors is the most promising approach for more than one reason. First, controlling the upstream regulators might not be able to block the STAT3 pathway due to the presence of multiple cross talkings and single targeted therapy might not be efficient. Second, RNA targeting still facing the problem of stable delivery issues, cell permeability and solubility of those oligonucleotides, thus clinical trials are still limited. Third, the preclinical data reveals that small molecule inhibitors are showing significant growth inhibition in cancer cells *in-vitro* and in animal models.[73]

2.12 Novel small molecule, LLL12

LLL12 is a small molecule that targets STAT3. It was found that LLL12 inhibits STAT3 phosphorylation at the tyrosine site. It has been tested with different cell lines; pancreatic, breast, and glioblastoma cells expressing high levels of pSTAT3. Studies showed that LLL12 as well has the ability to inhibit pSTAT3 induced by IL-6. The mechanism by which LLL12 inhibits STAT3 phosphorylation is by inhibition of DNA binding activity. Down regulation of downstream targets such as Bcl-2, Cyclin and survivin was also observed with LLL12.[74] LLL12 showed higher potency than previously reported STAT3 inhibitors like WP1066 and S3I-201. LLL12 showed selectivity to STAT3 than STAT1 and STAT5 by specific inhibition of STAT3 DNA binding activity. This reflects how LLL12 is potent and specific to STAT3 owing to its interaction with pTyr705 site of STAT3, consequently preventing STAT3 dimerization, translocation into the nucleus and blocking any possibility for STAT3 to be recruited to the target receptors.[75]

LLL12 has been recently identified in 2010 after making comparative screening for the most potent STAT3 inhibitors. It has been revealed that anthraquinones and naphthoquinones show preferential targeting activity against STAT3, among all anthraquinones based on SAR studies LLL12 showed a potent activity owing to its sulfonamide group at position 1 as shown in **Figure 2.12-1**.[76] Previously, curcumin family showed good activity against STAT3, however this family showed off-target events together with STAT3 inhibition. On the other hand, LLL12 which is not a curcumin derivative showed selectivity towards STAT3.[77]

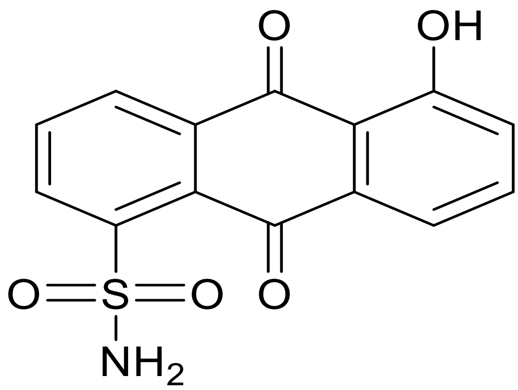

Figure 2.12-1 LLL12 structure

So far LLL12 is considered a promising agent for targeting cancer that express high levels of STAT3. Here we propose LLL12 to target immunosuppressed cells and helps restore the maturation inhibition that caused by high level of STAT3 expression in dendritic cells. To date, this is the first time LLL12 is used in the context of cancer immunotherapy.

Chapter three

3. Materials and Methods

3.1 First part: Synthesis of fluorescent labelled liposomes and testing them against *ex-vivo* cell lines

3.1.1 Materials

The Reactions were done under inert procedures. Cholesterol, Dichloromethane (DCM), unhydrous DCM, pyridine, methanol ethylenediamine, L-α-phosphatidylcholine (PC) were bought from SigmaAldrich (MA, USA). NHS-Fluorescein, Thermo Scientific (MA, USA). 1,2-dioleoyl-3-trimethylammonium-propane [DOTAP], 1,2-dioleoyl-sn-glycero-3-phospho-(1'-rac-glycerol) [DOPG], 1,2-dioleoyl-*sn*-glycero-3-phosphocholine [DOPC], 1,2-dipalmitoyl-*sn*-glycero-3-phosphocholine [DPPC], 1,2-Distearoyl-sn-Glycero-3-Phosphoethanolamine-N-[Amino(Polythylene Glycol)2000] (DSPE-PEG-Amino), 1,2-Distearoyl-sn-Glycero-3-Phosphoethanolamine-N- [methoxy (Polythylene Glycol)2000] (DSPE-PEG-methoxy), 1,2-Distearoyl-sn-Glycero-3-Phosphoethanolamine-N- [carboxy (Polythylene Glycol)2000] (DSPE-PEG-carboxy), Extruder kit containing Whatman Nucleopore Membrane 0.2 µm, filter supports and 1.0 mL syringes were bought from Avanti Polar Lipids (MA, USA). Anhydrous dimethylformamide (DMF) was bought from Acros Organics. Thin layer chromatography (TLC) was performed using precoated aluminum with silica gel from Fluka Analytical (MA, USA). Spots on the TLC plates were visualized using alkanine permanganate. 1H NMR (300 MHz) spectrum was obtained on a Varian Mercury 300 spectrophotometer. The chemical shifts are expressed in parts per million (ppm) using suitable deuterated NMR solvents with reference to TMS at 0 ppm. Column chromatography was conducted using silica gel (230-400 mesh) from Qualigens.

3.1.2 Synthesis of Cholesterol-fluorescein conjugate

Cholesterol-fluorescein conjugate was synthesized by reacting NHS-Fluorescein with Cholesterol-ethylene diamine in 1:1 molar ratio for 24 hr at room temperature in dichloromethane (1 ml) and pyridine (0.2 ml). The product was purified by column chromatography.

3.1.3 Preparation of fluorescent nanoliposomes

1- Organic solvent evaporation and lipid film formation

Initial trials started with PC, cholesterol and DSPE-PEG (amino or carboxy or methoxy) with different ratios in order to reach the best preparation in terms of stability, loading efficiency, size homogeneity and surface charge. The final optimized formulas were prepared as follows, in a round bottom flask, 3 different formulations have been prepared and dissolved in 3 ml anhydrous DCM; A) DOTAP:DPPC: Cholesterol-fluorescein: Cholesterol(for DOTAP liposomes), B) DOPG:DPPC: Cholesterol-fluorescein: Cholesterol (for DOPG liposomes) with mol % (20:60:5:15) respectively for both and C) DOPC:DPPC: Cholesterol-fluorescein: Cholesterol (for DOPC liposomes) with mol % (70:10:5:15) respectively. After that, the flask was mounted on the rotavap at slow speed under vacuum at room temperature for about an hour.

2- Lipid film hydration

At this step vacuum is completely released and 3 ml of double distilled H_2O were added to the flask. After that, the temperature of the water bath was kept from 50 °C to 60 °C. Rotation was maintained for another hour allowing the hydration of the lipid film layer.

3- Extrusion

For obtaining liposomes at size ranges between 150 to 200 nm, the whole suspension was forced through the polycarbonate Whatman membrane (0.2 or 0.4 µm) for about 25 times. Extrusion was done here at 60 °C **Figure 3.1-1**.

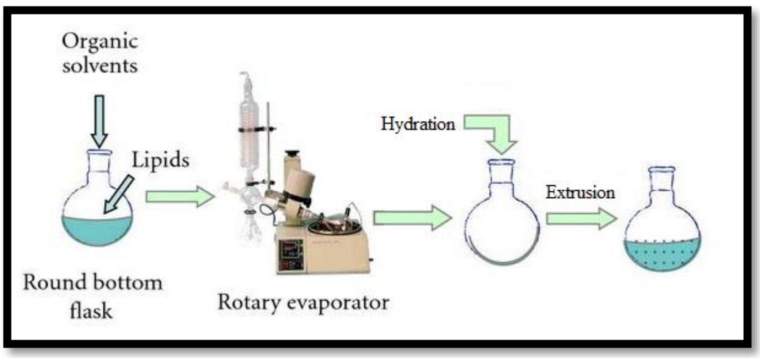

Figure 3.1-1 Conventional liposome preparation method (lipid film hydration)

3.1.4 Characterization and stability of the prepared nanoliposomes

The mean particle sizes of the 3 sets of nanoparticles were measured by Dynamic Light Scattering method using Zetasizer Nano ZS90, Malvern (Worcestershire, UK). 10µL of nanoparticles solution was diluted to 1ml using DI water and 3 sets of 10 measurements each were performed at 90 degree scattering angle to get the average particle size. The zeta potential was measured and the nanoparticles were diluted in water. The physical stability of the nanoparticles was evaluated by measuring changes in mean particle size and zeta potential during storage condition at 4ºC.

3.1.5 *Ex-vivo* studies on B16/F10 melanoma model:

B16/F10 cells (ATCC) were cultured in DMEM, life technologies (CA, USA) and suspended at 2 x10^6 cells per 0.5 ml in PBS (kept on ice) directly before injection. The right hind flanks of 20 C57BL/6 black mice (10 weeks age) were shaved before the subcutaneous injection of 100 µl of the cellular suspension. Mice were euthanized with carbon dioxide when any one tumor dimension was ∼100 mm3, when exhibiting any sign of sickness, or at 10 days post-treatment for FACS analyses studies. The mice were divided into 4 groups, each 5 mice were assigned to certain immune cell line **Figure 3.1-2**.

3.1.5.1 Isolation of tumor infiltrating immune cells

CD11c DCs, CD11b macrophages, CD90.2 T cells and CD49b NK cells were isolated from B16 melanomas according to Stem Cell Technologies. Subcutaneous tumors were removed from all mice, minced into tiny sections of approximately 3-4 mm then placed in 10 mL of serum free RPMI media, life technologies (CA, USA) containing 175 U/mL of Collagenase IA, Sigma (MA, USA). The tissue was manually homogenized for several times and the tissue suspension was kept for 1 hr at 37ºC, passed through a 70-µm tissue filter and cells were washed twice in serum free RPMI media and twice with PBS. The pellet was re-suspended in the recommended media

(PBS + 2% FBS with 1 mM EDTA) according to StemCell Technologies positive selection kit protocol for each cell line. The purity was assessed by FACS and reached to 85- 95% purity **Figure 3.1-3**.

Concept behind labelling of mouse cells: Initially cells of interest are labelled with PE-labeling agent. Followed by labeling with dextran-coated magnetic nanoparticles via Tetrameric Antibody Complexes. Magnetically labeled cells are then separated from unlabeled cells using the EasySep magnet **Figure 3.1-4**.

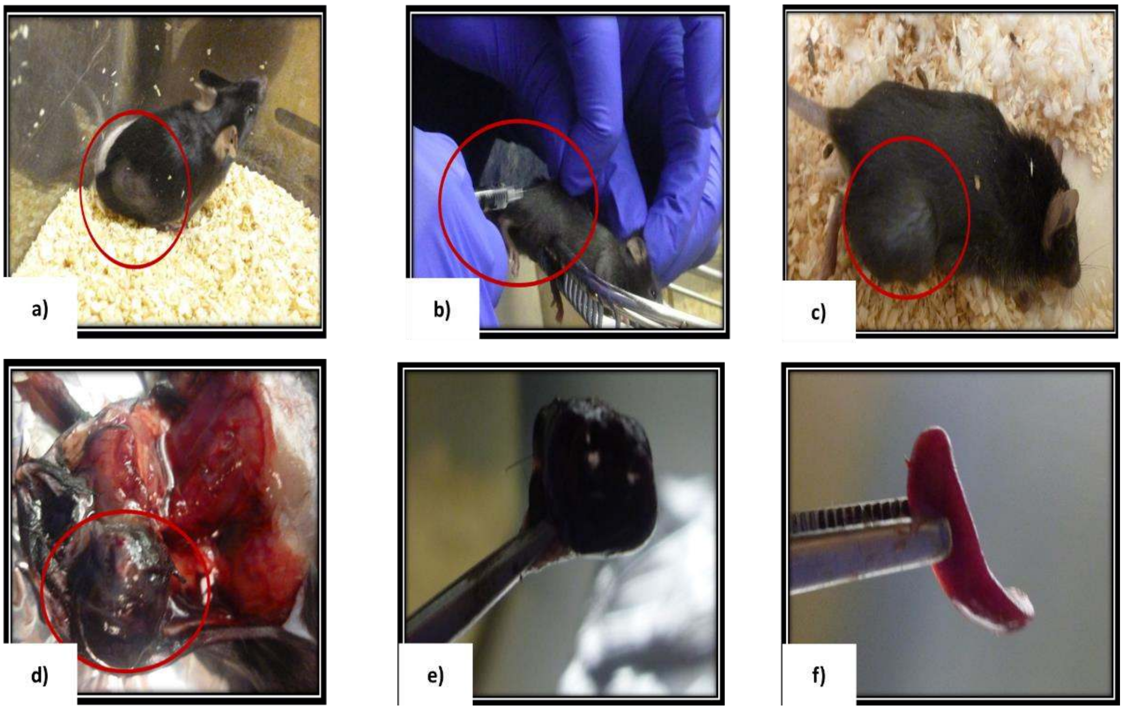

Figure 3.1-2 *Ex-vivo* studies on B16/F10 melanoma model. a) Shaving of the right hind flank. b) Subcutaneous injection of B16/F10 melanoma cells. c) Monitoring the tumor growth on daily basis. d-e) Resection of the subcutaneous tumor. f)Dissection of spleen.

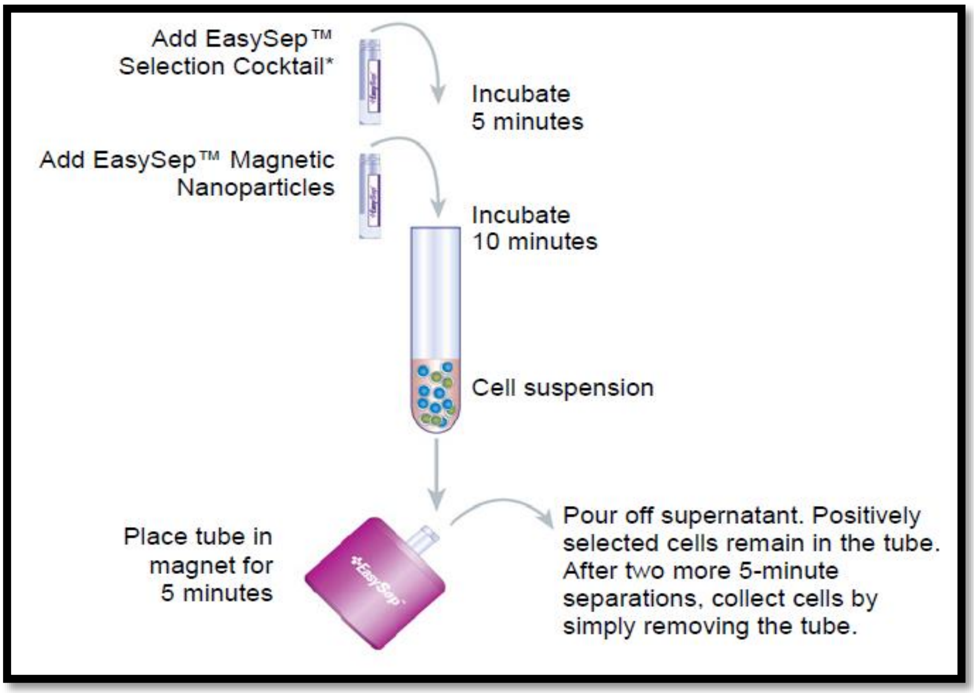

Figure 3.1-3 Steps for positive selection of labeled cells with EasySep® Mouse PE-labeling reagent. Same procedure for CD11c, CD11b, CD90.2 and CD49 cells, the only variable is the incubation times[78]

-

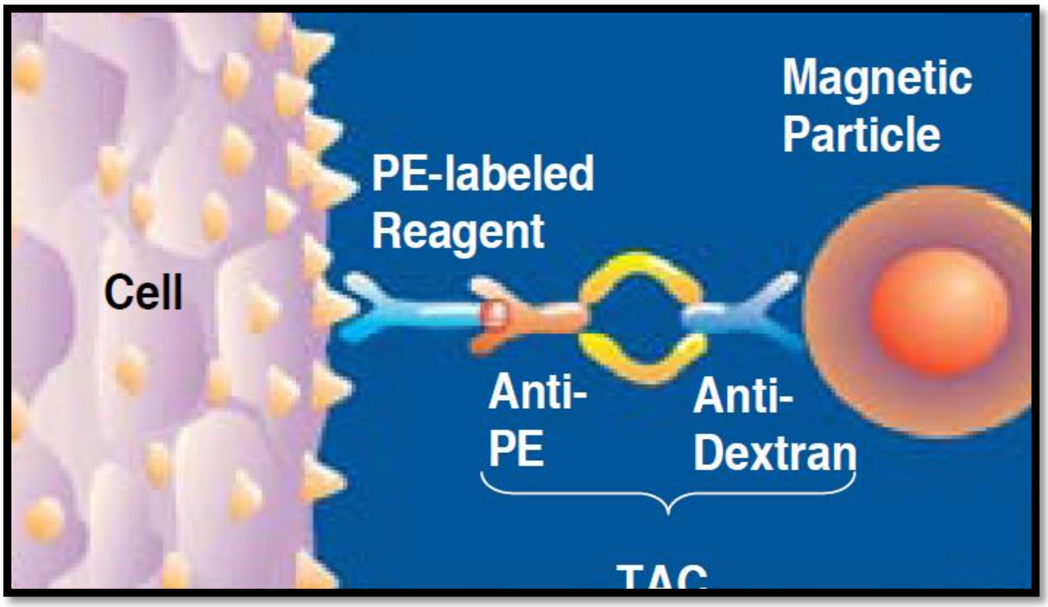

Figure 3.1-4 Scheme for magnetic labeling of cells via EasySep technique[79]

3.1.5.2 Isolation of spleen infiltrating immune cells

Spleens were dissected from the same 20 C57BL/6 black mice at the same setting of tumor resection. **For preparation of single cell suspension of CD11c DCs** according to Stem Cell Technologies protocol**,** spleen dissociation media (SDM) was used to get the optimum recovery of DCs from mouse spleen. The media contained DNase, Collagenase IV and Fetal bovine serum (FBS). Procedure as follows: In a 60 mm Treated Tissue Culture Dish, the freshly isolated spleens are minced using dissection scissors and forceps into a homogeneous paste. Contents of the SDM were poured into the dish and mixed using pipette. All spleen fragments were returned back to the original SDM tube, Incubated horizontally on rocking platform for 30 minutes at room temperature. Spleen fragments were dissociated by gentle passing through 16 gauge needle. The entire suspension then was poured through 70 µM mesh filter into a 50 mL conical tube. The empty SDM tube and mesh filter were rinsed with an additional recommended medium and added to 50 mL conical tube, centrifuged at 1000 rpm for 10 minutes. Supernatant was discarded and cells were resuspended in appropriate amount of recommended medium. Then the previous mentioned position isolation procedure was used.[78]

For preparation of single cell suspension of CD11b macrophages, CD90.2 T-cell and NK cells: Spleen was dissociated in the recommended medium. Remaining debris was removed by passing cell suspension through 70 µm strainer into a 50 mL tube, centrifuged and supernatant was discarded then pellet was re-suspended in the recommended media. After that, CD11b macrophages and CD90.2 T-cells were isolated by the previous mentioned positive isolation procedure, while NK cells were isolated by negative selection technique according to Stem Cell Technologies **Figure 3.1-5**. The unwanted cells this time were specifically labeled with dextran-coated magnetic particles.

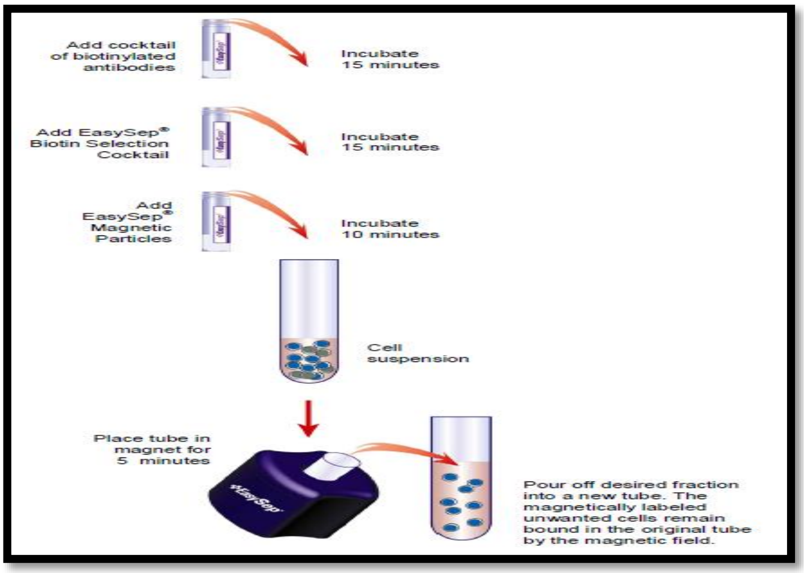

Figure 3.1-5 Negative Selection procedure for Mouse NK Cell[80]

After isolation of the target cells from the melanoma tumor and spleen, absolute cell numbers were assessed by direct counting on a Coulter cell counter then 10^^{5} cells were cultured in 24-well plates in a complete RPMI media (RPMI 1640, 10% FBS, 1mM sodium pyruvate, 0.05mM 2-mercaptoethanol, 100 µg/ml streptomycin and 100 µg/ml penicillin) at 37ºC in a 5% CO_2 humidified atmosphere for 24 hours.

3.1.6 Cellular uptake of nanoparticles by spectroflourometer and flow cytometry

The three types of nanoparticles (DOTAP, DOPG and DOPC) were added at equal concentrations 158µg/ml to the four immune cell lines in the 24-well plates and kept at 37ºC in a 5% CO_2 humidified atmosphere for 4 and 18 hrs. The treatment media were discarded, and the cells were then gently washed with PBS twice to remove unbound nanoparticles. A standard curve of Cholesterol-fluorescein was generated by measuring the fluorescence at 520 nm using spectroflourometer. A known concentration of nanoparticle was dissolved in DMF and the absorbance value at 520 nm was used to calculate the loading from standard curve. Loading efficiency was calculated as incorporated dye concentration / initial dye concentration x 100 and then normalized with amount of protein per cells measured by BCA assay. The uptake was expressed as the fluorescence associated with the cells (concentration of Cholesterol-fluorescein in µg) measured by spectrofluorometer (RF-5301PC, SHIMADZU) versus the protein concentration of these cells (concentration of protein in µg). Cells were then acquired to flow cytometry (accuri C6), gating was done based on CD11c-PE, CD11b-PE, NK-PE and CD90.2-PE expressions then florescence intensity was measured based on this gate. Mean fluorescence intensity was measured as well.

3.1.7 Statistical analysis

Statistical analysis was performed using one way and two way ANOVA. Differences were judged to be significant at $p < 0.05$.

3.2 Second part: Synthesis of pegylated LLL12 liposomes and testing against dendritic cells

3.2.1 Materials

All reactions were done under inert procedures. Dichloromethane (DCM), anhydrous DCM, Methanol, Cholesterol, Dimethylamino Pyridine (DMAP), Succinic Anhydride, Sodium Sulfate, Pyridine, 1-Ethyl-3-(3-dimethylaminopropyl)carbodiimide (EDC), L-α-phosphatidylcholine. LLL12 was purchased from Calbiochem. 1,2-Distearoyl-sn-Glycero-3-Phosphoethanolamine-N-[Amino(Polythylene Glycol)2000], PC and the Extruder kit were bought from Avanti Polar Lipids. Thin layer chromatography was performed using silica gel (Fluka Analytical). Spots on the TLC plates were visualized under UV light, and/or by treatment with alkaline permanganate solution followed by heating. MTS reagent was supplied by Promega. Column chromatography was conducted using silica gel (230-400 mesh) Qualigens.

3.2.2 Coupling of succinic anhydride to Cholesterol

200 mg cholesterol, 155 mg Succinic anhydride and 50 mg DMAP were dissolved in 1 ml anhydrous pyridine, 1 ml DCM and 1 ml methanol. The reaction was flushed with argon and allowed to stir under argon atmosphere for 24hr. Then pyridine was removed under vacuum. Completion of the reaction was confirmed by performing a TLC in 1% Methanol in DCM solvent mixture.

3.2.3 Synthesis of LLL12-Cholesterol conjugate

LLL12 (10 mg, 0.0330 mmol) was dissolved in 2 ml anhydrous DCM followed by addition of cholesterol-succinic acid (16 mg, 0.0330 mmol), EDC (12.65 mg. 0.0660 mmol) and DMAP (8 mg, 0.0660 mmol). The reaction mixture was flushed with argon and kept under argon atmosphere at room temperature for 48hr. Completion of the reaction was confirmed by performing a TLC in 1% Methanol in DCM solvent mixture, then the solvent was evaporated under vacuum and the crude product was obtained, yellow solid LLL12-cholesterol conjugate (10 mg).

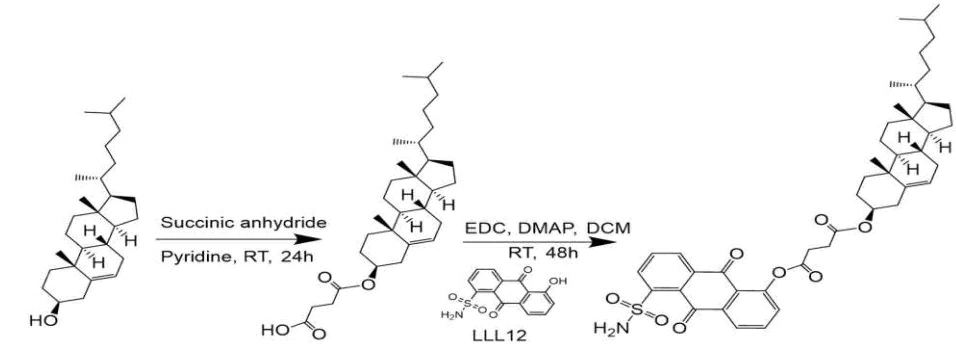

Cholesterol **Cholesterol_SA** **LLL12_Cholesterol**

3.2.4 Preparation of LLL12-Cholesterol nanoparticle

3 mg (60 mol %) of L-α-phosphatidylcholine, 0.5 mg (10 mol %) LLL12-cholesterol conjugate and 5.4 mg (30 mol %) of 1,2-Distearoyl-sn-Glycero-3-Phosphoethanolamine-N-[Amino (Polythylene Glycol) 2000] (DSPE-PEG) were dissolved in 1.0 mL anhydrous DCM. Solvent was evaporated into a thin and uniform lipid-drug film using a rotary evaporator. The lipid-drug film was then hydrated with 1.0 mL H_2O for 1 h at 55°C. The hydrated nanoparticles were yellow in color. Extrusion was done at 55°C to obtain sub 200 nm particles **Figure 3.2-1**. A standard curve of LLL12-Choletserol conjugate in DMF was generated by measuring absorbance at 389 nm using UV-Vis spectrophotometry (Shimadzu 2450). A known concentration of nanoparticle was dissolved in DMF and the absorbance value at 389 nm was used to calculate the loading from standard curve.

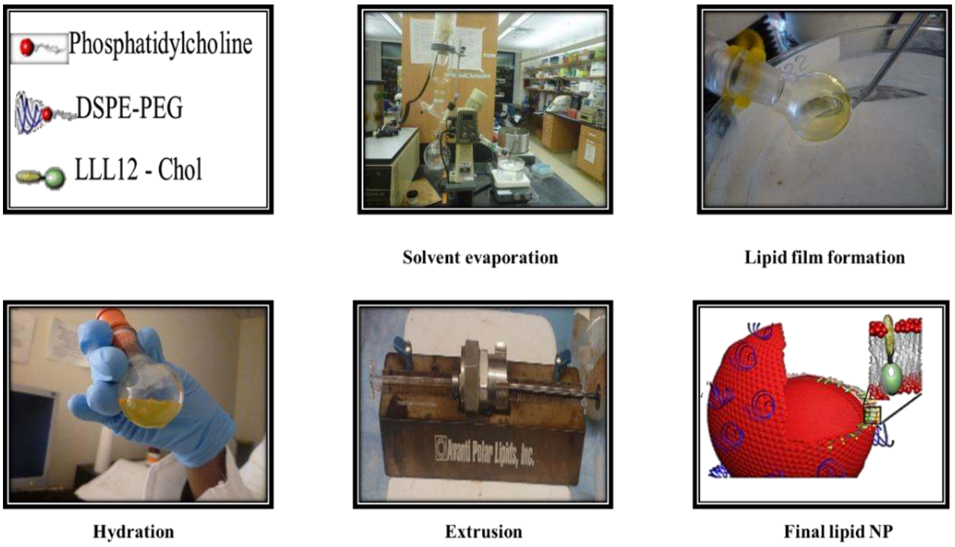

Figure 3.2-1 Steps of LLL12 nanoparticle synthesis

3.2.5 Nanoparticle characterization and stability studies

The mean particle size of the nanoparticles was measured by Dynamic Light Scattering method using Zetasizer Nano ZS90 (Malvern). 10µL of nanoparticles solution was diluted to 1ml using DI water and 3 sets of 10 measurements each were performed at 90 degree scattering angle to get the average particle size. The zeta potential was measured and the nanoparticles were diluted in water. The physical stability of nanoparticles was evaluated by measuring changes in mean particle size and zeta potential during storage condition at 4℃.

3.2.6 Cryo-Transmission Electron Microscopy for LLL12 nanoparticle

The sample was prepared by applying 3µL of sample suspension to a cleaned grid. Grids were stored in liquid nitrogen until transferred to the electron microscope for imaging.

3.2.7 Differentiation of DCs from bone marrow leukocytes

3.2.7.1 Bone marrow isolation

C57BL/6 mouse (4-10 weeks) was sacrificed by cervical dislocation, abdominal area was wiped with 70% ethanol. Small incision was made into the skin to expose the hind limbs. Tibia and femur were removed placed in HBSS (Hank's balanced salt solution) with 15% penicillin/streptomycin. Bones were washed six times in the same solution with strong shaking. Epiphyses of tibia and femur were cut off. 10 ml syringe was filled with HBSS plus (with 1 ml HEPES and 2ml FBS) and attached to 23G needle. Bone marrow (B.M) was flushed by inserting the needle in the core of the bone to an empty falcon tube, the red bone marrow at the core should come out, after emptying the whole marrow the bone turned into white transparent color. Bone marrow clumps were dissociated with 18G needle by drawing the solution from the falcon tube and forcefully shooting it back until no clumps were visible. Collected bone marrow solution was filtered through 70 µm cell strainer. 50 µL of the cell suspension was mixed with 50 µL RBC lysis buffer (1:1) and then counted using cellometer. The suspension was centrifuged at 1000 rpm for 10 minutes at 4°C and resuspended in the R10 media (RPMI supplemented with 5.5 mL P/S (100 U/ml Pencillin, 100 µg/ml streptomycin) 50 mL FBS (10%), 0.05 mM- 1.9 µL β-mercaptoethanol).

3.2.7.2 DCs differentiation

On day zero, bone marrow leukocytes were seeded at 2 million cells per 100 mm bacteriological petri dish in 10 ml R10 media containing 20ng/ml GM-CSF. On day three, another 10 ml R10 media with GM-CSF were added. On day six, half of the culture supernatant was collected, centrifuged and re-suspended in 10 mL fresh R10 media containing GM-CSF and added back into the original culture plate. By day seven, cells were ready for use and the purity of CD11c DC population was confirmed by flow cytometric analysis and was found to be between 70 and 80% for the non-adherent and semi-adherent cell population. Also, this CD11c population was compared with immature DC cell line (JAWSII – ATCC) in the sense of CD11c surface expression using flow cytometer also.

3.2.8 Analysis of CD11c DC purity by flow cytometry

Surface staining was done according to eBioscience surface staining protocols. 1 x 10^5 of DCs were washed with PBS and re-suspended in flow cytometry staining buffer. Then, cells were incubated with APC labelled anti-CD11c antibody or the corresponding isotype controls at 2µL / million cells for 1 hr. on ice and protected from light, followed by double wash with flow cytometry staining buffer then acquired to flow cytometry.

3.2.9 Generation of immunosuppressed high pSTAT3 DCs: Screening best condition media that can induce the highest pSTAT3

Conditioned basal media from 4T1, LLC and B16 were added to the culture of DCs on day 7 for 24hrs, stimulated with LPS (2µg/ml) for 15 hrs. The pSTAT3 levels were assessed by western blot, FACS and level of cytokines were determined by Luminex cytokine assay. In order to make 4T1, LLC and B16 condition media, cells were propagated in DMEM complete till they become confluent, then incubated in a serum free media (basal media) for 48hrs in 5% CO_2 atmosphere at 37°C, then added to DC culture reaching final concentration of 50%.

3.2.10 Analysis of pSTAT3 level by flow cytometry

Intracellular staining of pSTAT3 was done according to eBioscence two-step protocol. Cells were fixed with fixation buffer after intended time of incubation, kept in dark at room temperature for 60 min. After that, cells were centrifuged at 1000 rpm for 10 minutes at room temperature, supernatant was discarded and cell pellet was re-suspended in 1ml ice cold methanol and incubated for one 10 min. on ice. Cells were washed with flow cytometry staining buffer, centrifuged for 10 min at 1000 rpm, supernatant was discarded and pellet was re-suspended in flow cytometry staining buffer. PE labeled anti-pSTAT3 antibody or isotype control was added at 2µg / million cells and incubated in dark at room temperature for 60 min, then washed twice with flow cytometry staining buffer and acquired on a flow cytometer.

3.2.11 Western blot

After needed incubation period, cells were washed twice with ice cold PBS and protein was collected by scraping using RIPA buffer supplemented with protease and phosphatase inhibitor mini tablets (Thermo scientific). Amount of protein was measured by BCA assay and equal amount of protein lysates were electrophoresed on a 4-20% polyacrylamide gel, transferred to polyvinylidene membrane, and blocked in TBST in 5% BSA. Then membranes were incubated in TBST with Phospho-STAT3 (Tyr705) (1:500 dilution) and actin (1:2000 dilution) antibodies (all antibodies from Cell Signaling Technology) overnight at 4◦C. After washing with TBST, membranes were incubated with horseradish peroxidase–conjugated secondary antibody for 1 hour then washed again with TBST. Detection was done using G-box from Syngene.

3.2.12 Measurement of Cytokines

IL-2, IL-6, IL-10, IL-12, IFN-gamma and TGF-beta were measured in cell lysate using microbeads based assays in Dr. Joseph Bonventre's laboratory at Brigham & Women's Hospital. Briefly, cell lysate samples were incubated with microbeads coupled with different cytokine capture antibodies (R&D systems) and recombinant proteins for one hour, washed three times with PBST, and incubated with different cytokine detection antibodies (R&D systems) for 45 min on an orbital shaker at 300 rpm. After the incubation, beads were washed with PBST (3X) and incubated with streptavidin-PE (Invitrogen) for 15 min. Beads were washed and re-suspended in sample dilution buffer and analyzed using Bio-Plex 200 systems (Bio Rad). The signal from the flurochrome, which reflects the amount of antigen bound to the microbeads, was measured using Bio-Plex 200 systems. Standard curve was generated using five parametric logistic analysis and unknown values were interpolated.

3.2.13 Cell viability assay

Cancer cells like 4T1, B16F10 and MDA_MB_ 231 were cultured in DMEM, supplemented with 10% FBS and 1% of Antibiotic-Antimycotic 100x solution. For DC cell line, cells were cultured in Alpha minimum essential medium with ribonucleosides, deoxyribonucleosides, 4 mM L-glutamine, 1 mM sodium pyruvate and 5 ng/ml GM-CSF, 15% fetal bovine serum. For DCs derived from B.M, cells were cultured in RPMI supplemented with 5.5 mL P/S (100 U/ml Pencillin, 100 µg/ml streptomycin) 50 mL FBS (10%), 0.05 mM- 1.9 µL β-mercaptoethanol. 4T1, B16 F10 and MDA_MB_231 were seeded at 10,000 Cells into the 96-well flat-bottomed plates, while DC cell line and DCs derived from B.M seeded at 100,000 cell / well. Free drug and/or drug loaded nanoparticles (normalized to equivalent amounts of free drug) was added in triplicates in 96-well plate at appropriate concentrations (1, 10, 100 nM, 1, 10, 100 µM) and then plates were incubated in 5% CO_2 atmosphere at 37ºC. After desired period of incubation, cells were washed and incubated with 200 µl phenol-red free medium containing 25 µl of Promega aqueous solution. After the required time of incubation for optimum color change in a 5% CO_2 atmosphere at 37ºC, the absorbance in each well was recorded at 490 nm using plate reader. The absorbance reflects the number of surviving cells. Blanks were subtracted from all data and results analyzed using GraphPad Prism software. Data shown is mean ± SE of n=3.

3.2.14 Analysis of maturation status of immunosuppressed DCs before and after treatments addition using flow cytometry

DCs on their day 7 were incubated with B16 condition media for 16 hr at 50% final concentration followed by addition of IL-6 at 5µg/mL for 3 hr. then treatments were added (LLL12-np and LLL12-free) at 5µmole for 24 hr. in a fresh free serum condition media. After intended incubation period, cells were harvested, washed with PBS and acquired to FACS analysis for studying expression of CD11c, MHCII, CD80, CD86 (surface staining) and pSTAT3 (intracellular staining) according to eBioscence protocols. Consequently, cells were labelled with FITC conjugated anti-CD86, anti-CD80 antibodies and anti-I-A/I-E antibodies, APC conjugated anti-CD11c and PE labeled anti-pSTAT3 antibody and their corresponding isotype controls.

Chapter four

4. Towards understanding the preferential internalization of nano-liposomes with different surface charges in DCs, macrophages T-cells and NKs

4.1 Results and discussion

Immunomanipulation using material-based approaches lies under the field of immunobioengineering, where nanomaterials are designed as delivery vehicles to target and understand the immune system.[81]

Manipulation of the immune response by therapeutic intervention is becoming of great interest owing to the significant role of immunity in the general health and disease control.[3] APCs like Dendritic cells and macrophages are important targets for the particulate delivery system due to their ability to trigger cascade of events on both levels cellular and humoral immune response specially DCs. Successful targeting of DCs and macrophages will have a great impact on T-cell activation and priming.[37,82]

Targeting APCs in general can be achieved via surface functionalization of nanoparticles with antibodies against specific APC surface receptor. In DCs, there are several receptors that are considered possible targets such as CD205, CD206 (mannose receptor) and CD209 (DC- S1GN). However, there is no single receptor that is uniquely expressed on DCs in the tumor microenvironment.[83] The hypothesis here is whether we can target immune cells in the tumor microenvironment without the need of surface functionalization.

In the context of modifying the immune reactions in the tumor microenvironment, we know that the immune cells, have beneficial and deleterious influence on tumor growth. *In-vivo* studies revealed that animal models showed NK-cells and T-cells been involved in stress and damage removal that might turn into cancer. The design of cancer immunotherapy aims at directing the immune system against the tumor, and this is of a great interest since the success of the first cancer vaccine.[84] An essential need today for the design of successful particulate system that can elicit preferential targeting towards specific immune cell in the tumor microenvironment. This might represent a novel avenue for enhancing the antitumor immunity.

In most cases immune cells are infiltrating the progressing tumors. These immune cells comprise DCs, and tumor associated macrophages, Tregs and NKs. The TDFs act as a fuel for tumor growth rendering these tumor infiltrating cells malfunctioned.[85] A major hurdle facing cancer immunotherapy today is the high nonspecific systemic toxicity that is elicited by antibodies or stimulatory cytokines. Local immuno-targetting within the tumor microenvironment might provide efficient strategy that can avoid systemic toxicity. Providing passive targeting ability to the particulate system like surface charge might offer a platform for preferential targeting for critical immune cells residing in spleen and tumor. Moreover, test whether there will be differences in uptake according to certain preference towards certain surface charge in specific time frame.

Liposomes are made of phospholipid bilayer with a composite nature. Their properties are highly linked to their physicochemical characteristics such as size, surface charge and composition. These physicochemical properties can trigger certain immune response. Liposomal preparations are known with their improved stability either *in-vitro* or *in-vivo*.[86] Cationic liposomes like DOTAP and DOTMA are lipid vesicles with positive surface charge that have been extensively studied as successful delivery vehicles for nucleotides such as DNA, siRNAs, and others. They showed superior adjuvant effects in comparison to anionic and neutral charged liposomes.[87,88]

Many approaches have utilized different ways of actively targeting cancer cells using functionalized nanoparticles with antibodies or pH sensitive linkers, heat sensitive polymers, etc. The major hurdle in the nano-immunology field is to target immune cells within the tumor microenvironment, because most of the immune cells do not express unique surface marker that can be directly targeted in the tumor environment and ignore the other healthy populations in the rest of the human body. In addition, the ratio of cancer cells to immune cells in any tumor is very high which hinder reaching the immune cells. Today, there is crucial need to define a strategy to reprogram those immune cells to be able to reverse their downregulated status and render them immunoresponsive instead of immunosuppressive.

In the current study, we report rational design for fluorescent labelled nano-liposomes that are considered as a model for different surface charges. These liposomes were meant to have different surface charges according to the molar % of the lipid of interest. Incorporation of fluorescein as a stable fluorescent dye within the liposomal preparation that can be tracked *in-vitro* and in the future *in-vivo* studies requires rational design. Based on previous studies, the high stability of the incorporated moiety within liposome was observed when being conjugated to cholesterol. Cholesterol helps better physical attachment to the rest of the lipid structure[89]. Here, we conjugated Fluorescein-NHS to cholesterol via stable ethylene-diamine amide bond. The reaction was characterized by ^{1}H NMR spectroscopy as shown in the figure below. The ^{1}H-NMR spectra for cholesterol shows signals attributable to protons of methane, methylene and methyl groups ranges from δ 0.6 to δ 2.3. Ethylene diamine shows signals attributable to protons of amine groups at δ 4.5, δ 5.5 and to protons of methylene at δ 3.4, δ 3.5. Fluorescein shows signals attributable to protons of hydroxyl group at δ 7.9, carboxylic group at δ 8.1 and protons of aromatic rings at δ 6.5, δ 6.8, δ 7.2 and δ 7.4.

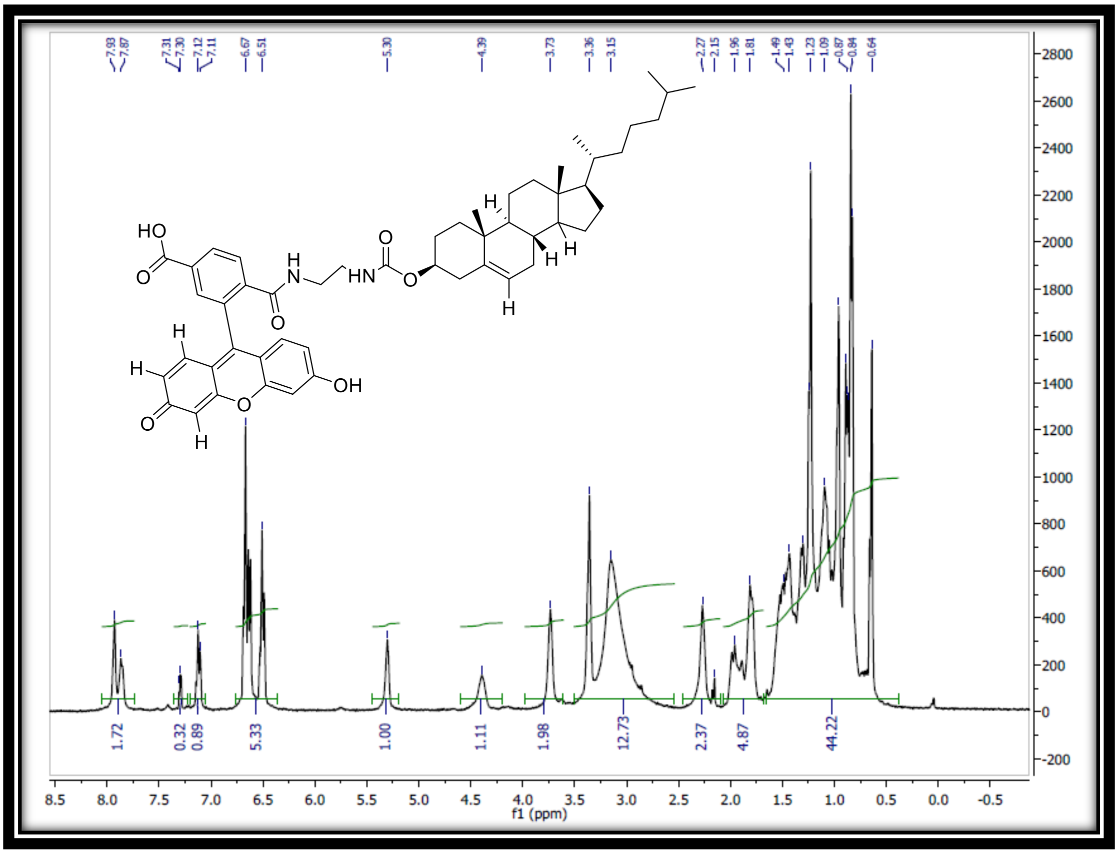

Figure 4.1-1 1H NMR spectra of cholesterol-ethylenediamine Fluorescein-NHS conjugate

4.2 Nanoparticles optimization

The main goal was to engineer three different nanoparticles via lipid film hydration method with nearly same size but different only in surface charge. Through utilizing three different surface charged liposomes, we will be able to establish a hit comparison between the internalization of specific charge among different immune cell lines in two different contexts, tumor microenvironment and lymphoid organ like spleen in two time frames 4 and 18 hrs.

Initial trials started with PC, cholesterol and DSPE-PEG (amino or carboxy or methoxy). Different ratios of each component have been tested in order to reach the best preparation in terms of stability, loading efficiency, size homogeneity and surface charge. Different PEG moieties have been used in order to establish different surface charges using PEG amino, carboxy or methoxy. PEG itself is a bulky group that has its own hydrophilic nature and stealth effect and also plays a major role in elongation of the circulation half-lives upon *in-vivo* studies. It was noticed throughout the optimization trials that PEG plays a role in hindering the charge of the linear chain moiety (amino, carboxy or methoxy) in a non-proportional manner. For example, it was expected that by decreasing the percentage of DSPE-PEG-methoxy from 10 to 1%, the overall surface charge will decrease in a proportional manner, but surprisingly the opposite happened. The same case happened also in case of DSPE-PEG carboxy and amino. **Table 4.2-1** illustrates the various preparations that have been tested. This led us to think of different compositions of liposomes without having any kind of surface modification, in order to have a systematic kind of surface changes that is to an extent in proportional to the lipid composition changes.

Table 4.2-1 Optimisation trials using different charged pegylated lipids

DSPE-PEG (type)	DSPE-PEG mol%	PC mol%	Cholesterol mol%	Mean particle diameter (nm)	Zetapotential (mV)
Amino	10% DSPE-PEG	70% PC	20% cholesterol	435 nm	+9.3
Methoxy	10% DSPE-PEG	70% PC	20% cholesterol	185 nm	-21.6
Carboxy	10% DSPE-PEG	70% PC	20% cholesterol	116 nm	-19
Carboxy	1% DSPE-PEG	75% PC	24% cholesterol	179.2	-45.2
Methoxy	1% DSPE-PEG	75% PC	24% cholesterol	181	-36.1

Consequently, in an attempt to achieve the previous mentioned goal, we decided to optimize the positive, negative and near neutral surface charges using liposomes with the required charge without having PEG. Meaning, in case of positive surface charge we used DOTAP, for the negative surface charge we used DOPG, and for the neutral we used DPPC, DOPC and PC. Cholesterol was meant to be added to increase the liposome stability. Different optimization trials have been done as shown in **Table 4.2-2** and **4.2-3** to reach a good magnitude of negative and positive surface charges and near neutral surface charge with near sizes. DPPC and cholesterol were coupled with the final optimized preparations as their presence neutralizes the charges, acts as neutral nontoxic co-lipid and enhances the overall stability.[90]

Table 4.2-2 Optimization trials using DOPC, DOPG, DOTAP and DPPC lipids

NP (type)	Lipid 1 mol %	Lipid 2 mol %	Cholesterol mol%	Mean particle diameter (nm)	Zeta potential (mV)
Anionic	20%DOPG	60%DPPC	20% Cholesterol	183	-33.9
Neutral	80% DPPC		20% cholesterol	315	-21.2
Cationic	5% DOTAP	75%DPPC	20%Cholesterol	177	+74.8
Cationic	20% DOTAP	60%DPPC	20%Cholesterol	210	+47.7
Cationic	35%DOTAP	35%PC	30% cholesterol	155	+42.8
Neutral	80%DOPC		20%Cholesterol	159	-4
Neutral	35%DOPC	35%DPPC	30% cholesterol	143	-11

Table 4.2-3 Final optimized fluorescent nano-liposomes

NP (type)	Lipid 1 mol %	Lipid 2 mol %	Cholesterol mol%	Mean particle diameter (nm)	Zeta potential (mV)
Cationic	20% DOTAP	60%DPPC	15% Cholesterol, 5%	220	+36
Negative	20% DOPG	60%DPPC	15% Cholesterol	190	-48
Near neutral	70% DOPC	10%DPPC	15% Cholesterol	210	-17.4

4.3 Nanoparticles characterization

4.3.1 Mean particle size and zeta potential for DOPG, DOTAP and DOPC

The mean particle size distribution, poly dispersity index and zeta potential of the nanoparticles were determined by Dynamic Light Scattering method (n=10 measurements per sample) and performed at 25ºC on a DLS-system (Malvern NanoZetasizer). We were able to engineer three sets of fluorescently labelled nano-liposomes as a model for different surface charges, the anionic DOPG NP, cationic DOTAP NP, and near neutral DOPC NP with mean diameter of 190, 220, 210 nm and Zeta Potential of -48, +36 and -17.4 mV respectively as shown in the figures below.

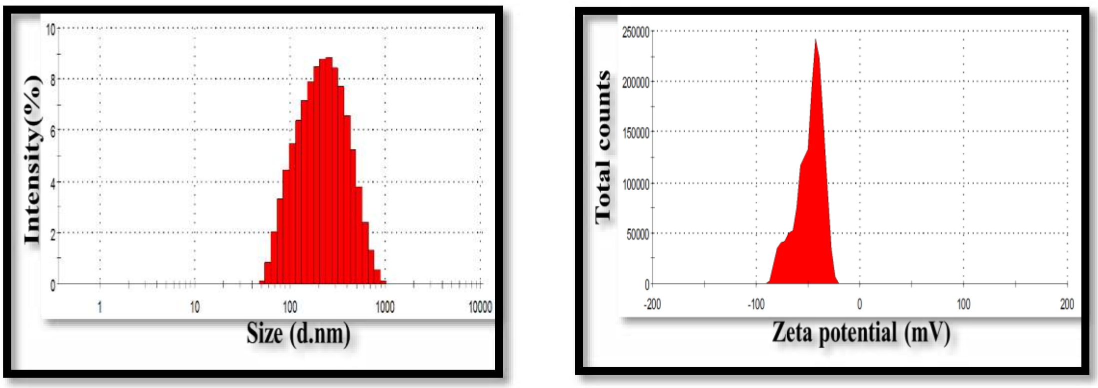

Figure 4.3-1 The distribution of hydrodynamic diameter and zeta potential of DOPG nanoparticle

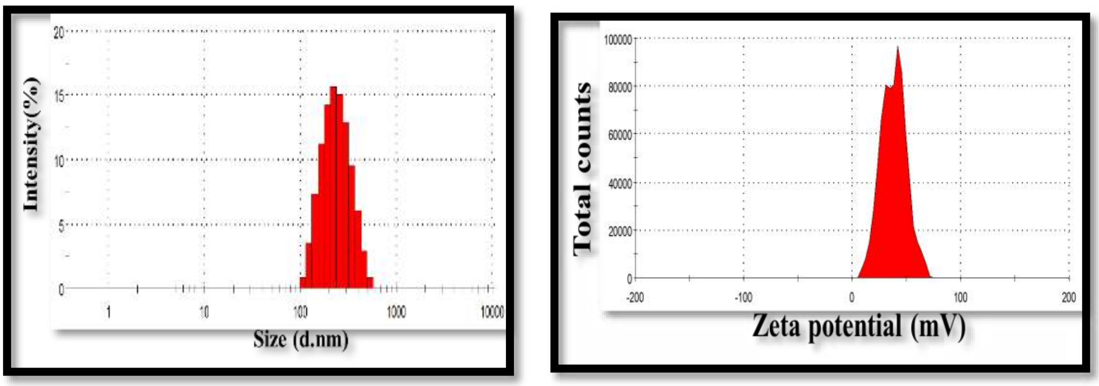

Figure 4.3-2 The distribution of hydrodynamic diameter and zeta potential of DOTAP nanoparticle

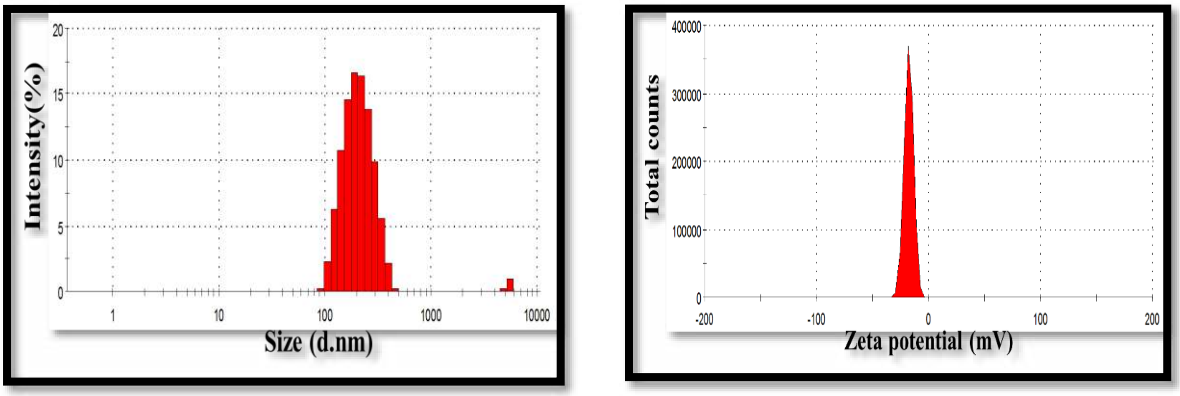

Figure 4.3-3 The distribution of hydrodynamic diameter and zeta potential of DOPC nanoparticle

4.3.2 Fluorescein loading efficiency (Spectrofluorimetric analysis)

The amount of Cholesterol-fluorescein that was incorporated successfully in the nanoparticles after extrusion step was determined using spectrofluorometer. Initially a standard curve was established using different serial dilutions for the three preparations by plotting absorbance intensity on Y-axis and the corresponding concentration on X-axis, given that the emission maximum of fluorescein is around 521 nm. Accordingly, the concentration of the nanoparticles was calculated from this standard curve using the following formula: $y = 133607x + 51.822$, $R^2 = 0.985$ **Figure 4.3-4**. The loading efficiency was determined as the concentration of fluorescein recovered after extrusion compared to the initial loading amount. It is important to mention that the 3 preparations were normalized to each other in terms of concentration before adding to the cells. As each well was loaded with exact same concentration of nanoparticles per volume and almost nearly same sizes, so the only variable was the surface charge.

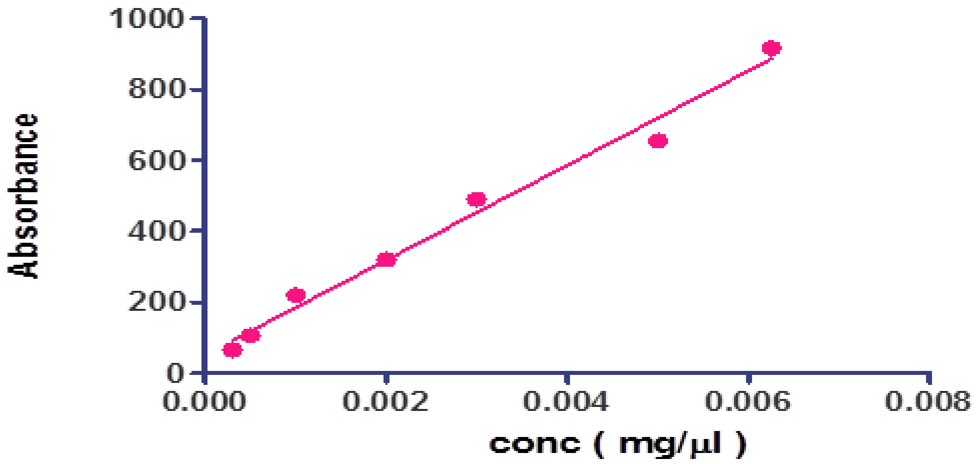

Figure 4.3-4 Cholesterol-fluorescein conjugate standard curve

4.3.3 Physical stability of the nanoparticles

The physical stability for the final optimized three types of fluorescent nano-liposomes was then assessed by monitoring the changes in particle size and zeta potential during storage at 4ºC, shown in **Figure 4.3-5**. The three preparations showed a stability to a great extent over a test period of 20 days. The magnitude of change either in the size or in the total surface charge was not that much significant. The stability data was collected on daily bases using DLS that was being used on triplicate basis for each single measurement. The most significant criteria was the absence of precipitation or turbidity during the test period. We can say that the three preparations are physically stable with minor non-significant changes which suggest a good and stable delivery system for future applications, given that the storage temperature is 4ºC.

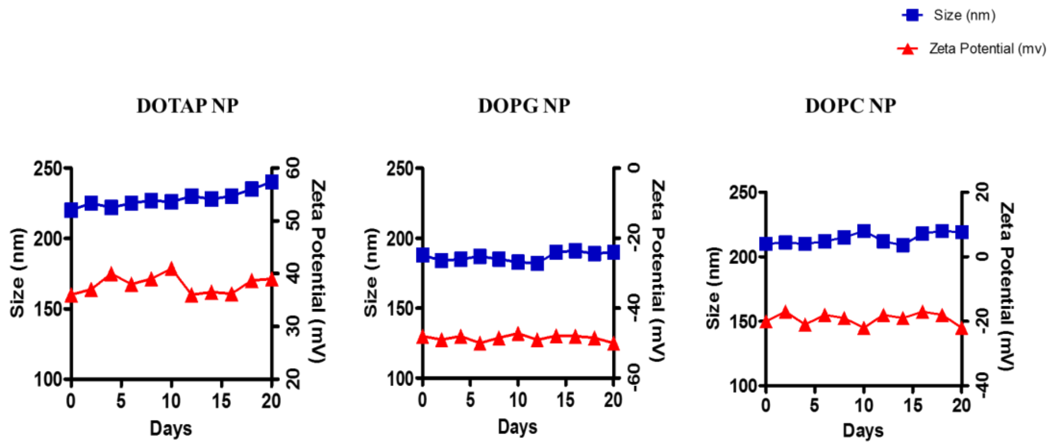

Figure 4.3-5 Physical stability of DOTAP, DOPG and DOPC nanoparticles respectively

4.4 Uptake efficiency and flow cytometric analysis

In agreement with previous studies that showed different uptake patterns of positive, negative and neutral surface charged liposomes with different cancer cell lines[91], results here reveal differences in the preferential uptake and internalization of different surface charged fluorescent labelled liposomes between different immune cell lines; macrophages, DCs, NKs and T-cells which were isolated from the tumor and from the spleen.

In case of DCs, two-way ANOVA analysis revealed that in spleen DCs, number of incubation hours was not significant ($p > 0.05$) , however type of NP was significant ($p < 0.001$) and the interaction between both number of incubation hours and type of NPs was significant as well ($p < 0.001$). In case of tumor DCs, number of incubation hours was significant by itself ($p < 0.01$), type of NPs alone or when combined with the effect of incubation hours were barely significant ($p < 0.05$). The previous results reflect how type of NPs and hence their surface charge showed significant effect in the uptake and hence the internalization pattern in both microenvironments (spleen or tumor). Also, number of incubation hours was not significant in case of spleen DCs in contrast to tumor DCs, which proves the sensitivity of tumor DCs to the incubation times. In order to reach more conclusive results and get detailed analysis for each NP, one-way ANOVA was used based on the previous preliminary statistics. In this test we analyzed the effect of NP type on combined conditions, type of cells and incubation hours. It has been revealed in case of spleen DCs of 4 hours incubation, DOTAP NP showed significant internalization ($p < 0.001$). In case of tumor DCs of 4 hours incubation, DOPC NP showed significant internalization ($p < 0.05$). DOPG NP did not show any significant pattern either in spleen or tumor DCs ($p > 0.05$). It is important to mention that 18 hours incubation in either tumor or spleen did not show any significant preferential internalization of a particular NP over another **Figure 4.4-1.**

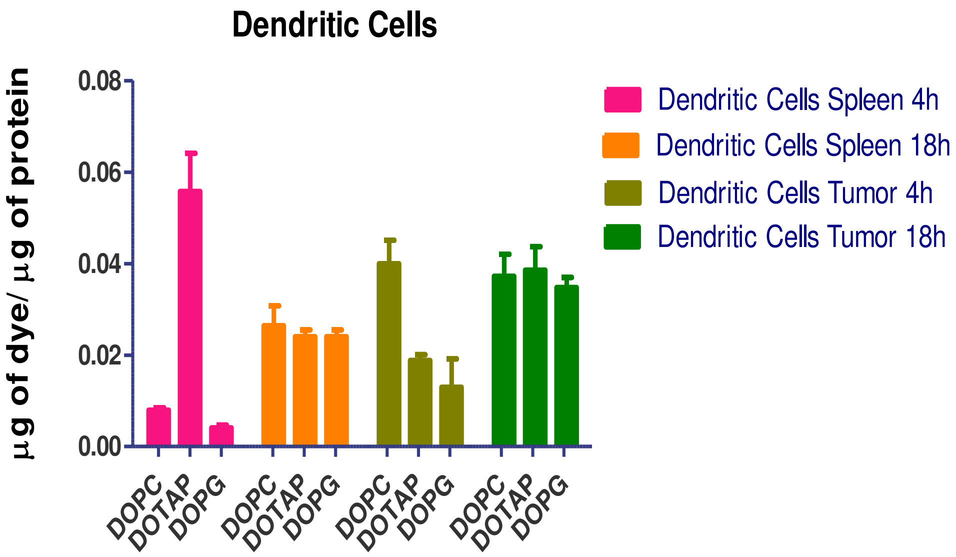

Figure 4.4-1 Uptake efficiency of DOTAP, DOPC, and DOPG NPs by DCS from spleen and tumor after 4 and 18 hours. The uptake was expressed as the fluorescence associated with the cells (concentration of fluorescein in µg measured by spectrofluorometer) versus the protein concentration of these cells (concentration of protein in µg measured by BCA assay).

A possible postulate is the variation of receptors distribution in DCs between tumor and spleen, i.e. the surface heparane sulfate proteoglycan which is negatively charged receptor might be expressed with higher levels in case of spleen DCs than tumor DCs that leads to a higher uptake of positively charged DOTAP NP in spleen than tumor. Although DOTAP has been mentioned extensively in the literature for being efficiently internalized within most of the cells owing to its cationic nature, DOPC which is neutral charge phospholipid was also used to deliver nucleotide cargos in tumor cells at 10 to 30 folds higher than cationic liposomes like DOTAP.[92] This can explain the preferential DOPC uptake in 4hr incubation time in case of tumor DC. One advantage of DOPC over DOTAP is the much less stress and toxic effects that could be elicited from the presence of cationic group.[93] The idea of having neutral liposomes as a delivery targeting carrier is of a great interest as their neutral nature limits the interaction with the DNA.[90] The mentioned results are particularly interesting because this could open a new avenue for developing therapeutic platform with a neutral charge that can efficiently targets DCs in tumor microenvironment. These results were confirmed by FACS analysis and mean fluorescence intensity as shown in **Figure 4.4-2**, where shifts in fluorescence NPs on x-axis (red histograms) are represented in comparison with untreated cells (black histograms). Higher shifts were observed in DOPC NP in tumor DCs and DOTAP NP in spleen DCs. The difference between uptake pattern in DCs in tumor and spleen is due to the difference in the microenvironment context.

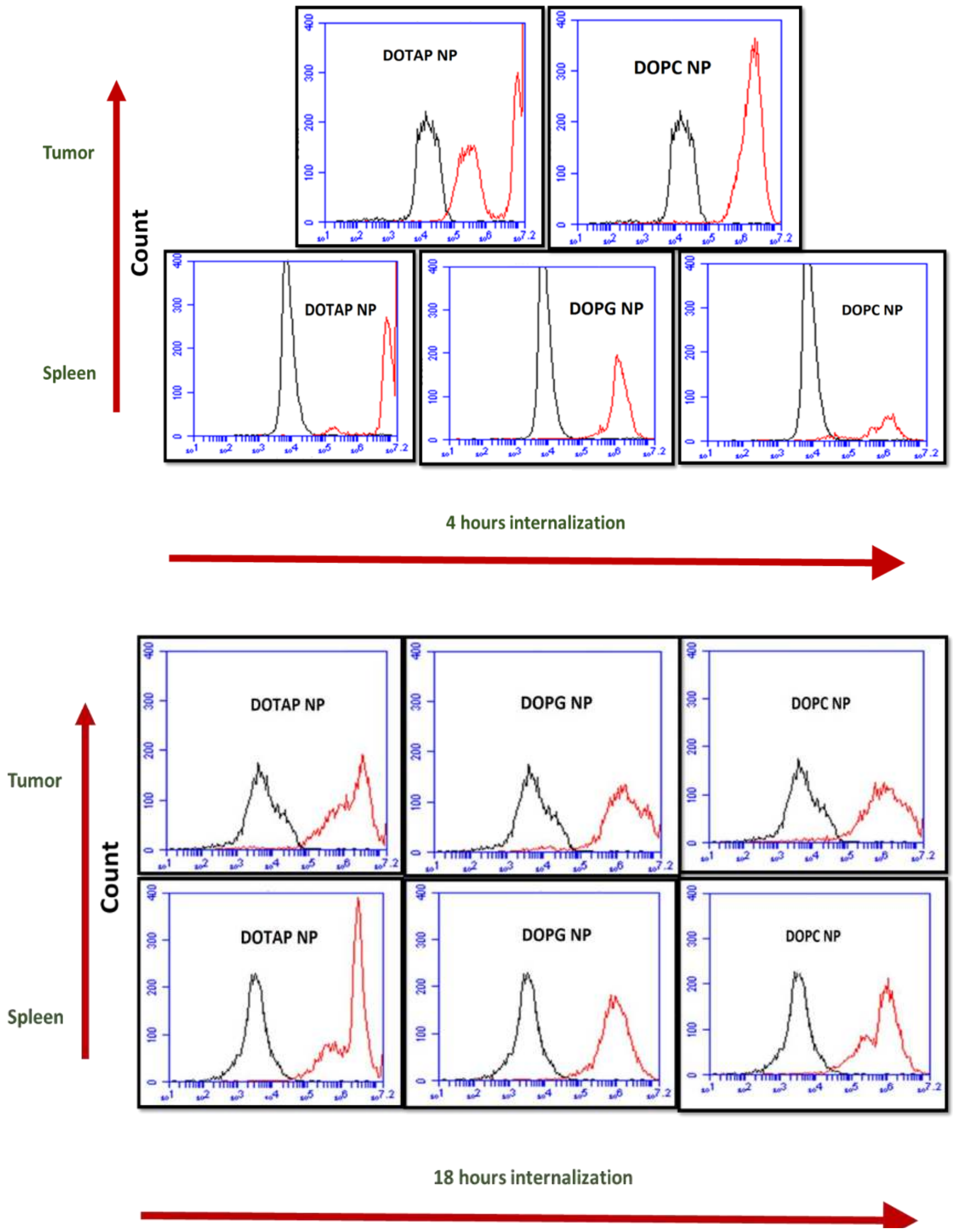

4.4-2 Representative FACS data of CD11c DCs isolated from tumor model and spleen treated with DOTAP, DOPG and DOPC nanoparticle. cells were incubated with the nanoparticles for 4hr (top) and 18 hr (bottom) kept at 37°C in a 5% CO_2 humidified atmosphere followed by washing with PBS to remove excess unbound nanoparticles. The mean fluorescence intensity of cells was measured by flow cytometry. Data shown are mean ± SD from n=3. Gating was done based on CD11c-PE expressions then fluorescein intensity was measured based on this gate. Shifts in fluorescence histograms on X-axis are shown in this figure. Mean fluorescence intensity was measured as well.

In macrophages **Figure 4.4-3**, two-way ANOVA analysis revealed that in spleen macrophages number of incubation hours and type of NP were significant ($p < 0.001$) however, interaction between these two parameters was not significant ($p > 0.05$). On the other hand, tumor macrophages showed the same pattern, except that number of incubation hours ($p < 0.001$) was much more significant than type of NP ($p < 0.01$) and this is in agreement with tumor DCs that showed high sensitivity to the effect of time. There was some interaction between incubation hours and type of NP in tumor macrophages that was barely significant ($p <0.05$). In the one-way ANOVA, DOTAP NP showed significant uptake pattern over other NPs in 4 and 18hr spleen macrophages and 18 hour tumor macrophages ($p < 0.01$, 0.05 and 0.05) respectively. The 4 hour tumor macrophages was not significant ($p > 0.05$). DOPC NP and DOPG NP did not show significant pattern ($p > 0.05$). These results were confirmed by FACS analysis and mean fluorescence intensity as shown in **Figure 4.4-4**. In which, DOTAP NP showed higher histogram shifts in spleen and tumor macrophages in comparison to DOPG and DOPC NP in 4 and 18 hr incubation time.

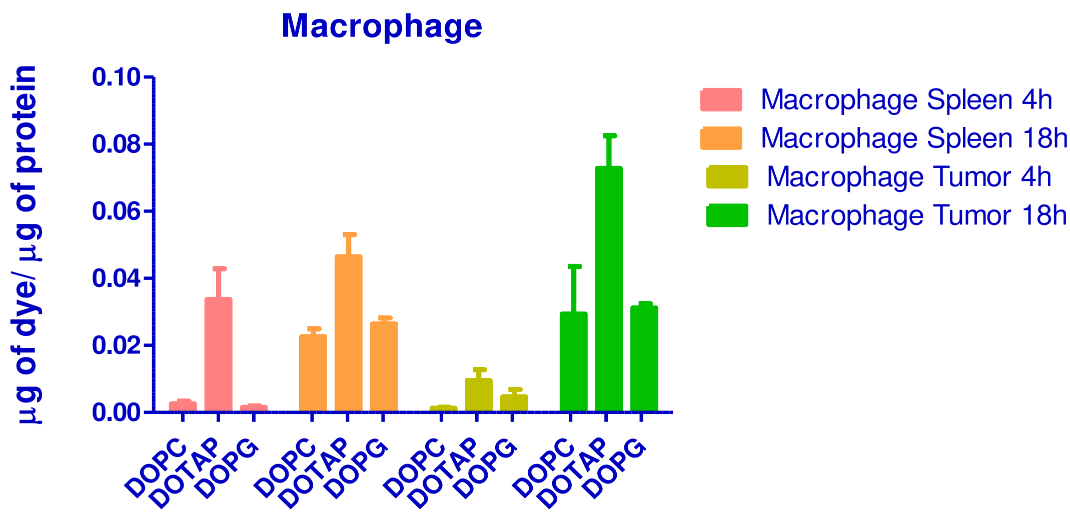

Figure 4.4-3 Uptake efficiency of DOPC, DOTAP and DOPG NPs by Macrophage from spleen and tumor after 4 and 18 hours. The uptake was expressed as the fluorescence associated with the cells (concentration of fluorescein in μg measured by spectrofluorometer) versus the protein concentration of these cells (concentration of protein in μg measured by BCA assay).

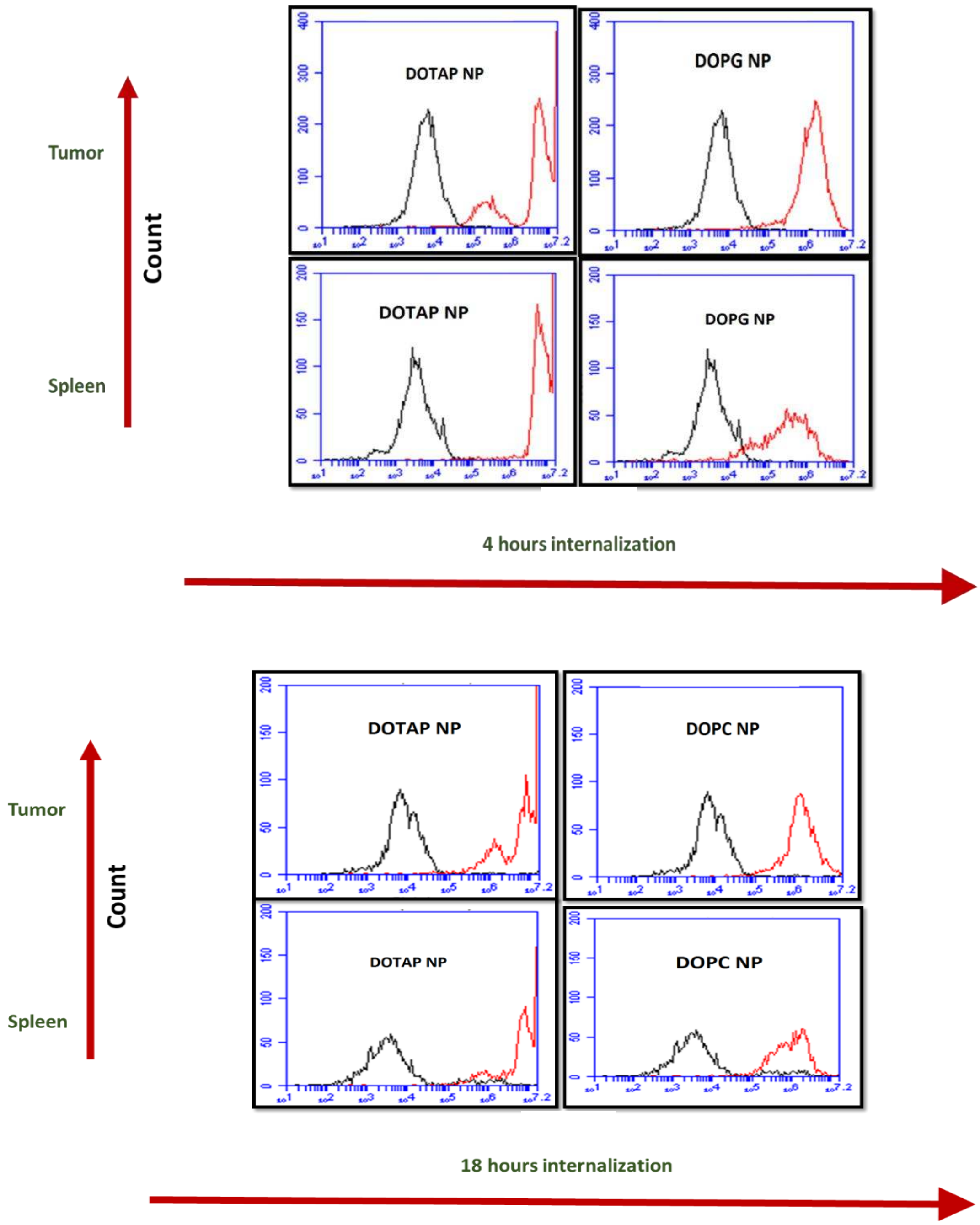

4.4-4 Representative FACS data of CD11b macrophages isolated from tumor model and spleen treated with DOTAP, DOPG and DOPC nanoparticle for 4 and 18hrs. Cells were incubated with the nanoparticles for 4hr (top) and 18 hr (bottom) kept at 37ºC in a 5% CO_2 humidified atmosphere followed by washing with PBS to remove excess unbound nanoparticles. The mean fluorescence intensity of cells was measured by flow cytometry. Data shown are mean ± SD from n=3. Gating was done based on CD11b-PE expressions then fluorescein intensity was measured based on this gate. Shifts in fluorescnece histograms on X-axis are shown in this figure. Mean fluorescence intensity was measured as well.

These results are inconsistent with previous studies that showed preferential uptake of anionic NPs due to the presence of scavenger receptors in macrophages that favor interaction with anionic groups.[94] The present results might be attributed to the existence of TLRs (Toll like receptors) which enhance the uptake of NPs. In some cases, TLRs are upregulated under stress conditions[95] which can explain why DOTAP NPs were internalized by high concentration in case of tumor and spleen macrophages. By comparing the behavior of macrophages versus DCs, it is observed that DCs show different uptake patterns between spleen and tumor microenvironments while macrophages showed almost the same uptake pattern in the two microenvironments. This is considered as a distinguished difference in particular between macrophages and DCs in the 4 hour time window. Selective targeting of DCs and macrophages separately in the tumor microenvironment i.e. DOPC NP for DCs and DOTAP NP for macrophages could be achieved via utilizing the release kinetics pattern of the nano-particulate system.

In case of T-cells and NK-cells, the first observation was that there is no preferential uptake of certain NP over the other. T-cells did not show significant uptake of particular NP either in spleen or tumor T-cells, actually most of NPs were internalized **Figure 4.4-5**. However, in case of NK-cells the incubation time was very significant in spleen and tumor NK-cells ($p < 0.001$). The degree of uptake of the three NPs in general was higher in case of 18hrs than 4hrs incubation time in both tumor and spleen **Figure 4.4-7**. The previous results were attributed to the absence of a parameter that controls the preferential uptake of specific charged NP. Flow cytometric analysis confirmed some of these observations as shown in **Figure 4.4-6** and **4.4-8**.

In this study, we have shown that some immune cells have different uptake pattern of different surface charged liposomes depending on the context they are presented in, whether spleen or tumor microenvironment. A full clear understanding of the optimum liposomal preparation that can be used as a platform for a therapeutic cargo still needs further investigations in terms of the nature of the uptake mechanism and the endocytic pathways. Interaction of lipid-based nanoparticles with immune cells offers a new avenue to explore targeting patterns within immune system and hence develop successful targeted delivery to certain subsets of immune cells.

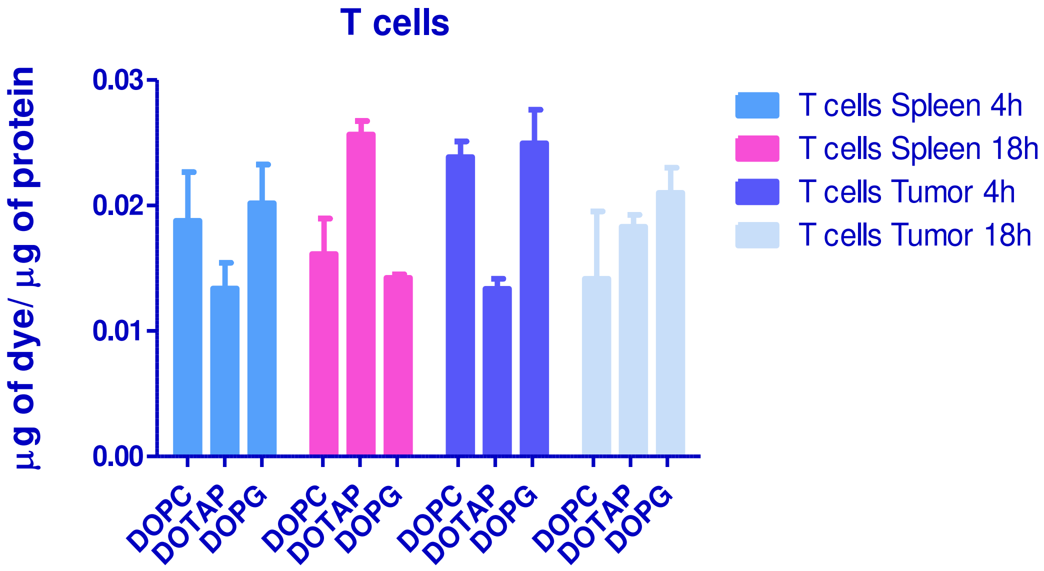

Figure 4.4-5 Uptake efficiency of DOTAP, DOPC, and DOPG NPs by T-cells from spleen and tumor after 4 and 18 hours. The uptake was expressed as the fluorescence associated with the cells (concentration of fluorescein in µg measured by spectrofluorometer) versus the protein concentration of these cells (concentration of protein in µg measured by BCA assay).

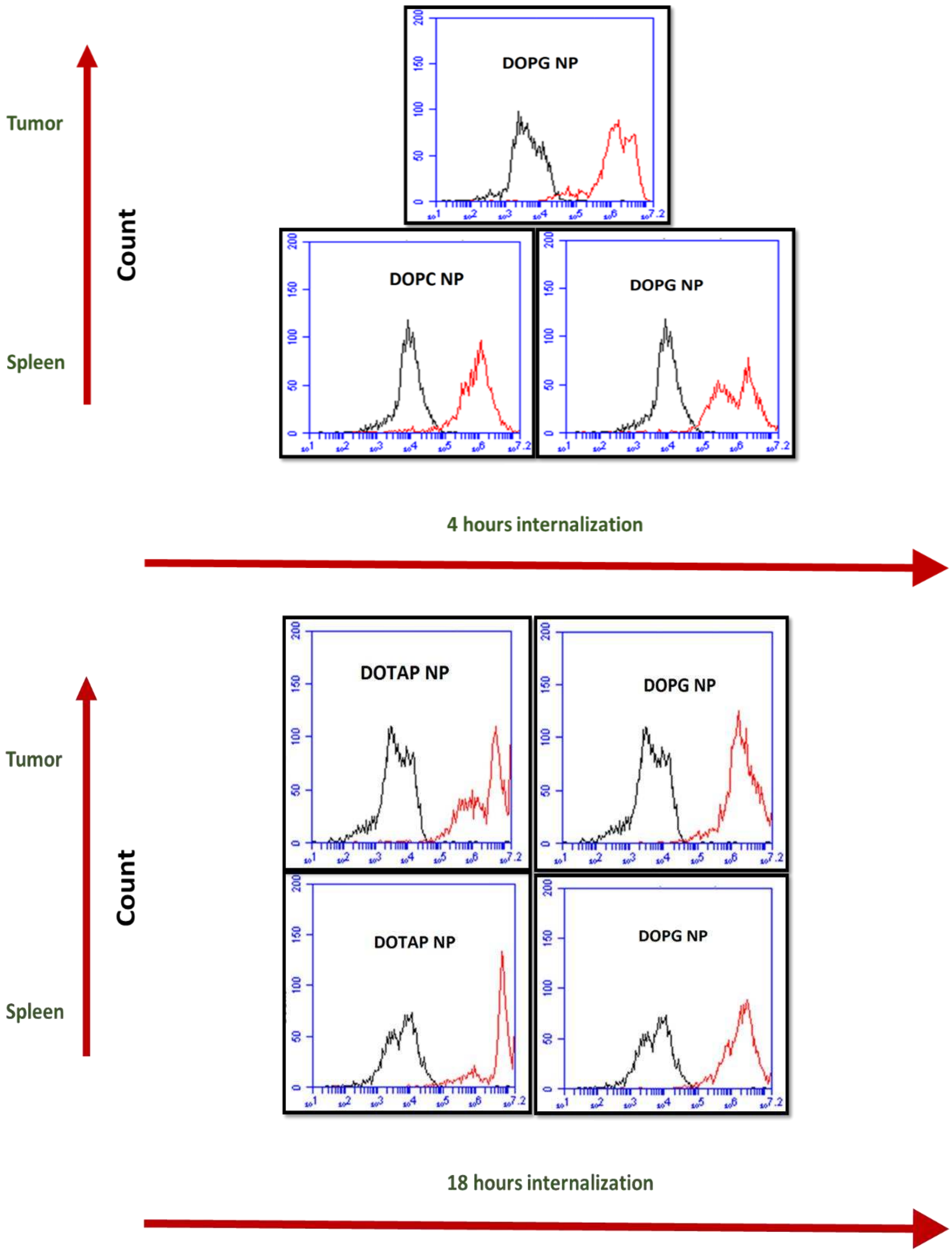

Figure 4.4-6 Representative FACS data of CD90.2 T-cells isolated from tumor model and spleen treated with DOTAP and DOPG nanoparticle for 4 and 18 hrs. Data shown are mean ± SE from n=3. Cells were incubated with the nanoparticles for 4hr (top) and 18 hr (bottom) kept at 37°C in a 5% CO_2 humidified atmosphere followed by washing with PBS to remove excess unbound nanoparticles. The mean fluorescence intensity of cells was measured by flow cytometry. Data shown are mean ± SD from n=3. Gating was done based on CD90.2-PE expressions then fluorescein intensity was measured based on this gate. Shifts in fluorescense histograms on X-axis are shown in this figure. Mean fluorescence intensity was measured as well.

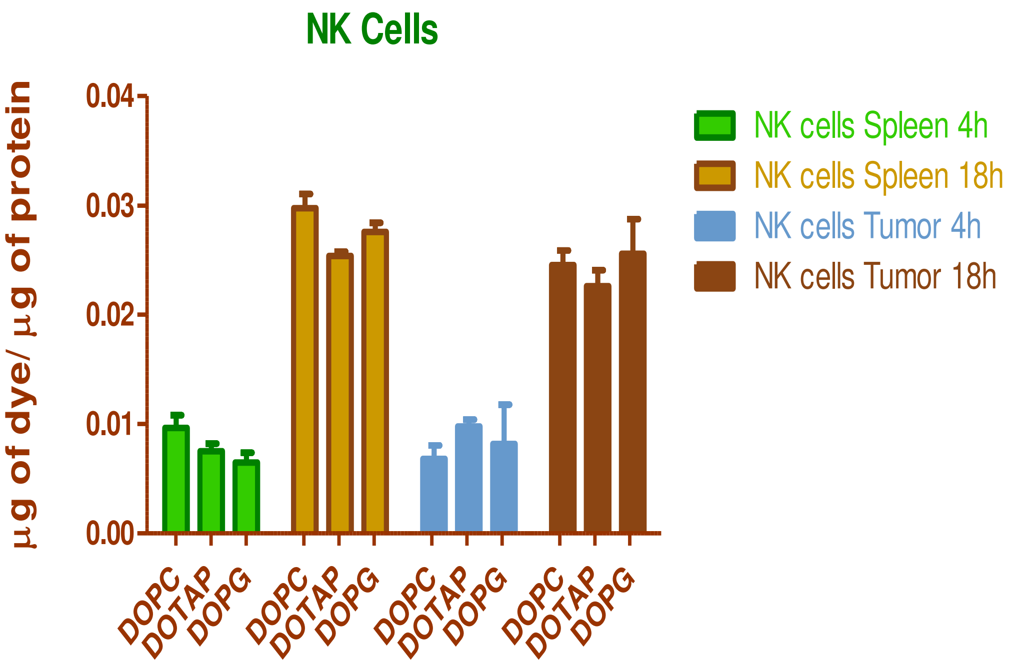

Figure 4.4-7 Uptake efficiency of DOTAP, DOPC, and DOPG NPs by NK cells from spleen and tumor after 4 and 18 hours. The uptake was expressed as the fluorescence associated with the cells (concentration of fluorescein in µg measured by spectrofluorometer) versus the protein concentration of these cells (concentration of protein in µg measured by BCA assay).

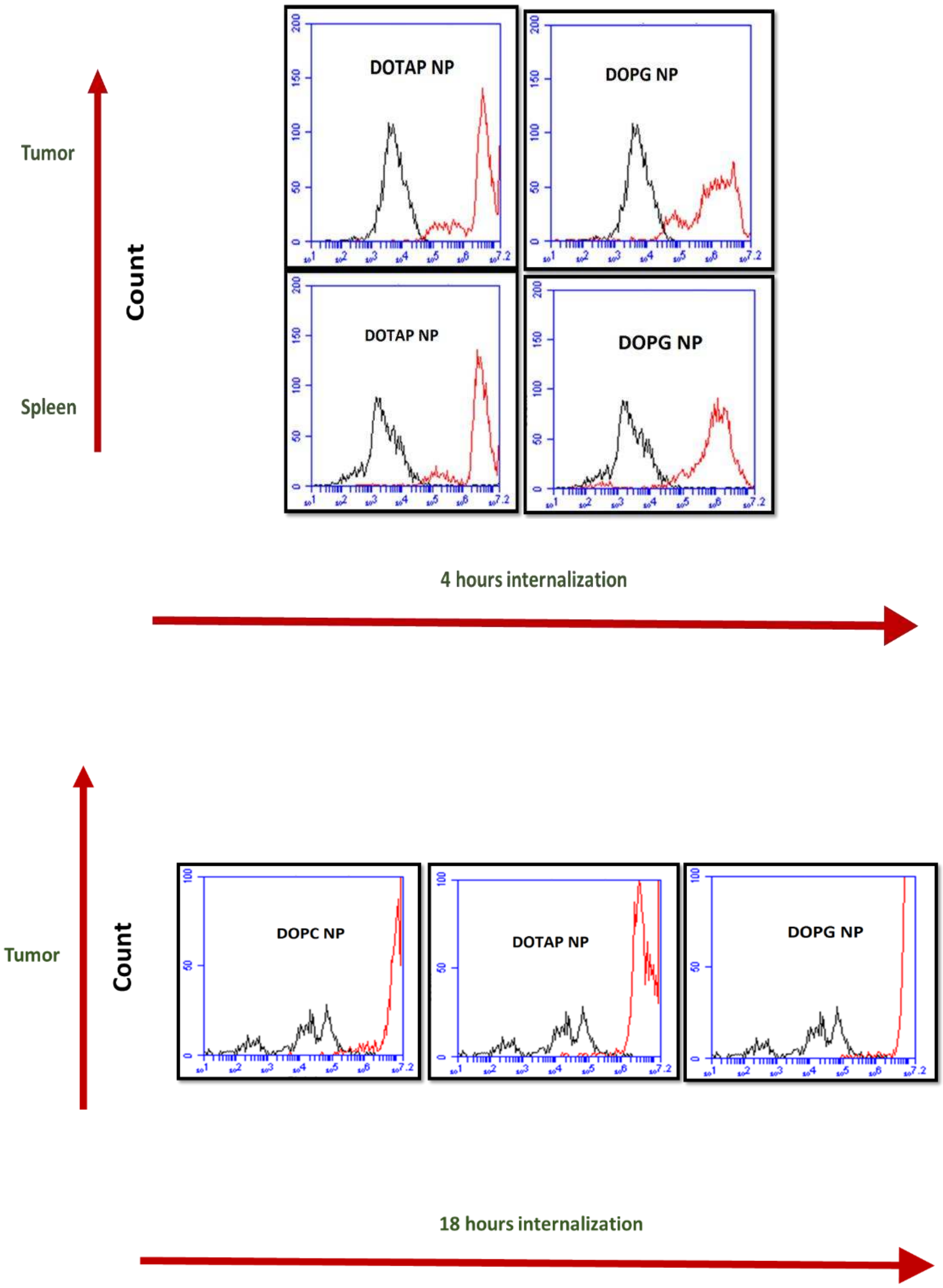

Figure 4.4-8 Representative FACS data of NK cells isolated from tumor model and spleen treated with DOPC, DOTAP and DOPG nanoparticle for4 & 18 hrs. Data shown are mean ± SE from n=3. Data shown are mean ± SE from n=3. Cells were incubated with the nanoparticles for 4hr (top) and 18 hr (bottom) kept at 37ºC in a 5% CO_2 humidified atmosphere followed by washing with PBS to remove excess unbound nanoparticles. The mean fluorescence intensity of cells was measured by flow cytometry. Data shown are mean ± SD from n=3. Gating was done based on CD90.2-PE expressions then fluorescein intensity was measured based on this gate. Shifts in fluoresence histograms on X-axis are shown in this figure. Mean fluorescence intensity was measured as well.

Chapter five

5. Towards development of novel pegylated LLL12 lipid nanoparticle as a STAT3 inhibitor in DCs: proof of concept

5.1 Results and discussion

A promising approach that can reverse the immunosuppressed status of DCs is STAT3 inhibition. In cancer, STAT3 is highly expressed in cancer cells as well as DCs. Despite the potent STAT3 inhibitory effects of LLL12, there are some limitations facing the clinical trials (in-*vivo*) which hinder the achievement of the high potency achieved on cell lines (*in-vitro)*, e.g. poor water solubility, nonspecific side effects and lack of sustained release over a certain window of time. Novel applications like nano-carriers represent a promising approach of drug delivery systems that will enhance the efficacy of the therapeutic agent and help overcome the existing limitations.

NPs loaded with small molecular inhibitor like LLL12 aim to inhibit STAT3 in a sustained fashion in comparison to free drug.[96] Development of pegylated liposomes containing chemically conjugated LLL12 to cholesterol is being investigated in this study as a strategy for a controlled delivery of LLL12 to tumor and dendritic cells. Liposomes act as a biocompatible and biodegradable lipid based carrier that is approved by FDA.[89] These lipid based nanoparticles can provide a platform for safe and sustained delivery to DCs, paving the way towards efficient cancer nano-immunotherapy. To our knowledge, this is the first time liposomes are used as a carrier for STAT3 inhibitor and LLL12 as well as is investigated for the first time against a new cell line like dendritic cells. The hydroxyl group of LLL12 was conjugated via an ester bond to cholesterol-succinate complex. The product was characterized by mass spectrometry, shown in **Figure 5.1-1**. The parent peak at 794.37 m/z is corresponding to LLL12-Cholesterol conjugate.

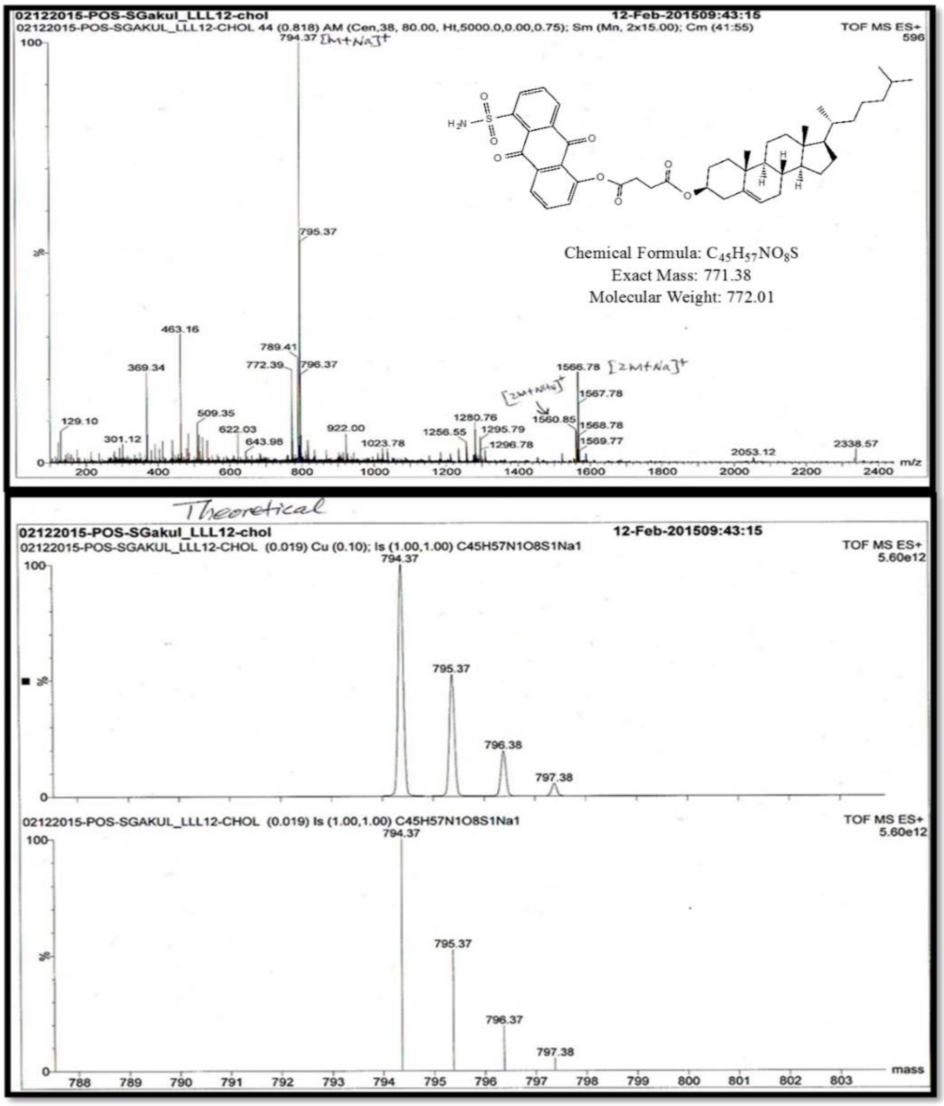

Figure 5.1-1 Mass spectra for LLL12-Cholesterol conjugate

In the present work, pegylated liposomes were chosen in order to achieve better *in-vivo* kinetics upon animal trial. PEG chain is cross linked to DSPE to elicit a lot of useful properties, as it is biocompatible, soluble and exert low antigenicity with a good excretion profile. Polyethylene glycols increase the stability of the drug and increase the circulation time of the cargo leading to an increase in the half-life and a decrease in the rate of clearance. A possible postulate for the reason behind eliciting extended half-life is the reduced interaction with the surface proteins due to the exerted steric hindrance.[97] PC and cholesterol were selected in the liposomal preparation as they are natural components of the biological membrane.[89] The engineered NP from DSPE-PEG, PC and LLL12-Chol at optimized molar ratios via lipid film hydration scheme is shown in **Figure 5.1-2**. The loading efficiency of LLL12-Chol was 82±4% as calculated from

LLL12-Chol standard curve according to the following equation: drug loading efficiency = loaded drug concentration /initial drug concentration x 100, shown in **Figure 5.1-3**.

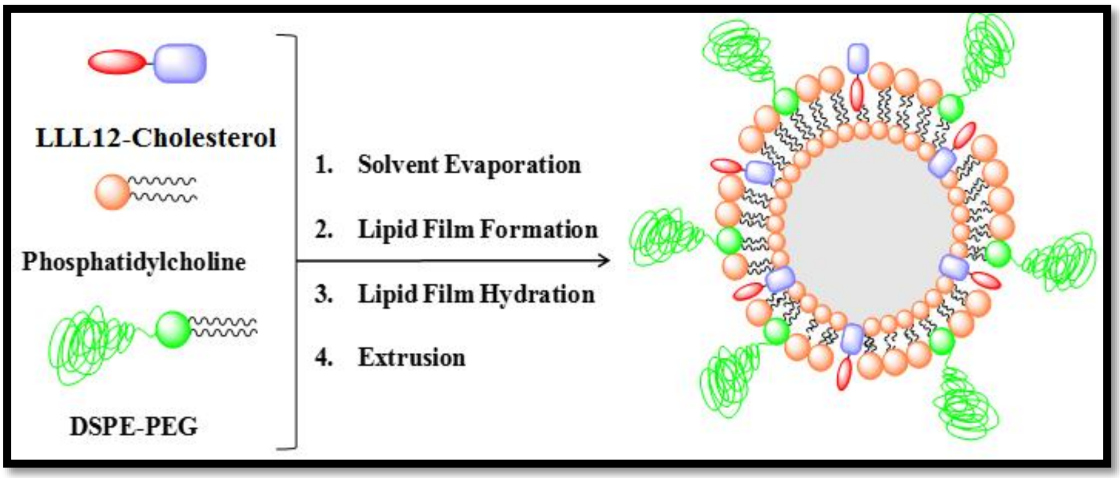

Figure 5.1-2 Schematic representation for the assembly of nanoparticles from phosphatidylcholine (PC), LLL12-cholesterol conjugate and DSPE-PEG

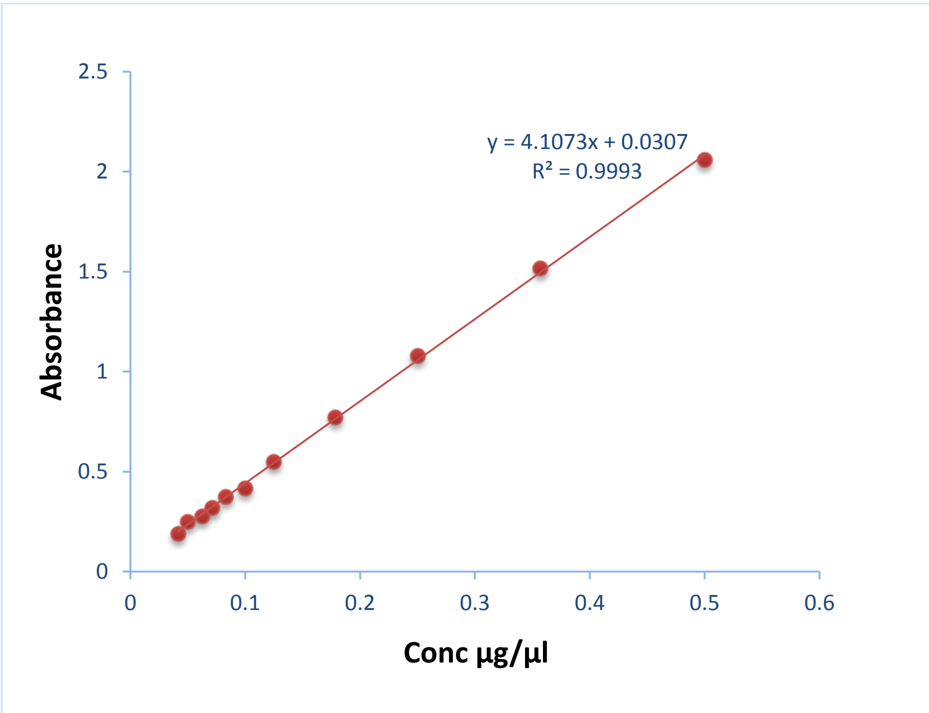

Figure 5.1-3 Standard curve of LLL12-Choleterol conjugate in DMF was generated by measuring absorbance at 398 nm

5.2 Characterization of LLL12-NP

The hydrodynamic diameter of this LLL12-NP is 190 ± 5 nm as determined by dynamic light scattering and zeta potential of 5.2 mV. Cryo-transmission electron microscopy (cryo-TEM) revealed the formation of predominantly unilamellar structures of diameter less than 200nm, shown in the figures below.

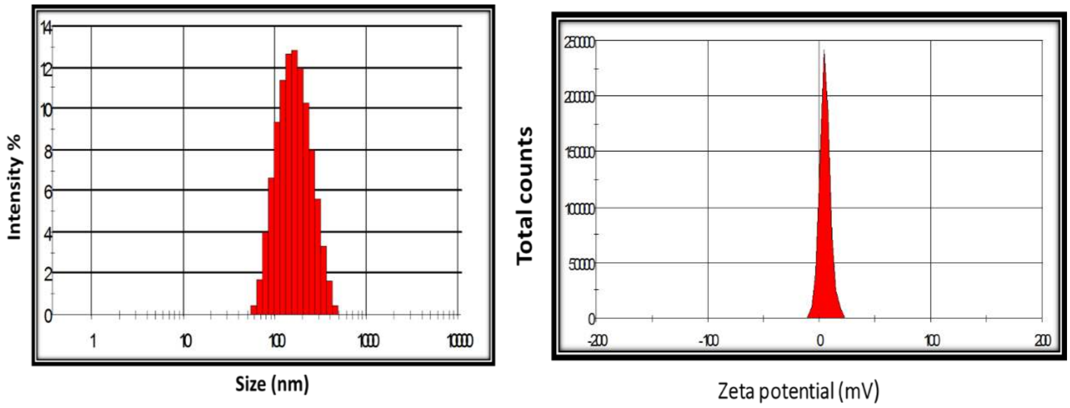

Figure 5.2-1 The distribution of hydrodynamic diameter (left) and zeta potential (right) for LLL12 NP

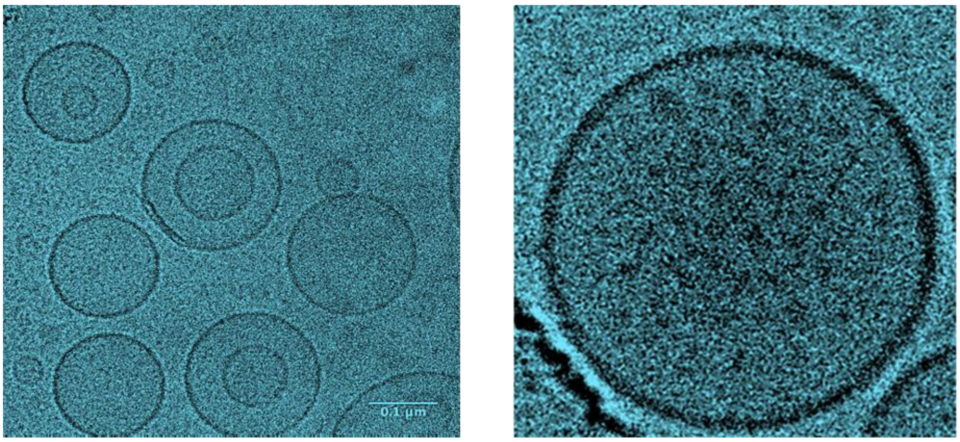

Figure 5.2-2 High-resolution Cryo-TEM image of LLL12-NP at low magnification (left) and high magnification (right). (Scale bar left, 100 nm)

5.3 Physical stability

To investigate whether the conjugation of LLL12 to cholesterol shows superior properties over the unconjugated form in terms of physical stability, two preparations were tested. One preparation was 30% DSPE-PEG, 60% PC and 10% LLL12-Chol (conjugated form) and the other was 30% DSPE-PEG, 60% PC and 10% LLL12 (unconjugated). By comparison, it was revealed that after day 2 the unconjugated preparation rapidly experienced precipitation as shown in **Figure 5.3-1 (left)**. This is consistent with the previous studies that utilized cholesterol-based derivative, facilitating supramolecular assembly with phosphatidylcholine and DSPE-PEG.[98]

The physical stability has been assessed by monitoring the changes in particle size and zeta potential during storage at 4°C, shown in **Figure 5.3-1 (right)**. The preparation showed a stability to a great extent over a test period of 15 days. The magnitude of change either in size or in total surface charge was not significant. The stability data was collected on daily bases using DLS which was being used on triplicate basis for each single measurement. The most significant criteria was that no precipitation or turbidity happened during the test period, given that storage temperature was 4°C. We can say that the preparation is stable and extended periods could be tested as well.

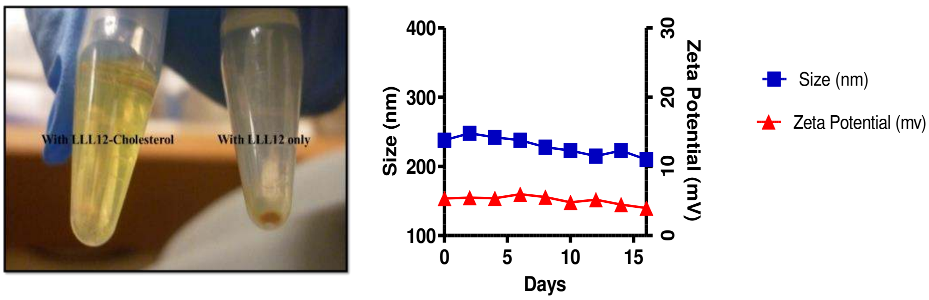

Figure 5.3-1 (left) Two formulations for LLL12 NP; left after conjugating LLL12 to cholesterol, right without conjugating LLL12 to cholesterol. (Right) graph shows the physical stability of LLL12-NPs during storage condition at 4°C as measured by changes in size and Zeta potential of nanoparticles

5.4 Cell viability assay

The efficacy of LLL12-NP was evaluated *in-vitro* using BMDC (bone marrow derived DCs), JAWSII (DC cell line), B16F10 (Melanoma cancer model), MDA-MB-231 (human breast cancer model) and 4T1 (murine breast cancer), ATCC **Figure 5.4-1**. IC_{50} values are shown in the table below. It has been observed and in agreement with previous studies that the conjugated form of LLL12 showed decreased potency than the free drug. This indicated that LLL12-NP behaves like prodrug status that needs time to be released with *in-vivo* conditions which will help its activation to the parent molecule for the ultimate efficacy.[98]

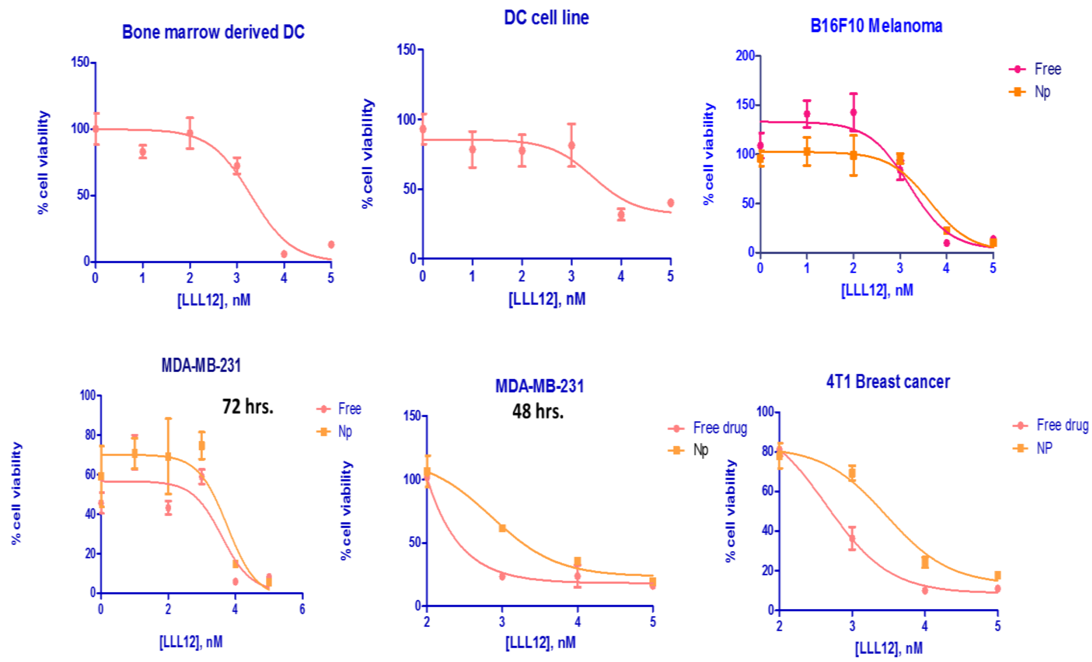

Figure 5.4-1 MTS assay showing the effect of free LLL12 or LLL12-NP at different concentrations on MDA-MB-231 cells at 72h and 48h; 4T1 cells at 48h; Bone marrow derived DC at 48h; DC cell line at 48h and B16F10 melanoma at 72h. Graphs show the effect of treatment with free LLL12 or LLL12-NP on viability on different cell lines. Table 5.4-1 shows IC50 of free LLL12 and LLL12 NP in different cell lines at 48h and 72h. Data shown are mean ± SEM (n=3, with at least triplicates in each independent experiment).

Table 5.4-1 IC50 values [µM]

Cell line	IC_{50} values [µM]	Treatment
MDA-MB-231, 72hrs	- 3.94 - 5.712	- Free - NP
MDA-MB-231, 48hrs	- 0.38 - 0.721	- Free - NP
4T1, 48hrs	- 0.443 - 2.954	- Free - NP
Bone marrow derived DC, 48hrs	- 2.08	- Free
DC cell line, 48hrs	- 2.7	- Free
B16F10, 72hrs	- 1.588 - 4.326	- Free - NP

5.5 CD11c DC purity by flow cytometry

Assessment of the purity of CD11c lineage has been done by staining the cells on day 7 with APC labelled anti-CD11c antibody and the corresponding isotype control. The purity was found to be 70-80%. Then, these DCBM were compared to the JAWSII (DC cell line) that showed purity of 85%. **Figure 5.5-1** shows FACS for DCBM on the left and DC cell line on the right. The cells were gated on CD11c APC channel.

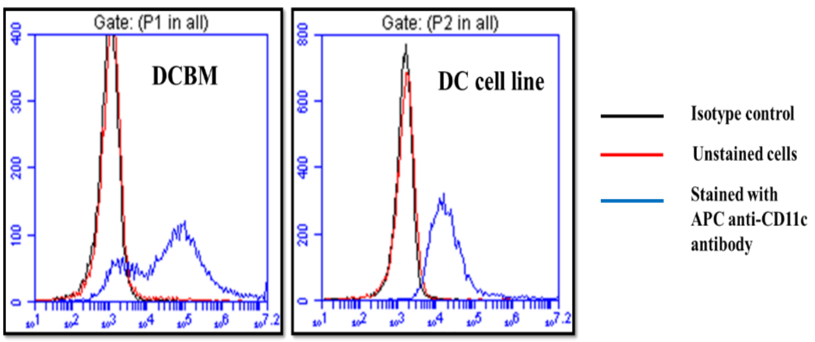

Figure 5.5-1 CD11 DC expression was evaluated by flow cytometry on day 7 for the DCBM and compared this expression level to DC cell line.

5.6 Screening best condition media that can induce the highest pSTAT3

In order to study which conditioning medium is potent to induce high levels of intracellular pSTAT3 and consequently mimic the immunosuppressed status of DCs within the tumor microenvironment, three conditioning media were tested against DCBM for 24hrs which are 4T1, LLC and B16 media. Cells were harvested and acquired for western blot, cytokine analysis and FACS. Western blot showed the highest intensity band of pSTAT3 in case of B16 condition medium. Cytokine analysis was performed to evaluate the highest IL-6 secretion which was observed also in B16, then final confirmation was done with FACS intracellular staining with PE labeled anti-p-STAT3 antibody, the result was in agreement with western blot and cytokine analysis, showing that B16 expressed pSTAT3 by 4.9% while 4T1 was 0.7% and LLC was 3.6% pSTAT3, **Figure 5.6-1**. In conclusion, B16 condition media is the best model that can be used to condition DCs and simulate a tumor microenvironment around them.

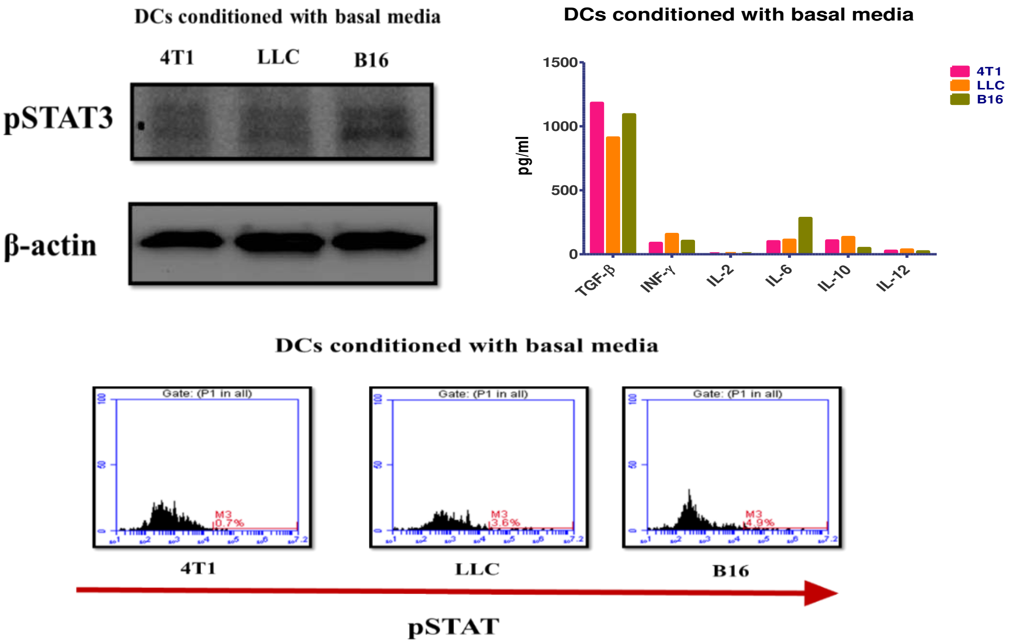

Figure 5.6-1 (top left) Western blot analysis showing expression of pSTAT3 in DCBM after conditioning in different tumor basal media and actin control. pSTAT3 optical density bands were normalized to actin bands using ImageJ software. (Top right) Cytokine levels measured for DCBM after conditioning in different tumor basal media. (Bottom) Representative FACS data for pSTAT3 expression level evaluated by flow cytometry on the different tumor basal media after 24 hrs

5.7 Assessment of maturation status of immunosuppressed DCs before and after LLL12 addition using flow cytometry

FACS analysis of CD86, MHCII and CD80 expressions were performed. MHCII, CD80 and CD86 were gated on CD11c double positive population. CD11c APC channel was on x-axis and FITC channel on y-axis. In **Figure 5.7-1 (a)**, normal expression of CD86, MHCII and CD80 were assessed in DCs in normal state on day 7. The isotype controls are also displayed. CD11c-CD86 showed 1.9% expression, CD11c-MHCII showed 22.8% expression and CD11c-CD80 showed 0.6% expression.

In **Figure 5.7-1 (b)** after conditioning BMDC with B16 basal media, down regulation occurred to the DC surface receptors and immunosuppressive state started to reveal. CD11c-CD86 showed 1.3% expression, CD11c-MHCII showed 5.3% expression and CD11c-CD80 showed 0.2% expression.

In **Figure 5.7-1 (c)**, after addition of IL-6 in order to induce more stress on DCs and add fresh stimulus that can activate the JAK-STAT pathway once again. CD11c-CD86 showed 0.3% expression, CD11c-MHCII showed 3.4% expression and CD11c-CD80 showed 0.1% expression.

Figure 5.7-2 (a), represents the pSTAT3 level in normal DCs after addition of B16 condition media and after addition of IL-6. The pSTAT3 level in normal DCs is 29.7%, in conditioned DCs is 77.8% and after IL-6 is 67.7%. These results are consistent and in agreement and with the previous results, where DCs upon conditioning, experience activation of JAK-STAT pathway that elicits high levels of pSTAT3 that cause the downregulation and immunosuppression of DC surface receptors.

Figure 5.7-2 (b), represents FACS data after addition of LLL12-NP (5 µmole) for 24hrs. pSTAT3 expression level decreased to 54.7% with slight upregulation in CD11c-CD86 that showed 0.4% expression, in CD11c-MHCII that showed 4.3% expression, while in case of CD11c-CD80 nothing was observed.

Figure 5.7-2 (c), represents FACS data addition of free LLL12 (5 µmole) for 24hrs. pSTAT3 level also decreased as in LLL12-NP. CD11c-CD86 showed 0.7% expression, CD11c-MHCII showed dramatic increase around 3 folds with 10.2% expression within only 24hrs and CD11c-CD80 almost showed no change. It is obvious that free drug showed significant upregulation of CD11c-MHCII than LLL12-NP. The free LLL12 results are consistent with the fact that NP is releasing the drug in a slow manner. This sustained behavior hinder the full potency of LLL12 in only 24hrs. Future work should test the LLL12 potency for 48hrs.

Activation of STAT3 play a major role in cancer development, it does not only provoke JAK-STAT cycle within the tumor, but also influences the tumor infiltrating immune cells. A major affected cell is the dendritic cell that suffers from immunosuppression and elicit increased numbers of immature DCs and regulatory T-cells.[99] Therefore, inhibition of STAT3 in tumor microenvironment and immunosuppressed DCs is a promising approach not only from the aspect of tumor proliferation reduction, but also to break a continuous cycle of tumor immunosuppression which will consequently lead to better therapeutic outcome.

LLL12 is a recently discovered molecular inhibitor for STAT3. It is selective for STAT3 inhibition with no off target properties, inhibits nuclear translocation and hence the DNA binding. Previous studies have used LLL12 for STAT3 inhibition in tumor cells, but in this study we investigate for the first time whether LLL12 will exert the same effect on STAT3 inhibition in DCs. In the present study, we generated immunosuppressed DCs that experienced high levels of induced pSTAT3 through exposure to melanoma cell line condition media as shown in **Figure 5.7-2 (a)**. This pSTAT3 induction significantly reduced DC functional maturation as shown in **Figure 5.7-1 (b)**. We tested whether LLL12 (5µmole) will exert immunomodulatory effects or no in 24hr based on its STAT3 inhibitory action. Here, we report a chemically conjugated LLL12 to cholesterol through esterification reaction between hydroxyl group of LLL12 and carboxylic group of Cholesterol-succinate. This preliminary step led to increase in the loading efficiency up to 80% within the lipid NP and tuned the release to cover extended period, and more importantly the stability of the formulation dramatically increased. In the future work, *in-vivo* studies will be performed as we predict that the potency of the LLL12-NP will get multiplied upon *in-vivo* trials, that is because prodrug will get activated when the ester bond get cleaved by the action of esterases, and fortunately, the acidic pH of the tumor will easily cleave the ester bond releasing the active LLL12. In summary, the chemical conjugation of LLL12 to cholesterol NP serve as an efficient drug delivery platform. The developed NP was found to have inhibitory effects on STAT3 in DCs, however future work will be done to test extended treatment periods and proceed to the *in-vivo* trials. *In-vitro* LLL12-NP (5µmole) reduced the pSTAT3 levels in melanoma cancer model in 24hr and restored the DC surface expression of CD86 and MHCII as shown in **Figure 5.7-2 (b)**. However, free LLL12 (5µmole) showed superior restoration of MHCII as shown in **Figure 5.7-2 (c)** which reveals that LLL12-NP needs longer time to elicit the full LLL12 effect.

These results demonstrate the potential of LLL12 to reverse the immunosuppressed status of DCs in tumor microenvironment and its immunomodulatory role. If this construct proven successful while *in-vivo* studies, it will offer a promising platform for novel immunotherapeutic strategy.

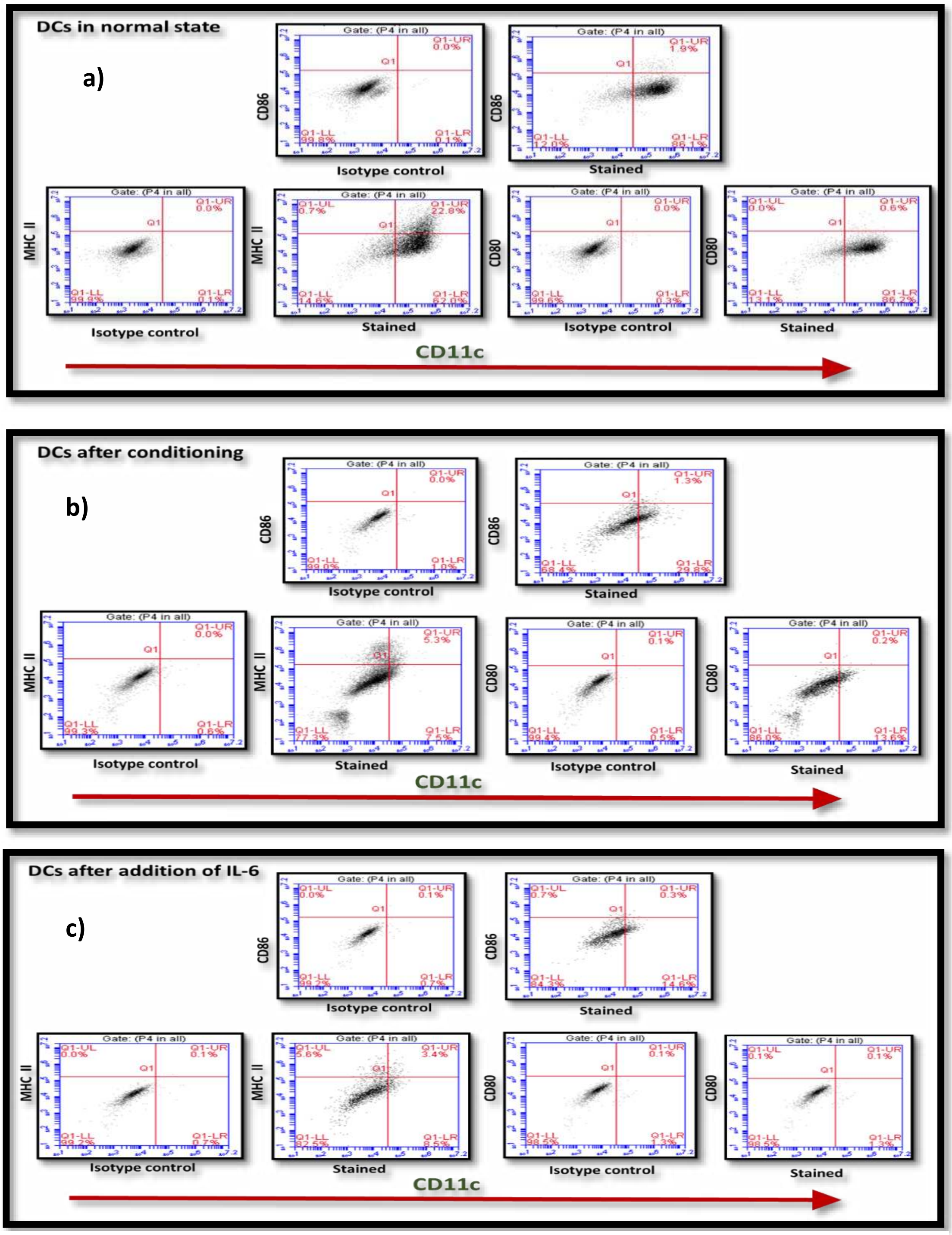

Figure 5.7- 1 Representative FACS data for the expression of MHCII, CD80 and CD86 on the gated CD11c double positive population. Gates were set using isotype controls. (a) Data shown for DCs in normal state, (b) Data shown for DCs after addition of B16 condition media (c) Data shown for the DCs after addition of IL-6

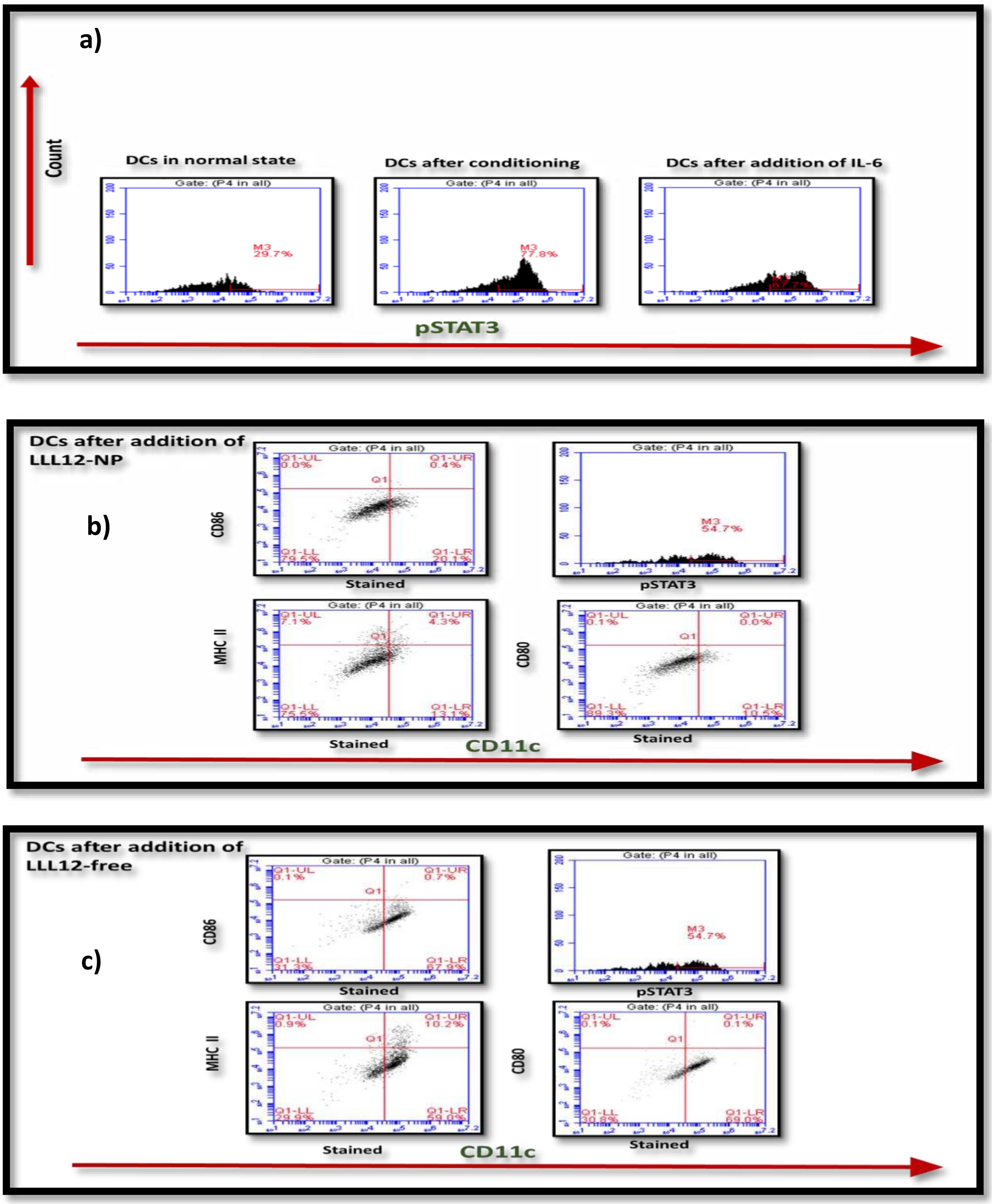

Figure 5.7-2 (a) Representative FACS data for the pSTAT3 expression in BMDC in normal state, after conditioning with B16F10 basal media and after addition of IL-6, FACS data for the expression of MHCII, CD80, CD86 on the gated CD11c double positive population and pSTAT3. Gates were set using isotype controls. (b) Data shown for the BMDC after addition of LLL12-NP at 5µm for 24 hrs. in a fresh B16F10 basal media, (c) Data shown for the BMDC after addition of Free-LLL12 at 5µm for 24 hrs. in a fresh B16F10 basal media

Chapter six

6. Conclusion and future prospectives

Material science has shown a new avenue of contribution which is the field of immune-bioengineering as a therapeutic drug delivery platform. This allowed us to better explore the interaction between different classes of immune cells and pathogens. Conventionally, the immune system used to instruct and dictate the fate of the material based intervention, however today the advances in material science are used to instruct the immunobiology.[81] Nanoparticle based immunotherapy is still at its infancy stage of development. It is crystal clear that this approach offers great potentials. Studies are still investigating the privilege of microparticles and nanoparticles as immunotargetting vehicle or immunomodulatory platform. Overall, these novel strategies showed better yield compared with the non-particle based conventional ones. Clinical translation of any of these approaches require first accurate optimization of the particulate system. So far and despite of the positive findings, physical and chemical properties of these particulate delivery systems need to be crucially defined.[100]

In summary, we have described different promising strategies either to target or modulate immune cells. More deep investigations are still needed to reveal the mechanisms and pathways by which certain immune cell can sense, interact and hence internalize certain NP. Understanding these properties will lead to improved targeted delivery to different immune cells.

Understanding the possibility of preferential uptake of certain surface charged liposome over another in specific cell line might serve as a guideline. This can help better design tailored NP for a successful targeting application. We observed a tendency of accumulation of DOPC NPs in tumor DCs and DOTAP NPs in spleen DCs within 4 hr. window. This suggests that DCs in two different contexts elicit different targeting affinities. In contrast to macrophages that showed constant pattern of DOTAP NPs uptake in both tumor and spleen macrophages. In T-cells, all NPs get internalized in both tumor and spleen T-cells. In NK-cells, all three NPs get internalized but with higher uptake efficiency in 18hrs treatments than 4hrs. In the future work related to this context, we are planning to investigate the mechanism of internalization of NPs per each cell line and find out the predominant endocytic pathway. In addition, we will study the *in-vivo* biodistribution in different organs in animal trial.

On the other hand, STAT3 is a new player in the field of cancer therapy. It has been proven that STAT3 represents a vital role in cancer progression, in terms of proliferation, invasion, angiogenesis and most importantly immunosurveillance escape. According to several studies, STAT3 activation is attributed to various types of human cancers, in addition to the immunosuppression it elicits which is our scope here. The inhibition of DCs functional maturation that hinders from normal expression of its surface receptors is a major challenge today that renders STAT3 pathway a novel target for cancer immunotherapy. LLL12 is molecular STAT3 inhibitor that is used for the first time here in cancer immunotherapy context for targeting the most professional antigen presenting cells like dendritic cells. It has been revealed in the current study that LLL12 might serve as a new player in cancer immunotherapeutics. In either free or conjugated form, inhibition of pSTAT3 was observed and consequently restoration as well as upregulation of some surface markers.

STAT3 inhibition approach can be extrapolated to cover multiple targets at the same time by designing suitable combinations with chemotherapeutics. The goal is to reach synergy between the two therapeutic moieties. It has been revealed that STAT3 suppression enhance the sensitivity of the cells to chemotherapy such as cisplatin and taxol. That is why STAT3 today is an attractive target and therapeutic designs should go beyond monotherapy. Our future work will entail testing the LLL12-NP for extended periods 48 and 72hrs. After that, proceeding to animal trial with melanoma cancer model, where we will use combination therapy. We might use chimeric NP containing STAT3 inhibitor like LLL12 and immune check point inhibitor. Another thought is to combine STAT3 inhibitor with chemotherapy like cisplatin or paclitaxel.

References

(1) Lesterhuis, W. J.; Haanen, J. B. A. G.; Punt, C. J. A. Cancer Immunotherapy--Revisited. *Nat. Rev. Drug Discov.* **2011**, *10* (8), 591–600.

(2) Ochs, H. D.; Ziegler, S. F.; Torgerson, T. R. FOXP3 Acts as a Rheostat of the Immune Response. *Immunol. Rev.* **2005**, *203*, 156–164.

(3) Pulendran, B.; Ahmed, R. Immunological Mechanisms of Vaccination. *Nat. Immunol.* **2011**, *131* (6), 509–517.

(4) Belyakov, I. M.; Ahlers, J. D.; Brandwein, B. Y.; Earl, P.; Kelsall, B. L.; Moss, B.; Strober, W.; Berzofsky, J. A. The Importance of Local Mucosal HIV-Specific CD8(+) Cytotoxic T Lymphocytes for Resistance to Mucosal Viral Transmission in Mice and Enhancement of Resistance by Local Administration of IL-12. *J. Clin. Invest.* **1998**, *102* (12), 2072–2081.

(5) Holmgren, J.; Czerkinsky, C. Mucosal Immunity and Vaccines. *Nat. Med.* **2005**, *11* (4 Suppl), S45–S53.

(6) The Halsted Mastectomy. *West. J. Med.* **1981**, *135* (4), 338–340.

(7) Foray, N. [Victor Despeignes (1866-1937): How a Hygienist Became the First Radiation Oncologist]. *Cancer Radiother.* **2013**, *17* (3), 244–254.

(8) DeVita, V. T.; Chu, E. A History of Cancer Chemotherapy. *Cancer Res.* **2008**, *68* (21), 8643–8653.

(9) Mayer, E. L. Early and Late Long-Term Effects of Adjuvant Chemotherapy. *Am. Soc. Clin. Oncol. Educ. Book* **2013**, 9–14.

(10) Shaw, A. T.; Hsu, P. P.; Awad, M. M.; Engelman, J. A. Tyrosine Kinase Gene Rearrangements in Epithelial Malignancies. *Nat. Rev. Cancer* **2013**, *13* (11), 772–787.

(11) Fialkow, P. J. Clonal Origin of Human Tumors. **2003**.

(12) Feldmann, M.; Steinman, L. Design of Effective Immunotherapy for Human Autoimmunity. *Nature* **2005**, *435* (7042), 612–619.

(13) Hodi, F. S.; O'Day, S. J.; McDermott, D. F.; Weber, R. W.; Sosman, J. A.; Haanen, J. B.; Gonzalez, R.; Robert, C.; Schadendorf, D.; Hassel, J. C.; et al. Improved Survival with Ipilimumab in Patients with Metastatic Melanoma. *N. Engl. J. Med.* **2010**, *363* (8), 711–723.

(14) Kalos, M.; Levine, B. L.; Porter, D. L.; Katz, S.; Grupp, S. A.; Bagg, A.; June, C. H. T Cells with Chimeric Antigen Receptors Have Potent Antitumor Effects and Can Establish Memory in Patients with Advanced Leukemia. *Sci. Transl. Med.* **2011**, *3* (95), 95ra73.

(15) Vesely, M. D.; Kershaw, M. H.; Schreiber, R. D.; Smyth, M. J. Natural Innate and Adaptive Immunity to Cancer. *Annu. Rev. Immunol.* **2011**, *29*, 235–271.

(16) Stewart, T. J.; Abrams, S. I. How Tumours Escape Mass Destruction. *Oncogene* **2008**, *27* (45), 5894–5903.

(17) Shin, J.-Y.; Yoon, I.-H.; Kim, J.-S.; Kim, B.; Park, C.-G. Vascular Endothelial Growth Factor-Induced Chemotaxis and IL-10 from T Cells. *Cell. Immunol.* **2009**, *256* (1-2), 72–78.

(18) Curiel, T. J.; Coukos, G.; Zou, L.; Alvarez, X.; Cheng, P.; Mottram, P.; Evdemon-Hogan, M.; Conejo-Garcia, J. R.; Zhang, L.; Burow, M.; et al. Specific Recruitment of Regulatory T Cells in Ovarian Carcinoma Fosters Immune Privilege and Predicts Reduced Survival. *Nat. Med.* **2004**, *10* (9), 942–949.

(19) Gabrilovich, D. I.; Nagaraj, S. Myeloid-Derived Suppressor Cells as Regulators of the Immune System. *Nat. Rev. Immunol.* **2009**, *9* (3), 162–174.

(20) Mellman, I.; Coukos, G.; Dranoff, G. Cancer Immunotherapy Comes of Age. *Nature* **2011**, *480* (7378), 480–489.

(21) The Pulse on Global Trials By Matthew HowesCRI and Cancer Immunology | CenterWatch News Online http://www.centerwatch.com/news-online/article/7868/cri-and-cancer-immunology#sthash.CxxRDpdw.LTi5oxgV.dpbs (accessed Jun 16, 2015).

(22) Mullard, A. 2010 FDA Drug Approvals. *Nat. Rev. Drug Discov.* **2011**, *10* (2), 82–85.

(23) McAleese, F.; Eser, M. : Harnessing the Immune System To Kill Cancer Cells. *Futur. Oncol.* **2012**, *8* (6), 687–695.

(24) Dobrovolskaia, M. a; Aggarwal, P.; Hall, J. B.; Mcneil, S. E. Preclinical Studies to Understand NP Interaction with the Immune System and Its Potential Effects on NP Biodistribution. *Mol. Pharm.* **2009**, *5* (4), 487–495.

(25) Cho, N.-H.; Cheong, T.-C.; Min, J. H.; Wu, J. H.; Lee, S. J.; Kim, D.; Yang, J.-S.; Kim, S.; Kim, Y. K.; Seong, S.-Y. A Multifunctional Core-Shell Nanoparticle for Dendritic Cell-Based Cancer Immunotherapy. *Nat. Nanotechnol.* **2011**, *6* (10), 675–682.

(26) Noh, Y.-W.; Jang, Y.-S.; Ahn, K.-J.; Lim, Y. T.; Chung, B. H. Simultaneous in Vivo Tracking of Dendritic Cells and Priming of an Antigen-Specific Immune Response. *Biomaterials* **2011**, *32* (26), 6254–6263.

(27) Reddy, S. T.; van der Vlies, A. J.; Simeoni, E.; Angeli, V.; Randolph, G. J.; O'Neil, C. P.; Lee, L. K.; Swartz, M. A.; Hubbell, J. A. Exploiting Lymphatic Transport and Complement Activation in Nanoparticle Vaccines. *Nat. Biotechnol.* **2007**, *25* (10), 1159–1164.

(28) Huppa, J. B.; Davis, M. M. T-Cell-Antigen Recognition and the Immunological Synapse. *Nat. Rev. Immunol.* **2003**, *3* (12), 973–983.

(29) Steinman, R. M.; Hemmi, H. Dendritic Cells: Translating Innate to Adaptive Immunity. *Curr. Top. Microbiol. Immunol.* **2006**, *311*, 17–58.

(30) Balthasar, S.; Michaelis, K.; Dinauer, N.; von Briesen, H.; Kreuter, J.; Langer, K. Preparation and Characterisation of Antibody Modified Gelatin Nanoparticles as Drug Carrier System for Uptake in Lymphocytes. *Biomaterials* **2005**, *26* (15), 2723–2732.

(31) Hellstrom, I.; Ledbetter, J. A.; Scholler, N.; Yang, Y.; Ye, Z.; Goodman, G.; Pullman, J.; Hayden-Ledbetter, M.; Hellstrom, K. E. CD3-Mediated Activation of Tumor-Reactive Lymphocytes from Patients with Advanced Cancer. *Proc. Natl. Acad. Sci. U. S. A.* **2001**, *98* (12), 6783–6788.

(32) Owens, D. E.; Peppas, N. A. Opsonization, Biodistribution, and Pharmacokinetics of Polymeric Nanoparticles. *Int. J. Pharm.* **2006**, *307* (1), 93–102.

(33) Vonarbourg, A.; Passirani, C.; Saulnier, P.; Benoit, J.-P. Parameters Influencing the Stealthiness of Colloidal Drug Delivery Systems. *Biomaterials* **2006**, *27* (24), 4356–4373.

(34) Decuzzi, P.; Godin, B.; Tanaka, T.; Lee, S.-Y.; Chiappini, C.; Liu, X.; Ferrari, M. Size and Shape Effects in the Biodistribution of Intravascularly Injected Particles. *J. Control. Release* **2010**, *141* (3), 320–327.

(35) Devarajan, P. V; Jindal, A. B.; Patil, R. R.; Mulla, F.; Gaikwad, R. V; Samad, A. Particle Shape: A New Design Parameter for Passive Targeting in Splenotropic Drug Delivery. *J. Pharm. Sci.* **2010**, *99* (6), 2576–2581.

(36) Guy, B. The Perfect Mix: Recent Progress in Adjuvant Research. *Nat. Rev. Microbiol.* **2007**, *5* (7), 505–517.

(37) Steinman, R. M.; Banchereau, J. Taking Dendritic Cells into Medicine. *Nature* **2007**, *449* (7161), 419–426.

(38) Aslan, B.; Ozpolat, B.; Sood, A. K.; Lopez-Berestein, G. Nanotechnology in Cancer Therapy. *J. Drug Target.* **2013**, *21* (10), 904–913.

(39) Khan, D. R.; Rezler, E. M.; Lauer-Fields, J.; Fields, G. B. Effects of Drug Hydrophobicity on Liposomal Stability. *Chem. Biol. Drug Des.* **2008**, *71* (1), 3–7.

(40) Ewert, K.; Evans, H. M.; Ahmad, A.; Slack, N. L.; Lin, A. J.; Martin-Herranz, A.; Safinya, C. R. Lipoplex Structures and Their Distinct Cellular Pathways. *Adv. Genet.* **2005**, *53*, 119–155.

(41) Conniot, J.; Silva, J. M.; Fernandes, J. G.; Silva, L. C.; Gaspar, R.; Brocchini, S.; Florindo, H. F.; Barata, T. S. Cancer Immunotherapy: Nanodelivery Approaches for Immune Cell Targeting and Tracking. *Front. Chem.* **2014**, *2* (November), 1–27.

(42) Insmed – Proprietary Liposomal Technology http://www.insmed.com/product-candidates/proprietary-liposomal-technology (accessed Jun 30, 2015).

(43) Honary, S.; Zahir, F. Effect of Zeta Potential on the Properties of Nano-Drug Delivery Systems - A Review (Part 1). *Trop. J. Pharm. Res.* **2013**, *12* (2), 255–264.

(44) Cancer | Nanotechnology in Medicine http://ts-1.eee.hku.hk/ccst9015sp13/p13/drug-delivery/cancer-3/ (accessed Jul 18, 2015).

(45) 16:0PC https://www.avantilipids.com/index.php?option=com_content&view=article&id=216&Itemid=206&catnumber=850355 (accessed Jul 18, 2015).

(46) Gabrilovich, D. I.; Nadaf, S.; Corak, J.; Berzofsky, J. A.; Carbone, D. P. Dendritic Cells in Antitumor Immune Responses. II. Dendritic Cells Grown from Bone Marrow Precursors, but Not Mature DC from Tumor-Bearing Mice, Are Effective Antigen Carriers in the Therapy of Established Tumors. *Cell. Immunol.* **1996**, *170* (1), 111–119.

(47) Gabrilovich, D. I.; Corak, J.; Ciernik, I. F.; Kavanaugh, D.; Carbone, D. P. Decreased Antigen Presentation by Dendritic Cells in Patients with Breast Cancer. *Clin. Cancer Res.* **1997**, *3* (3), 483–490.

(48) Shurin, G. V.; Shurin, M. R.; Bykovskaia, S.; Shogan, J.; Lotze, M. T.; Barksdale, E. M. . J. Neuroblastoma-Derived Gangliosides Inhibit Dendritic Cell Generation and Function. *Cancer Res.* **2001**, *61* (1), 363–369.

(49) Menetrier-Caux, C.; Montmain, G.; Dieu, M. C.; Bain, C.; Favrot, M. C.; Caux, C.; Blay, J. Y. Inhibition of the Differentiation of Dendritic Cells from CD34(+) Progenitors by Tumor Cells: Role of Interleukin-6 and Macrophage Colony-Stimulating Factor. *Blood* **1998**, *92* (12), 4778–4791.

(50) Pardoll, D. Does the Immune System See Tumors as Foreign or Self? *Annu. Rev. Immunol.* **2003**, *21*, 807–839.

(51) Blattman, J. N.; Greenberg, P. D. Cancer Immunotherapy: A Treatment for the Masses. *Science* **2004**, *305* (5681), 200–205.

(52) Zou, W. Immunosuppressive Networks in the Tumour Environment and Their Therapeutic Relevance. *Nat. Rev. Cancer* **2005**, *5* (4), 263–274.

(53) Gabrilovich, D. Mechanisms and Functional Significance of Tumour-Induced Dendritic-Cell Defects. *Nat. Rev. Immunol.* **2004**, *4* (12), 941–952.

(54) Bissell, M. J.; Radisky, D. Putting Tumours in Context. *Nat. Rev. Cancer* **2001**, *1* (1), 46–54.

(55) Borys, N. J.; Walter, M. J.; Huang, J.; Talapin, D. V; Lupton, J. M. The Role of Particle Morphology in Interfacial Energy Transfer in CdSe/CdS Heterostructure Nanocrystals. *Science* **2010**, *330* (6009), 1371–1374.

(56) Yu, H.; Jove, R. The STATs of Cancer--New Molecular Targets Come of Age. *Nat. Rev. Cancer* **2004**, *4* (2), 97–105.

(57) Welte, T.; Zhang, S. S. M.; Wang, T.; Zhang, Z.; Hesslein, D. G. T.; Yin, Z.; Kano, A.; Iwamoto, Y.; Li, E.; Craft, J. E.; et al. STAT3 Deletion during Hematopoiesis Causes Crohn's Disease-like Pathogenesis and Lethality: A Critical Role of STAT3 in Innate Immunity. *Proc. Natl. Acad. Sci. U. S. A.* **2003**, *100* (4), 1879–1884.

(58) Kortylewski, M.; Kujawski, M.; Wang, T.; Wei, S.; Zhang, S.; Pilon-Thomas, S.; Niu, G.; Kay, H.; Mulé, J.; Kerr, W. G.; et al. Inhibiting Stat3 Signaling in the Hematopoietic System Elicits Multicomponent Antitumor Immunity. *Nat. Med.* **2005**, *11* (12), 1314–1321.

(59) Leeman, R. J.; Lui, V. W. Y.; Grandis, J. R. STAT3 as a Therapeutic Target in Head and Neck Cancer. **2006**.

(60) Takeda, K.; Noguchi, K.; Shi, W.; Tanaka, T.; Matsumoto, M.; Yoshida, N.; Kishimoto, T.; Akira, S. Targeted Disruption of the Mouse Stat3 Gene Leads to Early Embryonic Lethality. *Proc. Natl. Acad. Sci.* **1997**, *94* (8), 3801–3804.

(61) Miyoshi, K.; Takaishi, M.; Nakajima, K.; Ikeda, M.; Kanda, T.; Tarutani, M.; Iiyama, T.; Asao, N.; DiGiovanni, J.; Sano, S. Stat3 as a Therapeutic Target for the Treatment of Psoriasis: A Clinical Feasibility Study with STA-21, a Stat3 Inhibitor. *J. Invest. Dermatol.* **2011**, *131* (1), 108–117.

(62) Aggarwal, B. B.; Kunnumakkara, A. B.; Harikumar, K. B.; Gupta, S. R.; Tharakan, S. T.; Koca, C.; Dey, S.; Sung, B. Signal Transducer and Activator of Transcription-3, Inflammation, and Cancer: How Intimate Is the Relationship?. *Ann. N. Y. Acad. Sci.* **2009**, *1171*, 59–76.

(63) Burger, R.; Le Gouill, S.; Tai, Y.-T.; Shringarpure, R.; Tassone, P.; Neri, P.; Podar, K.; Catley, L.; Hideshima, T.; Chauhan, D.; et al. Janus Kinase Inhibitor INCB20 Has Antiproliferative and Apoptotic Effects on Human Myeloma Cells in Vitro and in Vivo. *Mol. Cancer Ther.* **2009**, *8* (1), 26–35.

(64) Wei, L.-H.; Kuo, M.-L.; Chen, C.-A.; Chou, C.-H.; Lai, K.-B.; Lee, C.-N.; Hsieh, C.-Y. Interleukin-6 Promotes Cervical Tumor Growth by VEGF-Dependent Angiogenesis via a STAT3 Pathway. *Oncogene* **2003**, *22* (10), 1517–1527.

(65) Sasse, J.; Hemmann, U.; Schwartz, C.; Schniertshauer, U.; Heesel, B.; Landgraf, C.; Schneider-Mergener, J.; Heinrich, P. C.; Horn, F. Mutational Analysis of Acute-Phase Response factor/Stat3 Activation and Dimerization. *Mol. Cell. Biol.* **1997**, *17* (8), 4677–4686.

(66) Darnell, J. E. STATs and Gene Regulation. *Science* **1997**, *277* (5332), 1630–1635.

(67) Shuai, K.; Liu, B. Regulation of JAK-STAT Signalling in the Immune System. *Nat. Rev. Immunol.* **2003**, *3* (11), 900–911.

(68) Vicari, A. P.; Caux, C.; Trinchieri, G. Tumour Escape from Immune Surveillance through Dendritic Cell Inactivation. *Semin. Cancer Biol.* **2002**, *12* (1), 33–42.

(69) Wang, T.; Niu, G.; Kortylewski, M.; Burdelya, L.; Shain, K.; Zhang, S.; Bhattacharya, R.; Gabrilovich, D.; Heller, R.; Coppola, D.; et al. Regulation of the Innate and Adaptive Immune Responses by Stat-3 Signaling in Tumor Cells. *Nat. Med.* **2004**, *10* (1), 48–54.

(70) Nefedova, Y.; Huang, M.; Kusmartsev, S.; Bhattacharya, R.; Cheng, P.; Salup, R.; Jove, R.; Gabrilovich, D. Hyperactivation of STAT3 Is Involved in Abnormal Differentiation of Dendritic Cells in Cancer. *J. Immunol.* **2003**, *172* (1), 464–474.

(71) Park, S.-J.; Nakagawa, T.; Kitamura, H.; Atsumi, T.; Kamon, H.; Sawa, S. -i.; Kamimura, D.; Ueda, N.; Iwakura, Y.; Ishihara, K.; et al. IL-6 Regulates In Vivo Dendritic Cell Differentiation through STAT3 Activation. *J. Immunol.* **2004**, *173* (6), 3844–3854.

(72) Fletcher, S.; Drewry, J. A.; Shahani, V. M.; Page, B. D. G.; Gunning, P. T. Molecular Disruption of Oncogenic Signal Transducer and Activator of Transcription 3 (STAT3) Protein. *Biochem. Cell Biol.* **2009**, *87* (6), 825–833.

(73) Couto, J. I.; Bear, M. D.; Lin, J.; Pennel, M.; Kulp, S. K.; Kisseberth, W. C.; London, C. a. Biologic Activity of the Novel Small Molecule STAT3 Inhibitor LLL12 against Canine Osteosarcoma Cell Lines. *BMC Vet. Res.* **2012**, *8* (1), 244.

(74) Lin, L.; Hutzen, B.; Li, P.-K.; Ball, S.; Zuo, M.; DeAngelis, S.; Foust, E.; Sobo, M.; Friedman, L.; Bhasin, D.; et al. A Novel Small Molecule, LLL12, Inhibits STAT3 Phosphorylation and Activities and Exhibits Potent Growth-Suppressive Activity in Human Cancer Cells. *Neoplasia* **2010**, *12* (1), 39–50.

(75) Bid, H. K.; Oswald, D.; Li, C.; London, C. a.; Lin, J.; Houghton, P. J. Anti-Angiogenic Activity of a Small Molecule STAT3 Inhibitor LLL12. *PLoS One* **2012**, *7* (4).

(76) Bhasin, D.; Etter, J. P.; Chettiar, S. N.; Mok, M.; Li, P. K. Antiproliferative Activities and SAR Studies of Substituted Anthraquinones and 1,4-Naphthoquinones. *Bioorganic Med. Chem. Lett.* **2013**, *23* (24), 6864–6867.

(77) Lin, L.; Benson, D. M.; Deangelis, S.; Bakan, C. E.; Li, P. K.; Li, C.; Lin, J. A Small Molecule, LLL12 Inhibits Constitutive STAT3 and IL-6-Induced STAT3 Signaling and Exhibits Potent Growth Suppressive Activity in Human Multiple Myeloma Cells. *Int. J. Cancer* **2012**, *130* (6), 1459–1469.

(78) EasySep™ Mouse CD11c Positive Selection Kit II http://www.stemcell.com/en/Products/All-Products/EasySep-Mouse-CD11c-Positive-Selection-Kit-II.aspx (accessed Sep 6, 2015).

(79) Fast, Easy & Column-Free Cell Separation Ready Sep Go w/ EasySep™ http://www.stemcell.com/en/Products/Popular-Product-Lines/EasySep.aspx (accessed Sep 6, 2015).

(80) EasySep™ Mouse NK Cell Enrichment Kit http://www.stemcell.com/en/Products/All-Products/EasySep-Mouse-NK-Cell-Enrichment-Kit.aspx (accessed Sep 6, 2015).

(81) Hubbell, J. a; Thomas, S. N.; Swartz, M. a. Materials Engineering for Immunomodulation. *Nature* **2009**, *462* (7272), 449–460.

(82) Schliehe, C.; Redaelli, C.; Engelhardt, S.; Fehlings, M.; Mueller, M.; van Rooijen, N.; Thiry, M.; Hildner, K.; Weller, H.; Groettrup, M. CD8- Dendritic Cells and Macrophages Cross-Present poly(D,L-Lactate-Co-Glycolate) Acid Microsphere-Encapsulated Antigen in Vivo. *J. Immunol.* **2011**, *187* (5), 2112–2121.

(83) Engering, A.; Geijtenbeek, T. B. H.; van Vliet, S. J.; Wijers, M.; van Liempt, E.; Demaurex, N.; Lanzavecchia, A.; Fransen, J.; Figdor, C. G.; Piguet, V.; et al. The Dendritic Cell-Specific Adhesion Receptor DC-SIGN Internalizes Antigen for Presentation to T Cells. *J. Immunol.* **2002**, *168* (5), 2118–2126.

(84) Di Lorenzo, G.; Buonerba, C.; Kantoff, P. W. Immunotherapy for the Treatment of Prostate Cancer. *Nat. Rev. Clin. Oncol.* **2011**, *8* (9), 551–561.

(85) Joyce, J. A.; Pollard, J. W. Microenvironmental Regulation of Metastasis. *Nat. Rev. Cancer* **2009**, *9* (4), 239–252.

(86) Szebeni, J.; Moghimi, S. M. Liposome Triggering of Innate Immune Responses: A Perspective on Benefits and Adverse Reactions. *J. Liposome Res.* **2009**, *19* (2), 85–90.

(87) Shirazi, R. S.; Ewert, K. K.; Leal, C.; Majzoub, R. N.; Bouxsein, N. F.; Safinya, C. R. Synthesis and Characterization of Degradable Multivalent Cationic Lipids with Disulfide-Bond Spacers for Gene Delivery. *Biochim. Biophys. Acta* **2011**, *1808* (9), 2156–2166.

(88) Akinc, A.; Zumbuehl, A.; Goldberg, M.; Leshchiner, E. S.; Busini, V.; Hossain, N.; Bacallado, S. A.; Nguyen, D. N.; Fuller, J.; Alvarez, R.; et al. A Combinatorial Library of Lipid-like Materials for Delivery of RNAi Therapeutics. *Nat. Biotechnol.* **2008**, *26* (5), 561–569.

(89) Sengupta, P.; Basu, S.; Soni, S.; Pandey, a.; Roy, B.; Oh, M. S.; Chin, K. T.; Paraskar, a. S.; Sarangi, S.; Connor, Y.; et al. Cholesterol-Tethered Platinum II-Based Supramolecular Nanoparticle Increases Antitumor Efficacy and Reduces Nephrotoxicity. *Proc. Natl. Acad. Sci.* **2012**, *109* (28), 11294–11299.

(90) Pisani, M.; Mobbili, G.; Bruni, P. Neutral Liposomes and DNA Transfection. *Non-Viral Gene Ther.* **2011**, 319–348.

(91) Miller, C. R.; Bondurant, B.; McLean, S. D.; McGovern, K. A.; O'Brien, D. F. Liposome-Cell Interactions in Vitro: Effect of Liposome Surface Charge on the Binding and Endocytosis of Conventional and Sterically Stabilized Liposomes. *Biochemistry* **1998**, *37* (37), 12875–12883.

(92) Gewirtz, A. M. On Future's Doorstep: RNA Interference and the Pharmacopeia of Tomorrow. *J. Clin. Invest.* **2007**, *117* (12), 3612–3614.

(93) Tanaka, T.; Mangala, L. S.; Vivas-Mejia, P. E.; Nieves-Alicea, R.; Mann, A. P.; Mora, E.; Han, H.-D.; Shahzad, M. M. K.; Liu, X.; Bhavane, R.; et al. Sustained Small Interfering RNA Delivery by Mesoporous Silicon Particles. *Cancer Res.* **2010**, *70* (9), 3687–3696.

(94) Canton, J.; Neculai, D.; Grinstein, S. Scavenger Receptors in Homeostasis and Immunity. *Nat. Rev. Immunol.* **2013**, *13* (9), 621–634.

(95) Kelly, C.; Jefferies, C.; Cryan, S.-A. Targeted Liposomal Drug Delivery to Monocytes and Macrophages. *J. Drug Deliv.* **2011**, *2011*, 727241.

(96) Moon, J. J.; Huang, B.; Irvine, D. J. Engineering Nano- and Microparticles to Tune Immunity. *Adv. Mater.* **2012**, *24* (28), 3724–3746.

(97) Immordino, L.; Dosio, F.; Cattel, L. Stealth Liposomes: Review of the Basic Science, Rationale, and Clinical Applications,. *Int. J. Nanomedicine* **2006**, *1* (3), 297–315.

(98) Kulkarni, A. A.; Roy, B.; Rao, P. S.; Wyant, G. A.; Mahmoud, A.; Ramachandran, M.; Sengupta, P.; Goldman, A.; Kotamraju, V. R.; Basu, S.; et al. Supramolecular Nanoparticles That Target Phosphoinositide-3-Kinase Overcome Insulin Resistance and Exert Pronounced Antitumor Efficacy. *Cancer Res.* **2013**, *73* (23), 6987–6997.

(99) Molavi, O.; Mahmud, A.; Hamdy, S.; Hung, R. W.; Lai, R.; Samuel, J.; Lavasanifar, A. Development of a Poly(d,l-Lactic-Co-Glycolic Acid) Nanoparticle Formulation of STAT3 Inhibitor JSI-124: Implication for Cancer Immunotherapy. *Mol. Pharm.* **2010**, *7* (2), 364–374.

(100) Clemente-Casares, X.; Tsai, S.; Yang, Y.; Santamaria, P. Peptide-MHC-Based Nanovaccines for the Treatment of Autoimmunity: A "One Size Fits All" Approach? *J. Mol. Med. (Berl).* **2011**, *89* (8), 733–742.